Model-Aided Design of a High-Performance Fly-by-Wire Actuator, Based on a Global Modelling of the Actuation System using Bond-graphs

Clément Coïc

Université Fédérale

Toulouse Midi-Pyrénées

THÈSE

En vue de l'obtention du

DOCTORAT DE L'UNIVERSITÉ DE TOULOUSE

Délivré par :

Institut National des Sciences Appliquées de Toulouse (INSA de Toulouse)

Présentée et soutenue par :
Clément Coïc

le jeudi 1 décembre 2016

Titre :

Model-Aided Design of a High-Performance Fly-by-Wire Actuator,
Based on a Global Modelling of the Actuation System using Bond-graphs

---

École doctorale et discipline ou spécialité :

ED MEGEP : Génie mécanique, mécanique des matériaux

Unité de recherche :

ICA, CNRS UMR 5312

Directeur/trice(s) de Thèse :

Jean-Charles Maré

Jury :

Eric Bideaux, Professeur, INSA de Lyon, Rapporteur
Esteban Codina, Professeur, Université Polytechnique de Catalogne, Rapporteur
Jean-Charles Maré, Professeur, INSA de Toulouse, Directeur de Thèse
Marc Budinger, Maître de Conférences (HDR), INSA de Toulouse, Examinateur
Boris Grohmann, Docteur, Airbus Helicopters, Examinateur
Jean-Romain Bihel, Ingénieur, Airbus Helicopters, Co-encadrant de Thèse
Bruno Chaduc, Ingénieur, Airbus Helicopters, Invité
Thibaut Marger, Docteur, Airbus Helicopters, Invité

ACKNOWLEDGEMENTS

The researches involved in this PhD dissertation are the fruit of collaboration between *Institut Clément Ader* (Toulouse) on one side and *Airbus Helicopters* (Marignane) on the other side. It is thus naturally that I would like to thank both entities for their agreement on supporting this work.

First, my gratitude is directed to my advisor Professor Jean-Charles Maré for his support all along these three years. By sharing his knowledge, he gave me the ambition to look always further in a direction. His availability was a key for my achievements: confirming, improving or correcting my ideas soon enough to put as much energy as possible on each subject. His motivation and assets for spreading the knowledge make me improve my rigor and communication skills. Also, the degree of freedom he let me is appreciated for making my own opinion on certain topics.

Naturally, I would like to thanks Jean-Romain Bihel (technical referent) and Bruno Chaduc (Head of the *Hydraulics & Flight Controls* department) both for their support on the "company-side" of this PhD. They supported me in so many aspects: technically – by their experience in hydraulics and flight controls, financially – defending the projects I worked on inside the company, humanly – by being giving the responsibilities and keys for my own evolution… For all that I consider them as an infinite support inside Airbus Helicopters and clearly as friends.

I would like to thank also the member of the committee that were a source of improvements for my dissertation. The time my reviewers, Professor Eric Bideaux and Professor Esteban Codina, dedicated for their deep study of my work and criticizing the dissertation is invaluable. Professor Marc Budinger always provided me helpful remarks. Dr. Boris Grohmann and Dr. Thibaut Marger, during the four and a half year at Airbus Helicopters shared their knowledge with me. The remarks provided by all the members of this committee surely made possible improving my dissertation.

Airbus Helicopters is, in my opinion, a single team spread in several departments that are all working for the best technical solution. Without this team the result of these researches would not have been the same. So many people are part of this team but I would like to name the main contributors. Pierre Heng taught me the Fly-by-Wire world; Jean-Marie Allietta shared with me his infinite knowledge in modelling and simulation; Dr. Pascal Izzo supported me in many activities (such as hardware-related during my test bench development); Roméo Byzery integrated my hydraulic actuation system modelling in its flight control laws so we could run full flight control system simulations; Jean-François Lafisse, Antoine Maussion, Emmanuel Beaud were always available for a talk and for jokes... The help of all these co-workers was possible thanks to Max Massimi and Dr. Jacques Bellera who opened me the doors of the Fly-by-Wire team and included me in their projects and developments.

ACKNOWLEDGEMENTS

In this team, I am really grateful to all my colleagues from the *Hydraulics & Flight Controls* department. I want to particularly name: Anthony Caila was a reference in all serial program and safety related questions I could have; Thomas Buro and Joseph Barthélemy were always available for discussion and constructive remarks on my work; the "Heavy-team" including Nicolas Avril, Jean-Yves Agresta and Bernard Gemmati were the source of many smiles in these last years; Gérard Couderc and Christophe Kilhoffer for the many lunched we spent together… And all the others!

This team included many invaluable supports in my journey: Pascal Leguay was THE hydraulic expert and a referent to me; Michel Vialle was the origine of the project behind this PhD; Emmanuel Mermoz enabled starting this project by a joint feasibility study; François-Xavier Filias was financially controlling and approving all the expenses required for test benches, travels... Finally, Pierre Maret and Fabienne Fraisse showed me an infinite support until my last day at Airbus Helicopters.

I could not forget to thank the French organisms who made this PhD possible. First, the French national research and technology association (*ANRT*) for enabling doctoral thesis to happen with an industrial partner. Then the French Directorate General of Armaments (*DGA*) for supporting research and technology programs.

Last but far to be the least, I am deeply grateful to my family to whom this dissertation is dedicated. My wife Tina and son Yann let me the time, during nights and weekends, to investigate more solutions, to write communications and this dissertation. Without their comprehension and support, this PhD might not have been possible.

CONTENTS

INTRODUCTION GENERALE

VERS DES COMMANDES DE VOL D'HELICOPTERE PLUS PERFORMANTES

Les commandes de vol d'hélicoptères intègrent généralement des actionneurs hydrauliques. Ils assistent le pilote et l'autopilote en effort en positionnant le plateau cyclique selon les ordres d'entrée (typiquement avec une bande passante de quelques Hertz) tout en rejetant les perturbations liées aux charges en provenance du rotor (typiquement quelques dizaines de Hertz). En réponse à une demande du marché, l'augmentation du confort des passagers, Airbus Helicopters souhaite implémenter de nouvelles fonctions au sein du système de commandes de vol, tel le contrôle actif du rotor. Ces dernières nécessitent le contrôle en position des actionneurs à des fréquences multiples de celle du rotor (par exemple, 19 Hertz pour le rotor 3-pales du SA 349 **[POL86]**).

Pour ce faire, deux axes principaux ont été identifiés et investigués dans ce manuscrit :

1. Développer de nouvelles technologies permettant l'implémentation de ces nouvelles fonctions.
2. Evaluer les nouveaux designs grâce à l'utilisation de modèles virtuels et leurs simulations.

En ce qui concerne le premier axe, le choix technologique des systèmes de guidage et d'étanchéité des vérins d'actionneurs actuels est incompatible avec des sollicitations hautes fréquences. Les moyens de guidage recentrent l'ensemble piston-tige dans le corps du vérin. Les moyens d'étanchéités empêchent le passage du fluide au niveau des surfaces étanchéifiées. Sur les actionneurs hydrauliques d'hélicoptère, la fonction de guidage est généralement réalisée par des paliers en aluminium ou en bronze alors que la fonction d'étanchéité est souvent assurée par une combinaison de joints élastomères et plastomères. Un déplacement de l'actionneur à haute fréquence endommagerait dramatiquement les joints et conduirait à une fuite hydraulique inacceptable au niveau des paliers de guidage. Cette fuite pourrait alors avoir lieu au niveau du piston (entre les chambres d'extension et rétraction) ou au niveau des paliers externes (entre les chambres et l'environnement). Un vérin d'actionneur hydraulique est présenté en Figure 1 détaillant les sous-ensembles dont la terminologie a été utilisée précédemment.

De nouvelles technologies avec un design adapté doivent donc être développées afin de permettre l'implémentation de ces fonctions nécessitant de hautes fréquences. Les vérins hautes performances disponibles dans l'industrie, notamment pour les bancs d'essais de fatigue ou d'endurance, utilisent des paliers linéaires fluides. Un palier fluide consiste à laisser passer un fin film de fluide pressurisé, lequel génère une force normale au palier. La contrepartie de cette technologie est une fuite fonctionnelle de fluide drainée vers la ligne retour. Leur développement et utilisation dans l'industrie est facilité par un apport en fluide à pression et température quasi-constante.

INTRODUCTION GENERALE

Le palier fluide est une solution technologique intéressante pour atteindre les hautes performances des actionneurs tout en maintenant une durée de vie acceptable. Cependant, dans le cas précis d'un système de puissance embarqué, tel que le système hydraulique d'un hélicoptère, le design des paliers fluides linéaires n'est pas trivial : la température du fluide varie énormément, typiquement cette variation peut représenter plus de 150°C, et avec elle, les propriétés intrinsèques du fluide. Une étude détaillée des performances du palier fluide sur l'ensemble du spectre de température est donc nécessaire.

D'autres avantages s'ajoutent à l'utilisation de paliers fluides, en plus de la potentielle augmentation des performances de l'actionneur :

- La défaillance du joint de piston est une panne dormante, ce qu'elle ne peut être détectée sans un test dédié. Cela contraint le planning de maintenance de l'actionneur et induit un coût non-négligeable pour le client. De ce fait, la suppression des joints de piston est une avancée considérable.
- Le fluide utilisé par l'actionneur peut être partagé avec d'autres composants. Par exemple, des ensembles mécaniques, telle la boîte de transmission principale, pourrait être lubrifiés par le fluide en provenance du drain de l'actionneur.
- Le partage du fluide permet d'envisager l'usage d'un unique échangeur thermique pour plusieurs sous-systèmes, conduisant ainsi à un gain de masse au niveau hélicoptère.
- Aussi, l'utilisation d'un unique échangeur thermique améliorerait son efficacité pour le système hydraulique et permettrait donc de réduire la plage de température dans lequel le fluide évolue. Le système d'actionnement de l'hélicoptère, composé de la génération de puissance hydraulique, sa distribution ainsi que sa consommation, pourra donc être optimisé dans le but de minimiser sa masse.

Au regard de tous ces avantages, l'utilisation de paliers fluides pour actionneurs intégrés dans une enveloppe a été breveté, avec notre contribution, par Airbus Helicopters **[COI15a]**. Une vue du brevet est présentée en Figure 2 (a). En continuité du brevet, l'auteur a aussi contribué à l'étude de possible implémentation dont une solution est montrée en Figure 2 (b). Cette invention possède l'avantage supplémentaire de protéger les actionneurs d'agressions extérieures (e.g. impact à l'oiseau).

Bien que ce ne soit pas une obligation pour l'application de ce brevet, l'utilisation d'un système de commandes de vol électrique contribue à augmenter la bande passante de l'actionnement, à faciliter l'introduction de nouvelles fonctions et à en améliorer la fiabilité.

Le temps nécessaire au développement de nouvelles technologies peut être réduit grâce à la modélisation et simulation virtuelle du système concerné. Les modèles virtuels doivent être conçus dans le but de reproduire le comportement du système et de ses sous-systèmes de manière à pouvoir réaliser les tests unitaires et d'intégration d'intérêt. Dans notre cas, le système d'actionnement doit être modélisé

afin de reproduire virtuellement les réponses d'une implémentation existante. Il doit aussi faciliter l'évaluation de nouveaux designs partiels ou complets du système. Sur la base de ces observations, un intérêt particulier a été porté sur l'architecture des modèles afin de permettre leur réutilisation et leur évolution incrémentale. L'impact de la technologie choisie sur la modélisation du système doit être minimiser afin d'évaluer de manière efficace plusieurs architecture. Cela a été possible grâce à un travail de standardisation des interfaces des modèles.

Ces travaux de recherche ont pour but l'investigation de l'augmentation de performance des actionneurs à commandes de vol électriques et l'impact induit sur le système de génération et distribution hydraulique. Ces recherches représentent donc un pas en avant dans l'application du brevet présenté ci-dessus. Dans le but de synthétiser ces travaux, ce mémoire est organisé en quatre chapitres :

Le **Chapitre 1** présente les concepts généraux d'un système de commandes de vol d'hélicoptère. Il met en évidence ses évolutions incrémentales dirigées par les besoins naissants, depuis les commandes de vol mécaniques jusqu'aux électriques. Une attention particulière est portée aux différentes architectures et technologies d'actionneurs conduisant à des recommandations sur le choix technologique en lien avec la criticité de la fonction à réaliser.

Le **Chapitre 2** propose une modélisation virtuelle du système d'actionnement avec l'aide du formalisme Bond-graph. Le modèle est adressé avec une vision orientée objet et de manière à ce que les paramètres à renseigner soient ceux dont les ingénieurs disposent. Cette modélisation a pour but de réduire le temps de développement d'un nouveau système d'actionnement de commandes de vol d'hélicoptère tout en assurant une meilleure satisfaction des exigences spécifiées. Elle permet aussi, dans le cadre de l'augmentation des performances du système d'actionnement, de prédire les limitations au niveau de l'actionneur induites par l'ensemble du système, par exemple dû à la température du fluide ou encore par la génération et distribution hydraulique.

Le **Chapitre 3** se focalise sur les technologies de paliers fluides linéaires. Dans un premier temps, l'équation de Reynolds est détaillée. Elle fournit une modélisation algrébrico-différentielle de la distribution de pression au sein du film de fluide. Sur la base de cette équation, différentes formes de paliers sont étudiées dans le but d'observer leur impact sur trois critères principaux de dimensionnement du palier : sa force normale, sa fuite et sa raideur. Ensuite, un processus de pré-dimensionnement d'une butée hydrostatique est proposé, en insérant un « orifice tube-court » en tant que restriction amont nécessaire à la raideur du palier. Ce type d'orifice introduit un paramètre de dimensionnement d'intérêt, lequel peut aisément être adapté de manière à répondre au dilemme force/raideur versus débit de fuite sur la plage de variation de température du fluide. Finalement, une étude de sensibilité est menée sur les paliers hybrides coniques. Elle adresse la variation des trois principaux critères de dimensionnement

face aux variables temporelles (i.e. température et excentration), ainsi que face aux paramètres de dimensionnement (i.e. la forme du palier).

Le **Chapitre 4** présente un développement, assisté par les modèles virtuels, d'actionneur hautes performances, utilisant une technologie de paliers fluides linéaires. Ce chapitre est une contribution à un projet de recherche Airbus Helicopters. Dû aux sauts technologiques portés par l'ensemble du projet, ce chapitre a été jugé confidentielle pour une durée de dix ans.

Finalement, la **Conclusion Générale** résume les principales avancées de ces travaux et liste les perspectives associées à chaque sujet traité dans ce mémoire.

DISSERTATION INTRODUCTION

A STEP TOWARDS HIGH-PERFORMANCE HELICOPTER FLIGHT CONTROLS

Helicopter flight control systems usually integrate hydraulic actuators. They assist the pilot and autopilot in effort by positioning the swashplate according to the input commands (typically with a bandwidth of a few Hertz) while rejecting the effect of load disturbances coming from the rotor (typically with a bandwidth of a few tens of Hertz). As a response to a market demand, which is to increase passenger comfort, Airbus Helicopters would like to implement new functions on the flight control system, such as active rotor control. This requires controlling the actuator position at the rotor frequencies (e.g. 19 Hertz for a 3-blade rotor **[POL86]**).

For this, two main axes have been identified and are investigated in this dissertation:

1. To develop new technologies enabling the implementation of these new functions.
2. To evaluate the new design by resorting to modelling and simulation.

With regard to technology improvement, current bearing and sealing devices on actuator cylinders are not designed to face such high frequencies. Indeed, bearing devices guide the actuator piston-rod assembly in the housing cylinder (or vice versa) while sealing devices prevent leakage through the sealed surfaces. On helicopter actuators, the guiding function is typically fulfilled by aluminium or bronze rings, whereas the sealing function is usually performed by a combination of elastomeric and plastomeric seals. High-frequency motion wears the dynamic seals dramatically, leading to unacceptable leakage at the guiding rings. Leakage can occur at piston level (between the extension and retraction chambers) and at bushing level (between one chamber and the environment). A hydraulic cylinder of an actuator is presented in Figure 1 and the elements corresponding to the terminology used are shown.

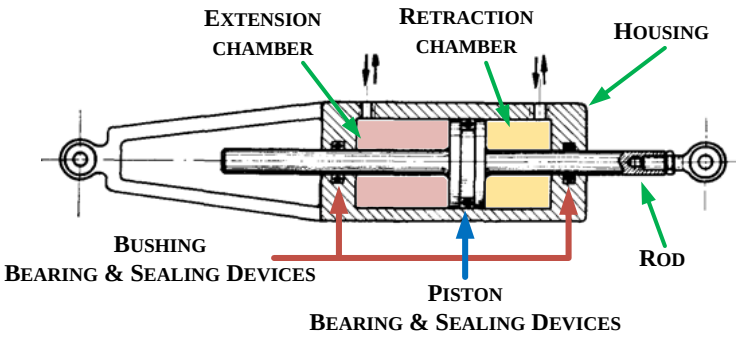

Figure 1 – Dynamic bearing and sealing devices in a hydraulic cylinder, modified from [FAI06].

A re-engineering of both the actuator bearing and the sealing functions is thus required in order to enable the implementation of high-frequency functions. Industrial high-performance actuators, typically

used for fatigue or endurance test benches, include piston and bushing linear fluid bearings at the cost of a functional leakage drained to the return line. A fluid bearing consists in a fluid film, the pressure of which generates a bearing force. Their development and operation is facilitated if the bearing is supplied at constant pressure and temperature.

The linear fluid bearing is an interesting technology to achieve high-performance actuators without excessive lifespan reduction. However, in case of embedded power systems such as the hydraulic network on helicopters, the design of linear fluid bearings is not simple: the temperature varies widely, typically within a range of more than 150°C, and with it the fluid properties. An investigation of the linear fluid bearing performances over such an extended range of temperature is thus required.

In addition to enabling enhanced performance, the removal of conventional sealing devices has other advantages:

- The piston seal failures are dormant, which means that they cannot be detected without a dedicated test. This constrains the maintenance planning of the actuator and has hence a non-negligible cost for the customers. From this point of view, removing seals obviously marks a step forward.
- The actuator fluid could be shared with other applications. For example, mechanical parts, such as the main gear box, could be lubricated with the fluid coming out of the actuator drain.
- The fluid sharing allows designing a single heat exchanger for the various applications. This leads to a mass reduction at helicopter level.
- Indeed, having a single heat exchanger ensures a more efficient fluid heating or cooling. Thus, the operating temperature range can be reduced. The Actuation System, composed of the hydraulic power generation and distribution and its consumers (such as the actuators) can thus be better optimized and its mass can be minimized.

With regard to these advantages, the use of fluid bearings for actuators integrated in an enclosure has been patented, with our contribution, by Airbus Helicopters **[COI15a]**. On the left side of Figure 2, a view of the patent drawing is shown. Following this patent, the author has also contributed to the study of a possible implementation, which is presented on the right side of Figure 2. Another advantage of this invention is actuator protection from external aggression (e.g. bird strike).

Although it is not mandatory for applying this patent, resort to a Fly-by-Wire flight control system contributes to an increased actuation bandwidth, the provision of new functions and improved reliability.

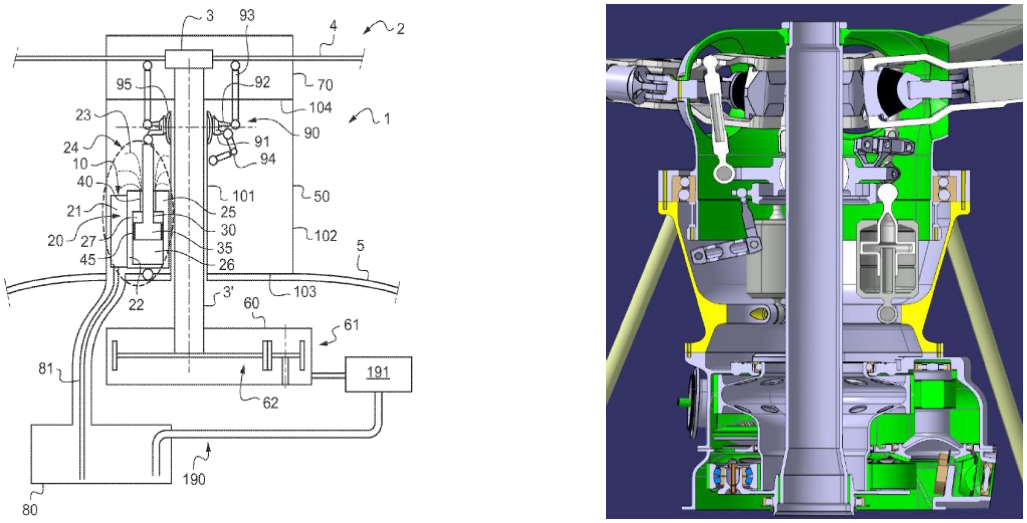

(a) –Variant as patented in **[COI15a]**

(b) – Possible implementation **[ETM14]**

Figure 2 – High-performance actuator in Main Gear Box.

The development time of new technologies can be reduced with the help of virtual model simulation. Virtual models should be designed to reproduce system and subsystem behaviour in order to perform unitary and integration virtual tests. In our application, the Actuation System must be modelled to reproduce the responses of existing designs and to facilitate and evaluate new designs of the entire system or some of its component. Based on these observations, a particular focus has to be put on architecting the model to allow its reusability and incremental evolution. The impact of the technology selection on the system modelling shall be minimized in order to be able to efficiently evaluate several architectures.

This research aims at investigating the Fly-by-Wire actuator performance improvements and its impact on the hydraulic power generation and distribution system, as a step towards the presented patent implementation. For this purpose, the dissertation is organized in four chapters.

Chapter 1 presents the general concepts of the helicopter flight control system. It highlights the incremental need-driven evolution from the mechanical to the Fly-by-wire technology flight control system. In this chapter, a particular focus is put on the actuator architectures and technologies. Recommendations on the actuator technology are given.

Chapter 2 proposes a virtual modelling of the Actuation System with the support of the Bond-graph formalism. The model is addressed in an object-oriented manner, paying attention to involve parameters that engineers are able to provide. It is aimed at reducing the development time of a new helicopter Actuation System and at ensuring a better fulfilment of its specification. Within the scope of increasing Actuation System performance, it permits predicting the limitations at actuator level, which are for example induced by the temperature or by the hydraulic power generation and distribution.

Chapter 3 focuses on the linear fluid bearing technologies. It starts by detailing the Reynolds equation, which provides the differential equation modelling the pressure distribution in the fluid film. Based on this, different physical shapes of the bearings are studied to observe their impact on the three main design criteria of fluid bearings: bearing force, leakage and stiffness. Then, a pre-sizing process of hydrostatic thrust bearings is proposed, introducing a short tube orifice as the fixed restriction required for stiffness. The short tube orifice introduces an interesting design parameter that can easily be managed to solve the sizing dilemma for meeting the bearing performance requirements. Finally, a sensitivity study is conducted on conical hybrid bearings. It addresses the variation of the three main design criteria with time variables (i.e. temperature and eccentricity) and then with design parameters (i.e. the physical shape of the bearing).

Chapter 4 is restricted and removed from this dissertation.

Finally, the Dissertation Conclusion summarizes the main achievements of this research and provides the perspectives for each subject dealt with in this dissertation.

BIBLIOGRAPHY

[COI15a] COÏC, C., BIHEL, J.-R., MARGER, T. & COUDERC, C., *Patent US2015298796 (A1) - Aircraft Hydraulic System Comprising at least one Servo-Control, and an Associated Rotor and Aircraft*. Airbus Helicopters, France, 2015.

[ETM14] ETM, *Flight Controls Inside the Rotor Mast*. Airbus Helicopters, France, 2015. (internal publication)

[FAI06] FAISANDIER, J., *Mécanismes Hydrauliques et Pneumatiques*. 9th edition, Dunod, Paris, 2006. (in French)

[POL86] POLYCHRONIADIS, M. & ACHACHE, M., *Higher Harmonic Control: Flight Tests of an Experimental System on SA 349 Research Gazelle*. 42nd Annual Forum of the American Helicopter Society, Washington, 1986.

CHAPITRE 1

ÉVOLUTION INCREMENTALE DES COMMANDES DE VOL D'HELICOPTERE

1.1 PRINCIPAUX ASPECTS DE LA MECANIQUE DU VOL HELICOPTERE

Les forces propulsive et sustentatrice de l'hélicoptère proviennent de rotors. La rotation des pales génère une force résultante, perpendiculaire au plan du rotor. L'orientation du rotor et la modulation de l'effort résultant permettent de contrôler la trajectoire de l'hélicoptère.

L'équilibre des forces appliquées sur un hélicoptère en vol d'avancement est présenté en Figure 1.2. La composante verticale de la résultante rotor est la portance (« lift » en anglais) – qui compense le poids de l'hélicoptère – tandis que la composante horizontale est la poussée (« thrust » en anglais) – qui fournit une accélération à la machine si elle est supérieure à la traînée aérodynamique engendrée par la vitesse.

L'intensité de la force résultante rotor peut être modulée en changeant l'incidence (ou pas) des pales– et donc l'angle d'attaque du flux d'air. Comme cette action est commune, en amplitude, à toutes les pales simultanément, elle est appelée variation du pas collectif (« collective pitch » en anglais).

L'orientation de cette force est possible grâce au pas cyclique qui change le pas des pales individuellement. Le terme cyclique provient du fait que, pour une commande de pas cyclique donnée, le pas des pales est le même à un azimut donné.

L'inclinaison de la résultante rotor induit des moments selon un des axes souhaités – présentés en Figure 1.3 – (ou la combinaison d'axes souhaitée) et provoque les rotations de l'appareil. La variation de la composante de cette résultante produira un déplacement dans la direction de l'axe associé.

Finalement l'hélicoptère peut évoluer selon les six degrés de liberté, car il est aussi capable tourner autour de son mât rotor (c'est l'axe de lacet). Le couple transmis par le(s) moteur(s) au rotor principal induit un couple de réaction dans la direction opposée sur l'hélicoptère qui doit être compensé. Une surcompensation ou sous-compensation de ce couple permet une accélération angulaire autour de l'axe de lacet – et donc de contrôler une position angulaire. Dans ce but, l'architecture la plus répandue d'hélicoptères inclue un rotor anti-couple – ou rotor de queue. La rotation de l'hélicoptère autour de l'axe de lacet est réalisée par action sur le pas collectif du rotor de queue.

1.2 ACTIONNEMENT A COMMANDES DE VOL MECANIQUES

Un hélicoptère présente ainsi classiquement quatre commandes de pilotage : le collectif, le tangage, le roulis et le lacet. Sur la plupart des hélicoptères, les pilotes agissent sur deux manches et une paire de pédales pour piloter l'attitude et la trajectoire de l'appareil :

- Le manche collectif qui contrôle le pas collectif des pales
- Le manche cyclique lequel oriente le rotor en tangage et roulis
- Les pédales pour le contrôle de l'axe de lacet

Les premiers hélicoptères furent élaborés de manière à ce que le pilote soit capable de piloter sa trajectoire, dans l'ensemble du domaine de vol, sans assistance hydraulique. Les commandes de vol se résumaient alors à une combinaison de bielles, renvoies, leviers mécaniques et/ou câbles pour assurer la transmission de la commande d'entrée pilote aux rotors principal et arrière. Pour exemple, l'Alouette II – dont le système de commande de vol est présenté en Figure 1.5 – est un hélicoptère de 5 places qui a réalisé son premier vol en 1955.

Le pas collectif des pales peut être contrôlé indépendamment des variations de pas cyclique, même si les deux actions agissent au final sur les mêmes ensembles mécaniques – le plateau cyclique. La commande de pas collectif est ajoutée à la commande de pas cyclique grâce au mélangeur (Figure 1.6).

L'augmentation des charges de vol conduit à l'ajout d'actionneur à commande mécanique et puissance hydraulique dans le but de réduire les efforts de pilotage. Seulement quatre ans après le premier vol de l'Alouette II, son successeur – l'Alouette III – apparut. Elle intégrait les premières servocommandes hydrauliques (Figure 1.8).

L'intégration des servocommandes à l'intérieur de l'armoire commande de vol n'est pas usuelle car elle nécessite de dimensionner les bielles qui vont jusqu'au rotor à l'effort de vol. La plupart du temps, les servocommandes sont positionnées au-dessus du plancher mécanique.

Ceci conduit à trouver une solution avec trois actionneurs de rotor principal en repère fixe, contrôlant l'orientation du plateau cyclique. Le rotor arrière est contrôlé par un seul actionneur.

Afin de garantir que la perte de la fonction commande de vol de l'hélicoptère est extrêmement improbable, les servocommandes des appareils Airbus Helicopters possèdent, à quelques exceptions près, deux corps hydrauliques positionnés en tandem (ou série) et alimentés par deux circuits hydrauliques ségrégués.

1.3 ACTIONNEMENT A COMMANDES DE VOL ÉLECTRIQUES HELICOPTERE

Les commandes de vol électriques consistent à transmettre les commandes des pilotes grâce à des signaux électriques jusqu'aux actionneurs via des calculateurs de contrôle de vol.

Pour cela, il est important de conserver les interfaces pilotes (manches et pédaliers) et les interfaces d'actionnement mais de réaliser un « re-engineering » de la fonction complète. En effet, l'ensemble des couplages de commandes de vol et limites des lois de pilotage sont intégrés dans le calculateur et peuvent

donc être plus facilement modifiés. Ceci conduit donc à une fonction réalisée de manière plus adaptée à l'appareil induisant de meilleures qualités de vol en termes de stabilité et facilité de pilotage.

Paradoxalement, malgré les problèmes de stabilité de mécanique du vol hélicoptère, en comparaison des caractéristiques aérodynamiques avions – plus stables – l'installation de commandes électriques sur avion est une solution banalisée, des avions militaires aux avions civils, alors que cette technologie reste marginale dans le monde hélicoptère.

La difficulté de transposition de la technologie d'actionneurs du monde avion au monde hélicoptère provient essentiellement du fait qu'il n'y a pas de redondance d'actionnement possible sur hélicoptère, et qu'en surcroit les actionneurs hélicoptère sont dans un environnement très sévère.

Ceci revient à considérer les technologies actuellement mise en œuvre dans un contexte avion à la lumière des contraintes particulières du contexte hélicoptère.

1.4 CONCEPTS D'ACTIONNEURS POSSIBLES A L'HORIZON 2020

A l'horizon 2020, différents concepts d'actionnements sont possibles pour application sur un futur hélicoptère à commandes de vol électriques, sur la base des technologies actuellement mises en œuvre dans le mode aéronautique. Dans ce chapitre, nous avons étudié les quatre technologies suivantes :

- L'actionneur électrohydraulique à actionnement direct du distributeur, référencé par DDV pour « Direct Drive Valve » en anglais.
- L'actionneur électrohydraulique à actionnement du distributeur par amplification hydraulique de la commande, appelé EHSV par la suite pour « Electro-Hydraulic ServoValve » en anglais.
- L'actionneur électromécanique en lieu et place de l'actionneur hydromécanique conventionnel, appelé EMA pour « Electro-Mechanical Actuator » en anglais.
- L'actionneur électromécanique, et son calculateur d'asservissement, pilotant le levier d'entrée d'une servocommande conventionnelle, dénommé SIA pour « Smart Interface Actuator » en anglais.

Une attention particulière est portée au deux premières technologies dans la suite du chapitre en anglais. Les deux autres sont pour leur part présentées en tant qu'opportunité pour le futur mais manquent de maturité à ce jour.

CHAPTER 1:

FROM MECHANICALLY POWERED TO ELECTRICALLY SIGNALLED, THE INCREMENTAL EVOLUTION OF HELICOPTER FLIGHT CONTROLS

As a basis for a new development, it has been decided to first introduce the needs behind former evolutions of the helicopter flight control system and their current and future trends. Airbus Helicopters, drawing on its experience acquired over more than 60 years of helicopter production, established a functional breakdown of rotorcraft. The titles of the first section of this chapter refer thus to the functional breakdown of helicopters. Some functions have been slightly adapted to the particularities of flight control systems, which are the scope of this chapter.

In order to understand the role of flight controls on helicopters, section 1 synthetically introduces the principles of flying and details some existing architectures at rotorcraft level. Section 2 focuses on mechanically signalled flight controls. The need-driven incremental evolution of flight control systems is presented. Section 3 addresses the technological step from conventional to Fly-by-Wire (FbW) flight controls. Two main technologies are used for electro-hydraulic actuators of FbW helicopters. A particular focus is laid on these solutions in this section. The most promising evolution perspectives of flight control systems are selected and shortly presented in section 4. Finally, section 5 concludes with the evolution of the helicopter flight control system and emphasizes the need for innovation in order to reach the maximum level of safety and customer satisfaction.

1. PROVIDE LIFT AND PROPULSIVE FORCES

1.1. Generate Aerodynamic Forces

When a relative speed is established between an airfoil and the air, a stream of air flows around it. The airfoil is designed in such manner that it causes curvatures of the air streamlines. As a consequence, it can be shown using Euler equations that the air pressure increases on its lower surface and decreases on its upper surface. Therefore, a differential pressure exists between the upper and the lower surfaces of the airfoil, creating an aerodynamic force. The modulation of this force is made possible thanks to the variation of the angle of attack. Figure 1.1 is a representation of such force.

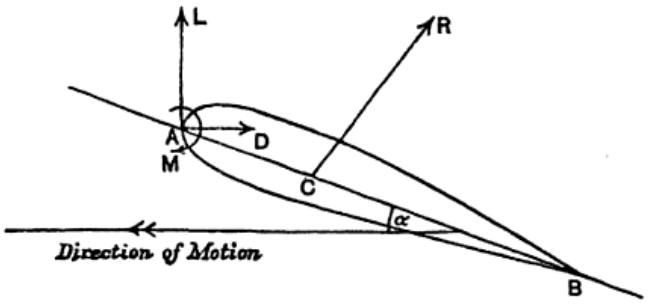

Figure 1.1 – Balanced forces on airfoil in motion as viewed by [GLA26].

To generate an aerodynamic force, aircraft require a means to create relative airspeed. To modulate such a force with a high bandwidth, the inclination of the control surfaces (orientable airfoils) has to be managed. This is performed by the flight control system and rotor kinematics.

1.2. Generate Lift

Airplanes use engines – usually jet engines or propellers – to create relative airspeed, which generates aerodynamic forces. Therefore, the lift (vertical component of this aerodynamic force) of an airplane is directly linked to its relative airspeed, and control surfaces enable trajectory control.

Almost all helicopters generate mechanical power with the help of engines. This power is modulated and propagated to the rotors – and to the equipment, e.g. hydraulic pumps. In helicopters, this power is used to rotate the blades, thus creating a relative speed between the blades and the air, and consequently a lift force. The lift is, at first sight, not dependent on the helicopter airspeed but on the angular velocity of the rotor – and thus blade speed – and blade inclination. Therefore, unlike airplanes, helicopters are able to take off or land vertically and to hover. On the downside, the blade rotation has three main consequences:

- The loads applied to the airframe are cyclic and induce a high level of vibration.
- The maximum angular speed of the rotor is limited by the linear speed at the tip of the blades – which leads to an undesired shock phenomenon if the speed of sound is reached. For this reason, the angular speed of the rotor is usually comprised between 250 and 400 rpm. This consideration has a direct impact on the maximum forward speed of the helicopter, which is usually lower than 180 knots (nearly 93 m/s in SI units or 330 km/h).
- Performances of the helicopter blades are mainly related to air density and the square of the blade airspeed. As angular speed of the rotor is limited, altitude of flight is also limited.

1.3. Control and Withstand Lift Forces

A simplified balance of forces on a helicopter in forward flight is shown in Figure 1.2. The aerodynamic force generated by the rotor rotation can be broken down into two functional forces. The vertical component of the rotor aerodynamic force (the lift) compensates the rotorcraft weight. The horizontal component (the thrust) provides acceleration if it is higher than the aerodynamic drag induced

by the rotorcraft speed. Steady state is reached once both thrust and drag are balanced. The magnitude of the rotor force can be modulated by changing the incidence (or pitch) of all blades – and therefore their angle of attack. As this action is applied simultaneously to all the blades, it is called *collective* pitch. The orientation of the rotor force is made possible by changing the cyclic pitch of the blades individually. The term *cyclic* comes from the fact that, at a given cyclic pitch command and at a given azimuth with respect to the airframe, the blade pitch remains unchanged.

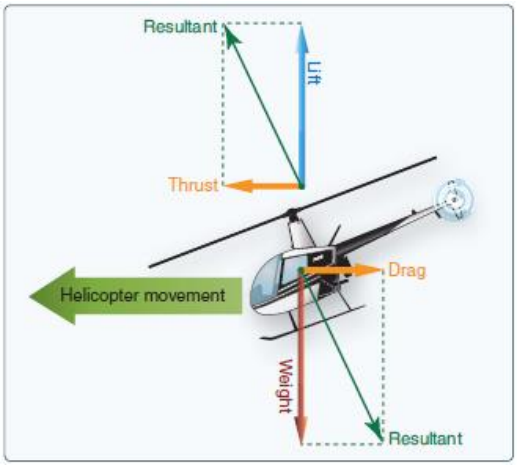

Figure 1.2 – Balanced forces in forward flight [FAA12].

The resultant force inclination induces moments on one axis or a combination of desired axes and generates rotorcraft rotation. Pitch, roll and yaw – rotations around, respectively, lateral, longitudinal and vertical axes – are shown in Figure 1.3. Changing the magnitude of the force component on the desired axis thus produces a motion of the rotorcraft in the respective direction.

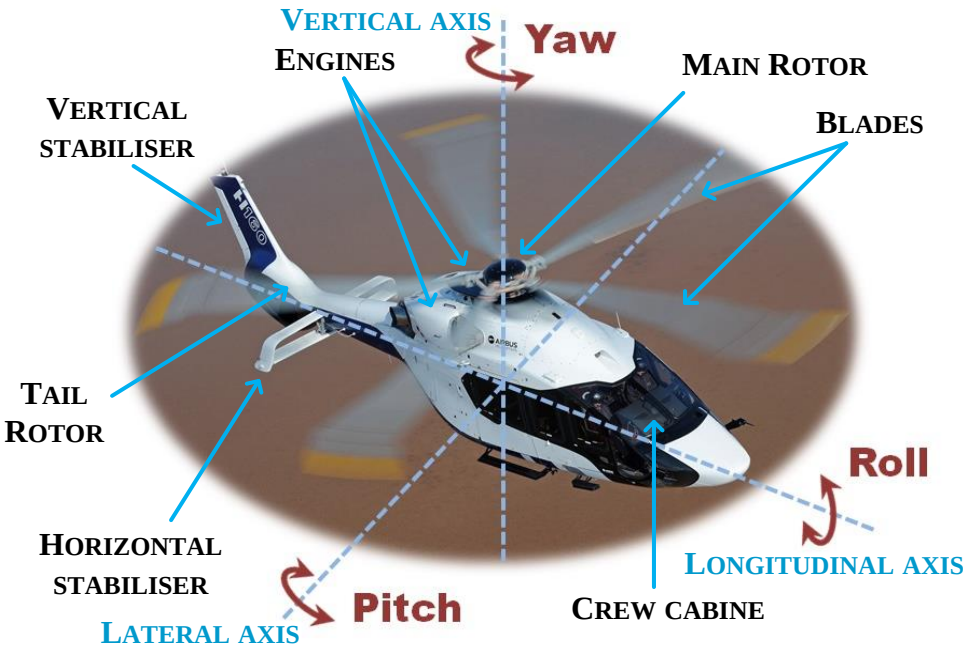

Figure 1.3 – Piloting axes of a helicopter (H160) and main contributors to resultant force.

On a helicopter, the blades rotate but, fortunately, the pilot is on a fixed reference (the airframe). The helicopter thus needs a specific assembly that allows transmission of flight control commands from the fixed reference to the blades. This function is today realized by the rotor hub, which transmits the power driving the rotor, coming from the engines, to the blades through its mast and ensures the command transformation from fixed to rotary domains by means of a swashplate.

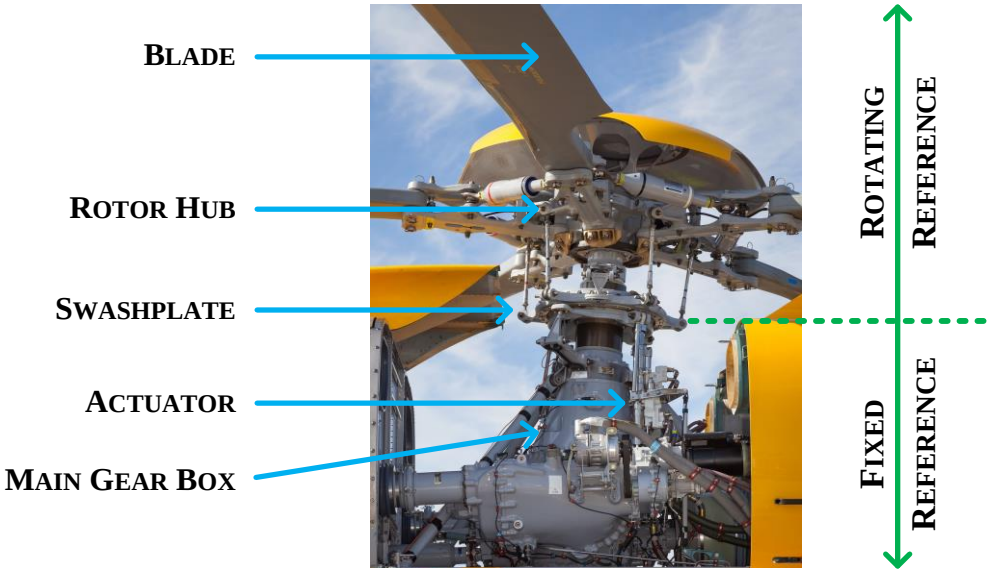

Figure 1.4 – Fixed and rotating references, main components near the rotor hub.

1.4. Control and Withstand Anti-Torque Forces

The torque produced by the engine(s) and transmitted to the rotor induces a reaction torque in the opposite direction on the helicopter airframe that has to be compensated. Over- or under-compensation of this torque results in an angular acceleration around the yaw axis – and causes the frame to rotate around the yaw axis. Two main groups of solutions to generate such torque compensation can be distinguished: those who tend to avoid torque creation and those who counteract the existing torque.

In the first group, usually two main rotors rotating in opposite directions are used. Coaxial rotors are common on Russian helicopters and on Sikorsky high speed prototypes. Tandem rotors, such as on the Boeing CH-47 Chinook, allow for a large centre of gravity range, making this architecture well suited for cargo helicopters. A particular design that avoided torque generation was developed in the early 1950s by Airbus Helicopters (SNCASO at the time). The Djinn helicopter was driven by compressed-air jets at the end of each blade. The yaw was then piloted by means of a vertical stabilizer that deflected the turbine exhaust jet.

The second group includes most of today's helicopters. Usually, helicopters feature a tail rotor with variable pitch. Motion around the yaw axis is thus controlled by action on the collective pitch of the tail rotor blades that rotate at a nearly constant speed. Unless otherwise specified, this helicopters

architecture (and associated flight controls) is the reference architecture in this PhD dissertation. Another, singular architecture also belongs to this group: the NOTAR (NO TAil Rotor) architecture, based on the Coanda effect, was developed by Hughes Helicopters and then implemented on some McDonnell Douglas (e.g. MD 900).

2. PROVIDE HELICOPTER CONTROL AND STABILIZATION – CONVENTIONAL FLIGHT CONTROLS

2.1. Capture Pilots Intentions on Control Axes

Historically, a helicopter is piloted through a control vector with four dimensions: collective, pitch, roll and yaw. Pilot inceptors typically include two sticks and a pair of pedals in order to control the rotor blade pitches and, consequently, the rotorcraft's trajectory. These sticks and pedals are:

- The collective stick, which acts on the collective pitch of the main rotor blades.
- The cyclic stick, which orientates the main rotor disk for pitch – resulting in forward/backward motion – and roll – resulting in left/right motion – commands.
- The pedals for the yaw control, which change the collective tail rotor blade pitch.

It is possible to see an analogy with the flight controls of an airplane, where the collective stick is substituted by the thrust lever.

2.2. Transmit and Process Pilot Orders to Main and Tail Rotors

The first helicopters were designed in such a way that the pilot was able to control the flight trajectory without any hydraulic assistance. The flight controls were a mere combination of mechanical links, cables and bell cranks that transmitted the pilot's commands to the main and tail rotors. As an example, the Alouette II – the flight control system of which is presented in Figure 1.5 – is a five seat helicopter that realized its first flight in 1955. Such design allowed only for limited flight duration and flight domains where piloting efforts remained acceptable.

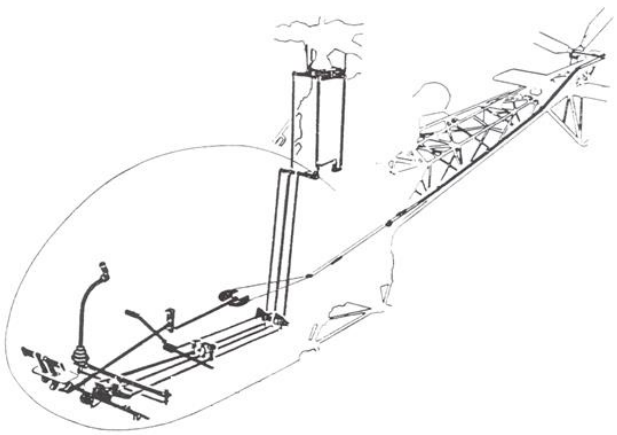

Figure 1.5 – Flight controls on Alouette II representation [SNC55].

As detailed above, it is convenient for the pilot to control the magnitude of the resultant force generated by the main rotor independently of the rotation around the control axes: pitch, roll and yaw. To satisfy this need, two components have been added to the flight control kinematics: the mixing unit (Figure 1.6) and the phasing unit (Figure 1.7).

The mixing unit receives collective and cyclic input, adds them together and provides a combined output, so that the sum can act on the swashplate at the end of the kinematic linkage.

Near the Main Gear Box (MGB), the interactions with other equipment generate a number of environmental constraints. Therefore, the swashplate actuating rods are not always positioned on the pure pitch and roll axes at swashplate level and the displacement of one actuating rod could contribute to both actions. This becomes transparent to the pilot via the phasing unit, which distributes the pilot's commands to the three actuating rods in order to obtain the desired cyclic pitch.

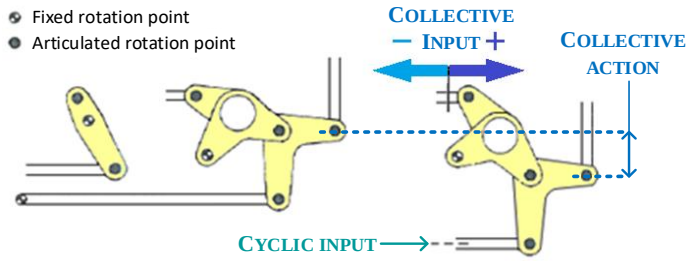

Figure 1.6 – Mixing unit on Alouette III from [SUD59].

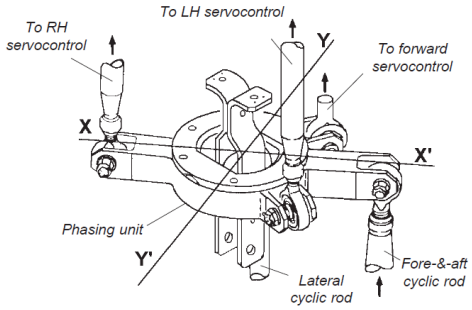

Figure 1.7 – EC 225 Phasing unit from [EUR04].

Helicopter payload (and thus mass) and speed increased and the flight domain was enlarged. These evolutions increased the flight loads and led to the addition of hydraulic actuators in order to reduce pilot efforts on sticks and pedals. Only four years after the first flight of the Alouette II, its successor – the Alouette III – was developed. It was designed with two additional seats and hydraulic actuators integrated in the flight controls (Figure 1.8).

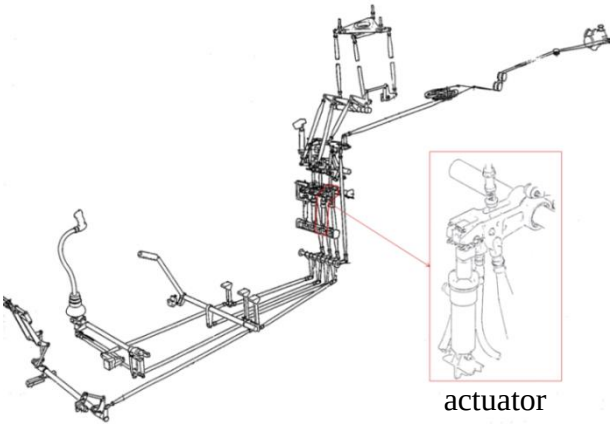

Figure 1.8 – Flight controls on Alouette III [SUD59].

Figure 1.9 – Actuators on H175.

The integration of the actuators in the flight control bay, as for the Alouette III, is not usual. The mechanical linkages between the actuators and the rotors have to withstand dynamic loads and shall be sized accordingly. Therefore, the actuators are usually located on the upper-deck of the helicopter. As an example of such implementation, Figure 1.9 shows the three main rotor actuators of an H175, with the fixed casings attached to the main gear box and the rods linked to the rotor swashplate.

Hydraulic actuators obviously require hydraulic power. In this PhD dissertation, the Actuation System includes hydraulic power generation and distribution, and main and tail rotor actuators. A detailed modelling of the Actuation System is described in Chapter 2.

Finally, a command variation on one axis can induce an undesired change on the helicopter attitude on another axis. For example, an increase of collective pitch generates a higher reaction torque exertion on the structure. Therefore, a collective/yaw coupling has been implemented on heavy helicopters so that the tail rotor thrust is modified in order to keep the helicopter in its trajectory.

The next technological step was the addition of the Stability and Control Augmentation System (SCAS), which is detailed in the following paragraph. Figure 1.10 represents a summary of the flight control architecture in a block diagram with the function associated to each subsystem.

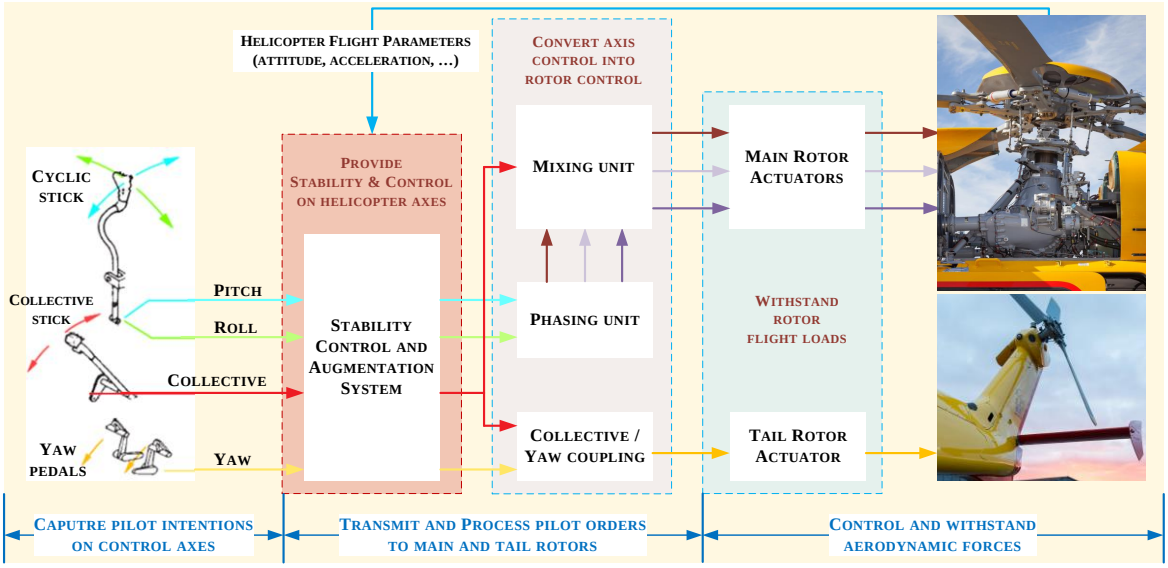

Figure 1.10 – Synthesis scheme of H/C flight control system with functional view.

2.3. Provide Stability & Control on Helicopter Axes

The stability and control augmentation system (SCAS) was developed in order to reduce pilot workload; it assists the pilot controlling the helicopter. Two main functions were identified and introduced: to follow a trajectory of flight and to reject the disturbances. The first function reduces the pilot workload for manoeuvers and level flights (constant altitude). The second function is aimed at compensating the natural instability of helicopters.

For these needs, SCAS actuators are integrated in almost all medium and heavy helicopters. Two main principles are used on the conventional flight control system:

– Added motion in series with the pilot input. This motion is not perceived by the pilot. Actuators in series usually generate high speed and high bandwidth SCAS orders with limited authority. In comparison with pilot orders, their maximum amplitudes are low. They are mainly used for stabilization. This function is usually realized with one of the following solutions:
  1. Smart Electro Mechanical Actuators (SEMA): These actuators were originally called serial actuators. They integrate electronic hardware and are controlled by a digital signal (Figure 1.11).
  2. Automatic Stabilization Equipment (ASE): This equipment was first introduced on the Sikorsky S55. In some designs, the flight control kinematic friction is too high regarding the SEMA capabilities. ASE then fulfils this function with the help of hydraulic power (Figure 1.12).

Figure 1.11 – SEMA.

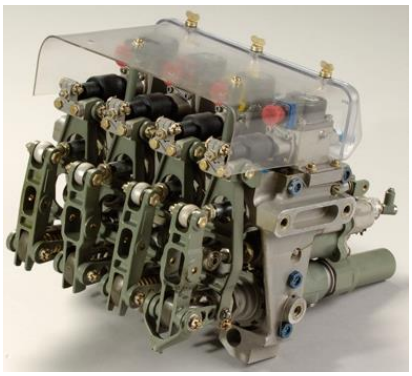

Figure 1.12 – ASE [webSITEC].

– Added motion in parallel with the pilot input. In this case the stick moves in the same proportion as the autopilot order. TRIM actuators (Figure 1.13) ensure this function. They have low speed but full authority on the pilot command. They can be used either by the pilot to hold a position order without effort, or by the autopilot to re-centre the SEMAs in order to keep a symmetrical margin of travel.

Figure 1.13 – Trim actuator.

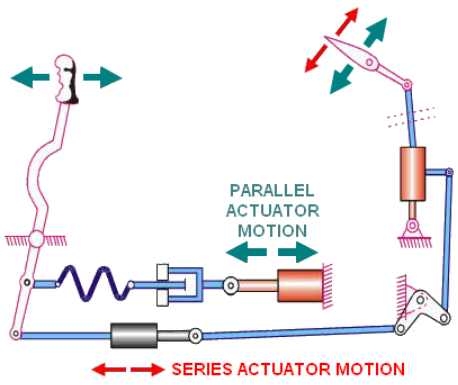

Figure 1.14 – SCAS actuation concept.

Figure 1.14 is a simple representation of both series and parallel actuators in the conventional flight control system and their impact on the blade pitch.

The control of the SCAS actuators is made possible by the Automatic Flight Control System (AFCS) computer called Auto-Pilot Module (APM) at Airbus Helicopters. It receives helicopters flight parameters from dedicated sensors to generate the series and parallel actuator commands. The criticality associated to this equipment, if the helicopter is naturally aerodynamically stable, is "major" as defined in Table 1.1 taken from **[SAE96]**.

Probability (Quantitative)	Per flight hour 1.0	1.0E-3	1.0E-5	1.0E-7	1.0E-9
Probability (Descriptive)	FAA	Probable	Improbable		Extremely Improbable
	JAA	Frequent / Reasonably Probable	Remote	Extremely Remote	Extremely Improbable
Failure Condition Severity Classification	FAA	Minor	Major	Severe Major	Catastrophic
	JAA	Minor	Major	Hazardous	Catastrophic
Failure Condition Effect	FAA & JAA	- slight reduction in safety margins - slight increase in crew workload - some inconvenience to occupants	- significant reduction in safety margins or functional capabilities - significant increase in crew workload or in conditions impairing crew efficiency - some discomfort to occupants	- large reduction in safety margins or functional capabilities - higher workload or physical distress such that the crew could not be relied upon to perform tasks accurately or completely - adverse effects upon occupants	- all failure conditions which prevent continued safe flight and landing
Development Assurance Level	ARP 4754	Level D	Level C	Level B	Level A

Note: A "No Safety Effect" Development Assurance Level E exists which may span any probability range.

Table 1.1: Failure condition severity taken from [SAE96].

This table regroups the qualitative and quantitative probability of failure per flight hour for both the Federal Aviation Administration (FAA) and the Joint Aviation Authorities (JAA – that preceded the European Aviation Safety Agency (EASA) now the European reference for aviation safety).

2.4. Withstand Rotor Flight Loads – Hydro-Mechanical Actuators

2.4.1. Generic Hydraulic Actuator

The hydraulic actuators are inserted in the flight control kinematics in order to implement the pilot orders and provide hydraulic assistance to face the aerodynamic loads. The force to be applied by the pilot to the stick should not exceed 0.25 daN in nominal operation. In contrast, within the flight domain, the aerodynamic load that is reflected to one main rotor actuator of a medium helicopter such as the AS365 can reach up to 300 daN **[MARG11]**. These static and dynamic loads can be much higher for heavier rotorcraft such as the H225 or NH90.

In order to keep a normalized vocabulary throughout this PhD dissertation, a generic hydraulic actuator is introduced with a word Bond-graph in Figure 1.15. The Bond-graph formalism is introduced in Chapter 1. However, some conventions shall be explained in advance. Half arrows (bonds) transmit power, while complete arrows stand for signals. Dashed lines are optional power/signal paths. The colour denotes the physical domain (here: blue for hydraulics, green for mechanics and black for a non-defined domain depending on the chosen technology). This representation makes the order of magnitude of the involved variables perceptible: pilots provide mechanically signalled commands and actuator output is mechanical power. This coincides with the orders of magnitude given at the beginning of this section. The functions fulfilled by the subsystems are the following:

- **The interface stage:** to receive the input signals and transmit them to the pilot stage.
- **The pilot stage:** to drive the power modulation stage based on the output of the interface stage.
- **The power modulation stage:** to receive the hydraulic power supply and to modulate it to provide flow and pressure to the cylinder.
- **The cylinder:** to receive the modulated hydraulic power and transform it into mechanical power.
- **The closed-loop:** to control the actuator movement versus the input signals. Helicopter flight control actuators are position-controlled.

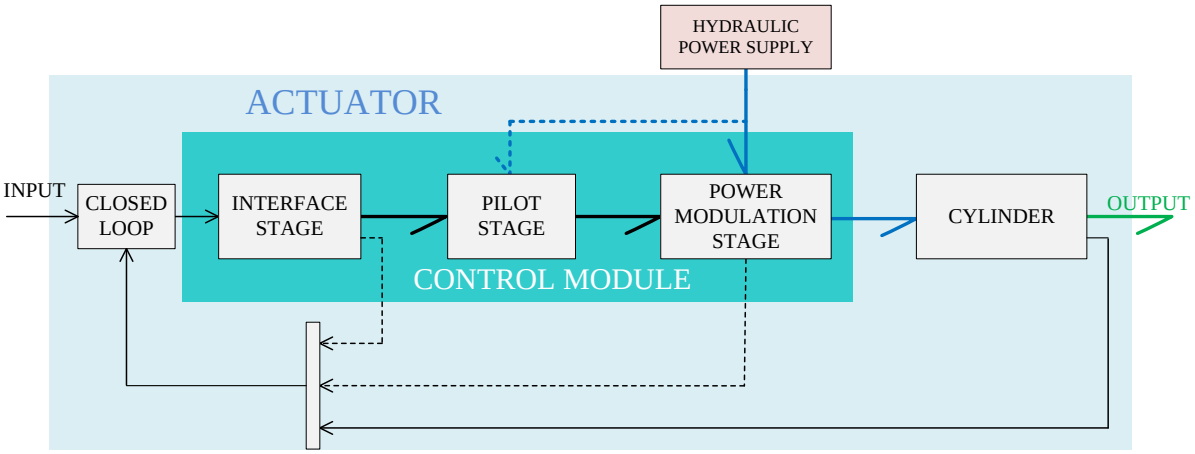

Figure 1.15 – Actuator word Bond-graphs from [COI15b].

2.4.2. Actuator Architecture Driven by Response to Failure

As the flight control system is a safety-critical function, response to failure drives the architecture of aerospace actuators. This section introduces some general safety requirement impacts on actuators and their consequences for a hydro-mechanical actuator.

2.4.2.1. Generalities

"*The rotorcraft systems and associated components, considered separately and in relation to other systems, must be designed so that (…) the occurrence of any failure condition which would prevent the*

continued safe flight and landing of the rotorcraft is extremely improbable" JAR 29.1309-(b)-(2)-(i) **[JAA99]**.

Safety requirements are legitimate for the flight control system as it ensures a critical function on the helicopter. Loss of the helicopter control leads to the loss of the rotorcraft. Therefore, the architecture of the flight control system components is highly impacted by these requirements.

Subpart *(c)* of paragraph *§695* in the main certification regulations (FAR 29 **[FAA65]** and CS29 **[EAS07]** for heavy helicopters) states that *"the failure of mechanical parts (such as piston rods and links), and the jamming of power cylinders, must be considered unless they are extremely improbable"*[1]. A correct sizing including stress and fatigue analyses with the right safety coefficients enables considering one single mechanical path for the flight control system (safe-life).

However, hydraulic and electrical individual faults and failures are not extremely improbable and shall thus always be considered in actuator architecture and design. It is also important to note that the jamming of the power modulation stage is not covered by paragraph §695 – (c). The actuator's architecture and design shall meet the safety objectives with respect to its own failure and possible cross failures with external events. Typically, external events that shall be considered in an actuator development are **[COI14]**:

- Loss of the hydraulic power supply. There can be multiple root causes: pump failure, pipe disconnection or rupture…
- Malfunction of the hydraulic power supply. For example, an increase of pump internal leakage leading to a decrease in pressure supply.
- Loss of the electrical input signal (in case of FbW flight controls). This could be due to the loss of one Flight Control Processing (FCP) or a cable disconnection.
- Erroneous electrical input signal (if FbW), e.g. malfunction of the FCP.

[1] The terms probable, improbable, extremely improbable or frequent, reasonably probable, remote, extremely remote, and extremely improbable relate to probability objectives **[SAE96]**.

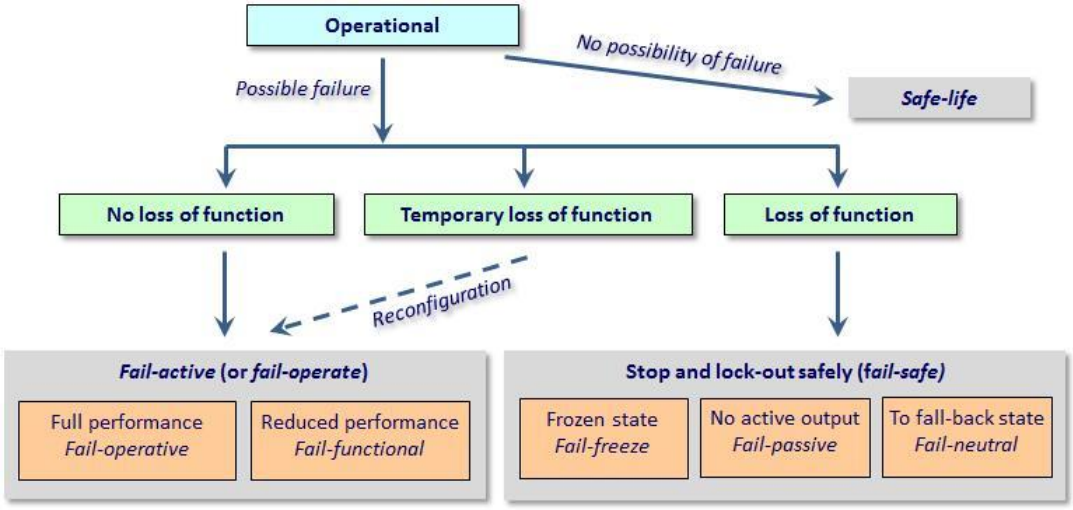

Figure 1.16 – System response to component failure [MAR16].

Figure 1.16 synthesizes the different manners in which a system can respond to a failure. Based on this terminology, actuator design shall be fail-active so the overall flight control system function is ensured. While satisfying this condition, redundant subsystems of the actuator can be fail-safe.

Once these generalities have been introduced, Figure 1.15 appears to be a simplification of the possible architecture for helicopter actuators. Redundancies are not represented: they include multiple interface and pilot stages, usually two (even three for the Bell 525 Relentless) power modulation stages and jacks. Passivation elements needed to avoid catastrophic response to failure are not shown either. The choice has been made to introduce such generic architecture so that each kind of actuator studied within the scope of this dissertation could fit to it. Specificities of each technology, mostly related to its response to failures, will be detailed in a dedicated part of this chapter.

2.4.2.2. Hydro-Mechanical Actuator

In conventional flight controls, pilot commands are transmitted to the actuators through a single path[2] of mechanical links (safe-life). The interface stage is thus usually a mechanical lever, the kinematic linkage of which corresponds to the pilot stage. Action on the lever induces a displacement of the control valve (power modulation stage) to feed the hydraulic cylinder.

Valve jamming is extremely remote, but not extremely improbable. Therefore, a back-up spool (usually a concentric second valve) is integrated on the power modulation stage. Also, the loss of one hydraulic circuit is an external event that shall be considered. Therefore, two segregated hydraulic circuits are usually implemented. The power modulation stage and the cylinder are thus duplicated. Should a hydraulic circuit loss occur, the cylinder concerned will respond in a fail-passive way. The

[2] Military helicopters can have two segregated paths of mechanical links in order to reduce the vulnerability to bullets. This is for example the case on the Sikorsky S-92.

second cylinder enables the actuator to remain fail-operative or fail-functional depending on the design choices.

Position control is mechanically realized by comparing the (transformed) pilot orders and the position of the moving part of the cylinder. This can be performed in two ways depending on the type of actuator integration: fixed or moving body (Figure 1.17).

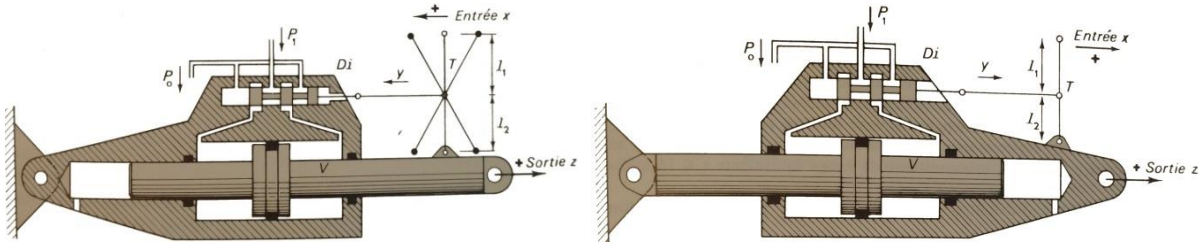

(a) Fixed body (b) Moving body

Figure 1.17 – Position control of a hydro-mechanical actuator adapted from [GUI72].

3. PROVIDE HELICOPTER CONTROL AND STABILIZATION – FBW FLIGHT CONTROLS

FbW flight controls correspond to a market demand, providing enhanced handling qualities and superior manoeuvrability **[MIL93]**. The FbW technology reduces friction and increases the sensitivity of flight controls, simplifies the integration and maintenance on aircraft and finally reduces vulnerability for military application **[GUI92]**. It consists of converting pilot commands into electronic signals and transmitting them to the actuators via the FCP.

Removing the mechanical links induces a global re-engineering of the helicopter's flight controls, from the pilot inputs to the actuators' flanges. The FCP needs to be highly reliable in order to compute the control of the flight – where the automatic pilot laws are integrated – and generate the actuator control signals. Due to this high level of reliability, more authority can be given to the flight control system. The integration of sensors in the pilot sticks and pedals could also facilitate the evolution of the cabin into a more ergonomic piloting environment – the mechanical implementation (routing and friction) no longer being a constraint.

At actuator level, new sensors are needed in order to close the control loop electrically. This has the significant advantage that these sensors can also be used to implement new functions – such as monitoring – without additional recurrent costs.

In contrast with all these advantages, FbW flight controls are more expensive than the conventional ones and induce new constraints: need of highly reliable electrical power at actuator level, resistance to electro-magnetic interferences, management of lightning protection, component obsolescence, to name but a few. The lack of redundancy on control surfaces on rotors combined with the harsh environment

(vibrations, high temperature, etc.) make the implementation of FbW more complex and more risky on helicopters than on fixed wings. This explains why commercial airplanes have integrated FbW flight controls since the late 1960s (Concorde) but only a single rotorcraft (NH90) has been produced in series with this technology since 2006.

The trade-off between mechanical and FbW flight controls reveals many advantages and disadvantages for both technologies. The chosen solution may differ from one helicopter to another, according to the customers' needs or the market target.

3.1. Capture Pilot Intentions on Control Axes

FbW flight controls do not necessarily modify the pilot's control interfaces: sticks and pedals can remain unchanged. However, new opportunities are introduced as sensitivity of command can be managed electrically. As an example, mini-sticks are tested in combination with FbW flight control systems **[SED89]** to improve piloting ergonomics.

Also, the removal of mechanical linkages enables the implementation of new flight control laws. One concrete example would be the advanced control laws in which pilot input (stick or pedal deflection) is directly translated into piloting objectives such as helicopter attitudes (e.g. pitch angle, bank angle, heading, etc.).

3.2. Transmit Pilots Orders to Main and Tail Rotors

Pilot intentions, once converted into electrical signals by means of the sensors, are transmitted to the FCPs. In case of conventional flight laws, the FCPs perform the same functions as conventional flight controls (control gain, mixing, coupling and phasing), as detailed in section 2.

Implementation of complex mechanical components such as phasing units is easily performed in an FCP: it is only a change of reference frame, i.e. a matrix. Therefore, the integration of the actuators around the main gear box is less constrained and weight can be minimized at system level with low implementation costs.

Particular attention is required when developing an FCP. It is indeed a key component of the flight control system as all orders transit through it. The right level of redundancy and dissimilarity has to be selected in order to meet the safety requirements of the entire flight control system.

3.3. Provide Stability & Control on Helicopter Axes

As detailed at the beginning of section 3, one of the main advantages of FbW flight control systems is the extremely high reliability of the FCPs. This allows implementing stabilization and control functions at any time of the flight and after any failure combination, occurrence of which is extremely improbable. Such new functions can be added at FCP level without the need of additional actuators.

Serial actuation (SEMA or ASE) is thus no longer required, which reduces weight and increases overall flight control system reliability. The parallel actuation (Trims) remains unchanged as there is still a need for moving the inceptors to provide information on the actuator position to the pilot in case of conventional sticks (it is no longer needed for mini-sticks).

3.4. Withstand Rotor Flight Loads – FbW Actuators

When the FbW flight control system is implemented, the actuator input is no longer mechanical but performed by electrical signals. Therefore, actuator control modules need to integrate interface stages able to receive these signals. The position closed loop requires position sensors at jack level. The control signal is generated by the Actuator Control Loop (ACL).

Initially, FbW actuators were developed for military needs – fighter aircraft, radar drives, guidance platform drives, controls for missile launchers and spaceships – using Electro-Hydraulic ServoValves (EHSV) as an interface between the signal and the hydraulic power domains: the control module. EHSV provides high power gains – on the order of 10^4 to 10^6 – with low command currents – less than ±40 mA for the industry and usually ±8 mA for aeronautic applications **[MAS78]**.

However, the use of the EHSV technology on helicopters is not trivial. Performances at low temperature, reliability in a vibrating environment, response to failure and hydraulic continuous power consumption are its main challenges.

With the arrival of the electrical power generation system on aircraft for many uses such as air conditioning, a new technology has become a reference in flight controls for piloting a jack: the Direct Drive Valve (DDV). The use of a DDV as a control module removes the drawbacks listed for the EHSV. On the other hand, it requires more electrical power: around 50 Watt in demanding configurations such as jamming issues.

These two technologies are described in this chapter as they represent opportunities for FbW flight controls on helicopters. Recommendations on their implementation perimeter are provided at the end of this part.

3.4.1. EHSV-Based Actuators

3.4.1.1. Control Module

The EHSV uses one or several motors (also referred to as coils by convention) as interface stage which receive a current as input. They act on a hydraulic potentiometer (pilot stage) that displaces the valve proportionally (power modulation stage). This combination of electric signal with a hydraulic potentiometer is at the origin of the term “electro-hydraulic” for the servovalves.

The embodiment of the pilot stage is usually realized using the Jet-Pipe technology for safety-critical applications such as primary flight controls because it is fail-safe in case of fluid pollution. However, the Nozzle-Flapper technology also exists and is widely used for industrial applications as it is less expensive than the Jet-Pipe technology. The Deviation-Jet technology is a variant to the Jet-Pipe technology. These three technologies are well described in the literature, e.g. **[ATT08]**.

A feedback loop inside the control module is mechanically and/or electrically implemented. Mechanical feedback usually consists in a spring that connects the armature of the hydraulic potentiometer to the main valve spool. On one side the current provides a torque via the coils, and on the other side the feedback spring generate a reaction torque proportional to the valve relative opening. Therefore, the feedback spring induces a mechanical control of the valve spool position to the input current. When electrical feedback is implemented (Figure 1.18), sensors are integrated at valve level to measure its position. A valve position (and optionally speed) control loop is implemented in the ACL. It is also possible to implement valve position sensors on an EHSV with mechanical feedback for monitoring purposes or for the static error correction of the valve position.

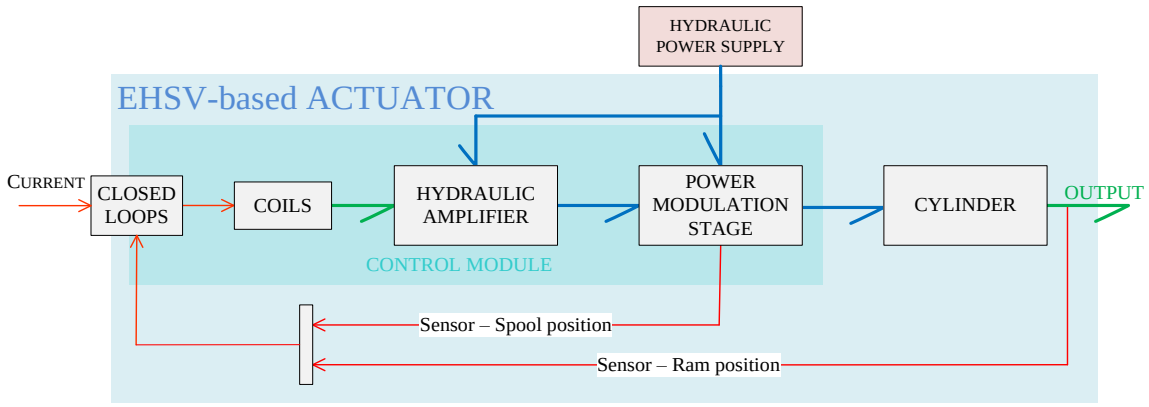

Figure 1.18 – EHSV based Actuator word Bond-graphs.

3.4.1.2. Actuator Architecture Driven by Response to Failure

EHSV is the reference technology for control modules of American FbW actuators in many developments: AH-64 **[OSD88]**, UH60 Blackhawk **[DON00]**, Sikorsky H92 **[BOC04]**, recently the Bell 525 Relentless **[KIM14]** or even the convertibles Bell-Boeing V22 **[STI04]** and Agusta-Westland AW609 (previously Bell-Agusta), which features the same architecture as the V22 for historical reasons.

The safety-critical aspect of the helicopter flight control system highly impacts actuator architectures in terms of redundancies and means to passivate failure **[MAR16]**. The EHSV-based reference architecture is detailed in the remainder of this section. Figure 1.19 is a representation of such architecture with two cylinders in parallel (most of US configurations). It is a simplified illustration of the H92 FbW actuators **[BOC04]**.

The EHSV-based reference architecture includes 2 (or even 3) segregated hydraulic circuits. Each of them supplies a control module that provides power to a cylinder. Both power outputs of the cylinder rod are mechanically linked by an attachment fitting, which adds up the forces.

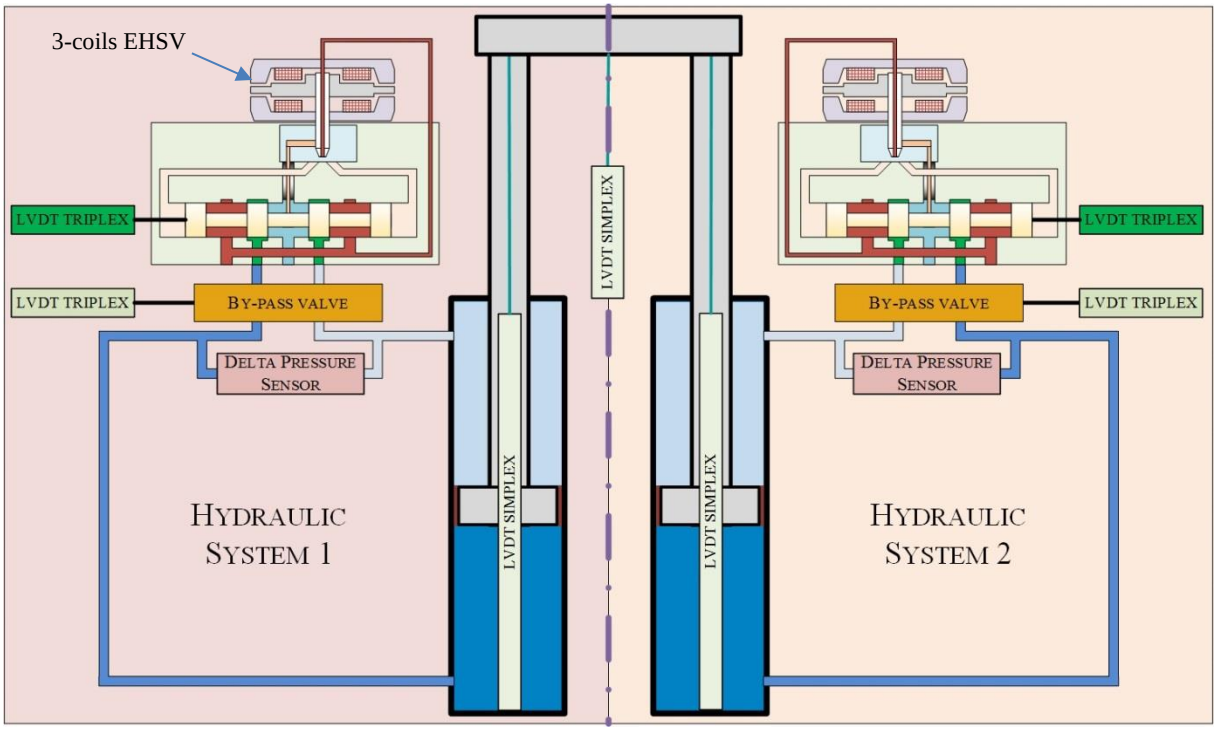

Figure 1.19 – EHSV based reference actuator.

Each control module includes a three-coil jet-pipe electro-hydraulic servovalve with mechanical feedback and sensors to monitor their main valve. Coil redundancy ensures that the generated torque remains sufficient (fail-operative) after the loss of one coil (or the loss of its command) and that degraded performances (fail-functional) after the loss of two coils remain acceptable. The three-coil design also enables the implementation of a monitoring strategy by comparison of the three currents. Finally, the risk of rupture of the feedback spring or valve jamming requires the addition of a by-pass valve between the control modules and the cylinders. The position of the by-pass is also monitored to prevent a dormant failure (jamming in open position). It is important to note that, unlike in hydro-mechanical actuators, the back-up spool solution to valve jamming is not implemented due to its integration complexity.

Pressure difference sensors are necessary to synchronise both servovalves. Both valves need to open at the same time, in the same proportion and in the same direction to avoid generating force-fighting at cylinder level.

This description is bottom-up, deducing the requirements from an existing design. However, the first designs were top-down approaches based on flight control system requirements and safety analysis support. It has been decided not to detail the safety analyses in this dissertation as they are realized by a

dedicated department at Airbus Helicopters. Candidate architectures shall meet the safety requirements. The aim is to ensure that single failure or failure combinations leading to the loss of the function are extremely improbable for safety-critical functions such as the flight control system. Tools such as Fault Tree Analysis (FTA) are used to validate this safety requirement.

3.4.1.3. Advantages and Disadvantages with Respect to Helicopter Application

Typically, the MIL-PRF-83282 can be used as hydraulic fluid for helicopters. Its operating temperature ranges from -40°C to +205°C **[SAE00]**. The associated variation of oil properties negatively impacts the actuator and hydraulic circuit sizing and, consequently, mass. Therefore, the embedded power system suffers severe environmental and power consumption constraints. Also, it is relevant to consider cost constraints in order to ensure economic viability of the product.

The advantages and disadvantages of the EHSV technology are multiple but it has been decided to focus on those who affect the three criteria listed above.

Main advantages selected:

1. Low electrical power consumption. For a typical servovalve used for aerospace application, a ±7.5 mA input current through a coil resistance of 400 Ω (the maximum electrical power is 22,5 mW) can control a flow of up to 150 L/min with a differential pressure of 200 Bar (the maximum hydraulic power is 50 kW). The hydraulic/electrical power ratio is 2.10^6 **[FAI83]**.
2. Low sensitivity to pollution of the power modulation stage. For a spool with a 4.62 mm diameter **[MOO87]** and a hydraulic power supply set at 206 Bar, the chip shear force – the capability to "cut" a particle blocking the valve – is up to 345 N.
3. Off-the-shelf parts. EHSV are well established as a reference component for aerospace and industrial actuators. The cost of off-the-shelf equipment is reduced compared to specific equipment.
4. EHSV with internal mechanical feedback requires only one ram position closed loop. This requires lower processing frequencies at ACL level in case of digital implementation.

Main drawbacks selected:

1. High hydraulic power consumption. Typically, the pilot stage consumes a permanent 0.5 L/min flow for a new EHSV and could reach 1.5 L/min at end of life. This corresponds to a power dissipation between 170 W and 500 W for a 206 Bar supply pressure. Considering two servovalves per actuator and four actuators per helicopter, power dissipation of the pilot stage can be up to 4 kW at helicopter level.
2. High sensitivity to fluid pollution of the pilot stage. In order to reduce the operating flow, pilot stages use very small hydraulic restrictions. These restrictions make the EHSV sensitive to fluid pollution. This effect is supposed to be minimized by the jet pipe technology, as it only introduces

a bias in the command and reduces performances instead of spool runaway of the main control valve.

3. Time for passivation (By-pass activation). Typically, the time needed for closing the by-pass valve is around 100 ms. The flight control system requires high actuator speed and bandwidth. Therefore, any transient position error of a helicopter's primary flight control actuator within this elapsed time is not acceptable.
4. Performances at low temperature. The performances of the pilot stage are highly dependent on the oil viscosity **[ATT08]**, which varies considerably with the temperature, by a factor of almost 3000 within the overall operating temperature range for the MIL-PRF-83282 **[COI16a]**.
5. Number of electrical input/outputs. The number of coils, position sensors and pressure sensors entails a high number of interfaces with the FCP. This constrains the number of inputs/outputs at computer level and the global weight of wires between the FCP and actuators.

These disadvantages are of primary importance for helicopter application. However, airplanes use EHSV for almost all control surfaces. The explanation lies in the airplanes' needs and design choices: EHSV first stage power dissipation has to be put in perspective with the global aircraft power generation; airplanes have control surface redundancy; their stability is better and allows more time for passivation; and finally, phosphate ester fluids used for commercial airplanes (e.g. Skydrol IV) are less viscous at low temperatures, which reduces the temperature-performance dependence.

3.4.2. Direct Drive Valve

3.4.2.1. Control Module

The Direct Drive Valve (DDV) technology is the FbW actuator architecture that seems closest to conventional hydro-mechanical actuators. It consists in using electrical motors (the interface stage) linked to the valve (the power modulation stage) for its command via a mechanical shaft (the pilot stage). The motors are thus mechanically connected to the main power valves. This is why the technology is called Direct Drive Valve technology.

A feedback loop, internal to the control module, is usually electrically implemented (Figure 1.20). Position sensors are integrated at valve or motor level to measure its position. Usually, valve opening and speed regulations are implemented in the ACL.

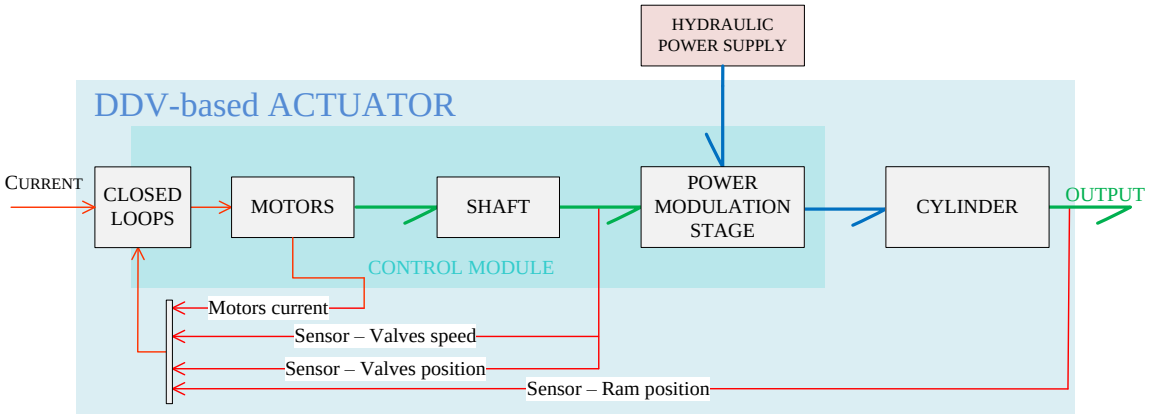

Figure 1.20 – DDV-based Actuator word Bond-graphs.

3.4.2.2. Actuator Architecture Driven by Response to Failure

This technology is already implemented on the Airbus Helicopters fleet for the NH90 electrohydraulic actuators. The NH90 is the only series-produced military helicopter with FbW flight controls being qualified based on the FAR 29 requirement **[FAA65]**.

The particular embodiment for NH90 actuators is presented in Figure 1.21. Four simplex[3] limited angle torque (LAT) motors are mounted on a single shaft with two rotary valves **[VID97]**. This shaft adds up the motors' torques (equality of speeds). Jamming of this shaft shall not occur as it is a common path for all commands and generates the opening of both valves. Therefore, many redundancies and passivation elements are introduced:

- Each motor rotor integrates a mechanical clutch (fail-passive). Declutching occurs when the resistant torque is greater than the maximum torque a motor can produce. Therefore, if one motor is jammed, only two motors are required to declutch it.
- Each power modulation stage includes a back-up spool (fail-functional).
- Clutches are also present on each position sensor of the valves (fail-passive).
- The shaft is guided by bearings with double load paths (fail-passive).

In terms of control, the motors' speed loops are implemented to get nominal performances after one motor jam and one motor loss. The angular position of the valve spool is measured with two duplex LVDTs and transmitted to the ACC[4] where spool position and speed (time derivated from position) closed loops are performed. Regarding the ram, a position control is implemented in the ACC with the signal provided by the rod internal quadruplex LVDT.

[3] Simplex motor means that the motor has only one electrical lane.
[4] On the NH90, FCP and ACL are two different computers. They are called Flight Control Computer (FCC) and Actuator Control Computer (ACC) respectively.

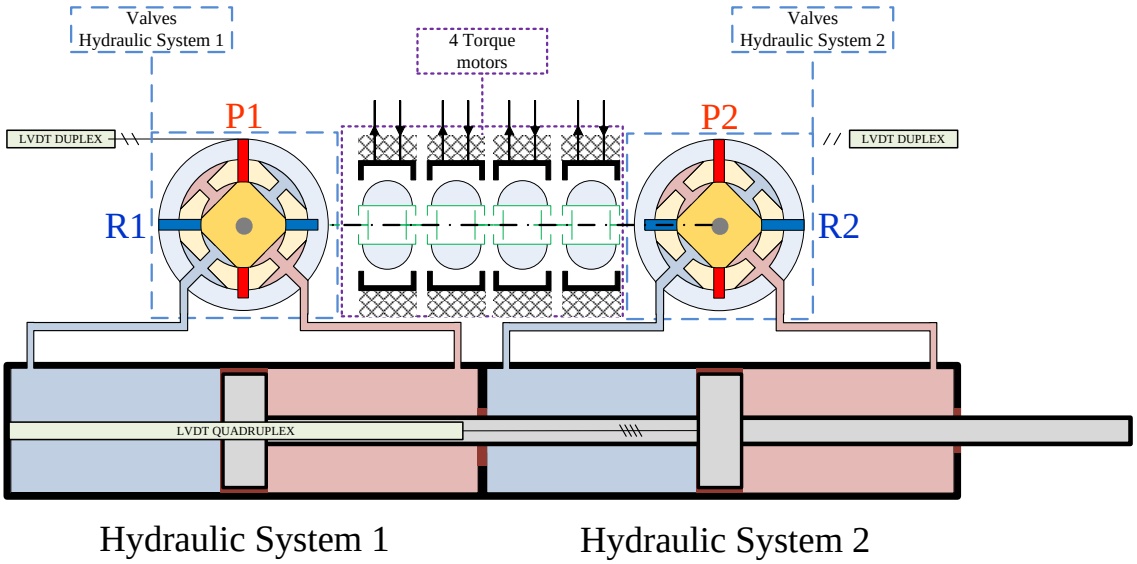

Figure 1.21 – NH90 Direct Drive Valve actuator.

The valves are mechanically synchronised by a precise positioning of the valves on the shaft to prevent force fight of the two actuator cylinders, as is the case for hydro-mechanical actuators.

3.4.2.3. Advantages and Disadvantages with Respect to Helicopter Application

With the same approach as for the EHSV, advantages and disadvantages of the DDV technology based on environmental, power consumption and cost constraints are listed in the following paragraph.

Main advantages selected:

1. Low transients after failure. The high stiffness and bandwidth of the motors' speed loop ensure a quick declutching in case of jamming.
2. Hydraulic and electric failure decoupling. The pilot stage (the shaft) is unique. This means that any interface stage can control both power modulation stages. For example, after a hydraulic circuit loss, the four motors still pilot – through the shaft – the valve associated with the remaining hydraulic power source. Also, such failure decoupling allows a take-off after the loss of one electrical lane as the three remaining motors can still pilot both main power valves.
3. No permanent operating flow and thus temperature-related performance of the pilot stage. The shaft drives the power modulation stages from the output of the interface stages. Such technical solution is almost insensitive to temperature variation and does not require any hydraulic supply.
4. Lighter technology. The weight of the motors is not in favour of the DDV solution, but as this technology does not need any further passivation components (e.g. by-pass valve) or pressure sensors, the global weight is lower than an EHSV-based actuator.

Main drawbacks selected:

1. Higher electrical consumption. Few amperes are needed for declutching. However, even if nominal power consumption is approximately 50 times smaller than declutching power, it is still 20 times higher than EHSV nominal power.
2. Control complexity inside the ACC. The DDV technology requires four control loops, as detailed in section 3.4.2.1. Each inner loop requires a higher bandwidth than the outer loop. Therefore, the current loops require several kilo-Hertz of bandwidth and thus an even higher sampling rate. Implementation of digital ACC becomes therefore more complex.

In addition to these points, Airbus Helicopters is familiar with this technology. A new development could be easier with a DDV-based actuator thanks to the experience acquired during NH90 development and service feedback. Benefits should be notable on development cost and schedule.

3.4.3. Technology Recommendation

In accordance with the arguments given above, this dissertation recommends using the DDV technology for primary flight control actuators on FbW helicopters for safety aspects, weight savings and performances at low temperatures[5]. Customer satisfaction is Airbus Helicopters' top priority and these points are all linked to this goal.

Nevertheless, the EHSV technology is well suited for functions with lower criticality. Secondary flight controls with low authority could be concerned. For a function on which failure is probable, the actuator architecture using a single hydraulic cylinder would be simplified and implementation with an EHSV-based control module would be easier.

[5] A safety-critical function, such as the flight control system, shall not be downsized.

4. FUTURE OF HELICOPTERS FLIGHT CONTROLS

It has been chosen to present a selection of previous and current works for their potential to improve helicopter flight controls.

4.1. FbW Retrofit – SIA

A recent technology – the Smart Interface Actuator (SIA) – has been recently patented **[GRO13]** and investigated by Pierre Estival within the scope of his PhD research **[EST15]** at Airbus Helicopters. The SIA is a position-controlled electro-mechanical actuator. It pilots the mechanical lever of a hydro-mechanical actuator which has its own mechanical position control loop.

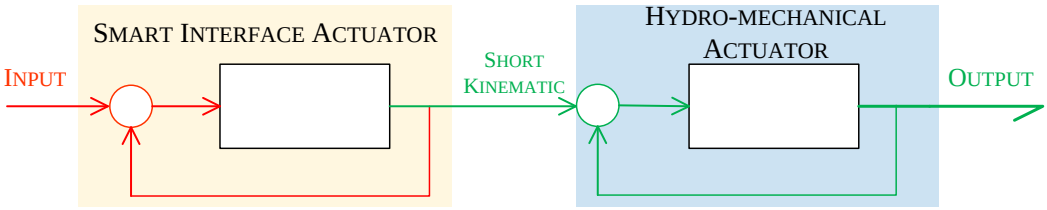

Figure 1.22 – SIA concept, in series with a conventional actuator.

This technology seems well suited for retrofitting conventional helicopters to equip them with FbW flight control systems. In fact, as the effort needed to move the input lever of a conventional actuator and the lever stroke are similar for all Airbus Helicopters fleet, only one SIA could be developed and fitted to the entire fleet retrofit. Helicopters with conventional flight controls could be upgraded with FbW flight controls at low development cost.

This technology suffers from a lack of maturity but could be very promising if efforts are made to develop a single SIA for the entire fleet.

4.2. Fly-by-Light

Information from pilot inceptors to FCPs and up to the FbW actuators is transmitted in the form of signals – which are represented by complete arrows in Figure 1.15, for example. The next evolution, which is already investigated at Airbus Helicopters Deutschland **[FOR88]** or on UH-60 **[STI04]** for example, could be to transmit this information using optical fibres.

The main advantage of Fly-by-Light (FbL) with respect to FbW is the electro-magnetic compatibility of the optical fibre, which is not the case for copper wire. The main drawback is that the conversion of optical information into electrical information is complex and induces a weight increase on the flight control system. Also, component dissimilarity required by safety requirements is hardly achievable making this technology not mature for aircraft flight controls.

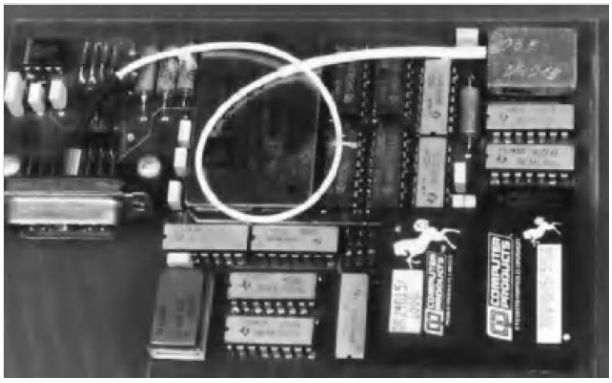

Figure 1.23 – Circuit element with optical interface copied from [HIR04].

4.3. Power-by-Wire

The tendency on fixed wings is to remove hydraulic circuits. Researches are to substitute hydraulically powerd actuators with Electro-Mechanical Actuators (EMAs) for primary flight controls. The term Power-by-Wire (PbW) is introduced as the power source becomes electric.

Although this technology is deployed daily on the airplane Boeing 787 Dreamliner **[KAS14]**, it is not set to appear soon on helicopters in serial production. The current design of PbW actuators is indeed not mature enough to face complex issues relative to rotorcraft in terms of safety and reliability (such as clutch reliability **[SEE12]**) or availability (e.g. excessive wear due to the aerodynamic loads in the HEAT program for the EH101 helicopter **[WRI99]**).

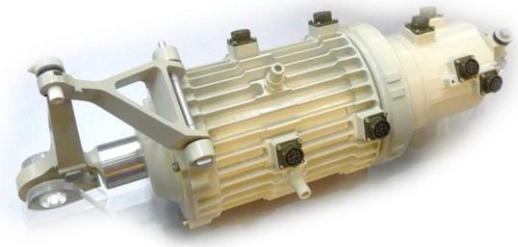

(a) HEAT EMA **[COI16b]**.

(b) 787 Dreamliner Spoiler EMA **[KAS14]**.

Figure 1.24 – Power-by-Wire actuators

4.4. Individual Blade Control

As detailed in paragraph 1.3, the main rotor actuators are usually placed in the fixed frame of the helicopter (on the upper deck) and the change of the incidence of the blades, which belong to the rotary frame is made possible by the swashplate. Current works investigate the substitution of this architecture. One candidate is the Individual Blade Control (IBC), where each main rotor blade incidence is piloted directly by an actuator. This technology requires high-performance actuators as each of them ensures the collective and cyclic (more constraining in terms of speed requirement) pitch. Research has been conducted on the UH-60 **[HAB02]** (Figure 1.25 – left) using electro-hydraulic actuators and then PbW actuators **[FUE07]**, and even recently on Agusta Westland's Project Zero **[GIA14]** (Figure 1.25 – right),

but the constraints imposed by the transmission of power from the fixed to the rotary frame seem to be difficult to overcome with today's technologies.

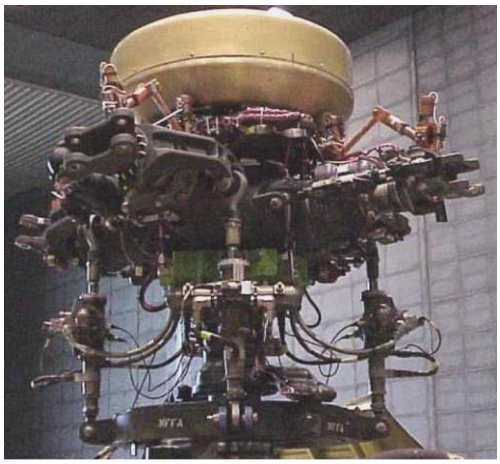

(a) IBC actuators on a UH-60 rotor head **[HAB02]**

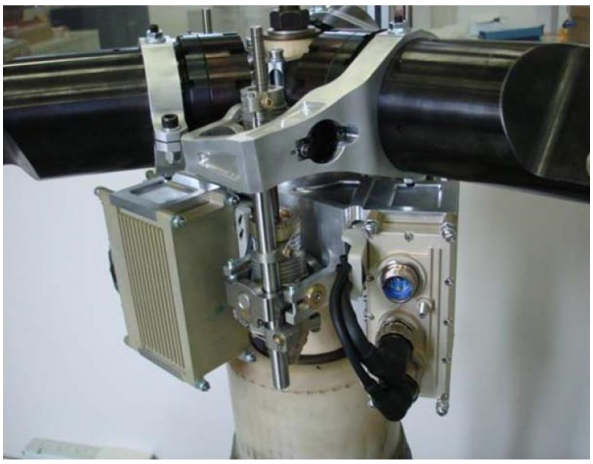

(b) IBC EMA on a Project Zero blade **[GIA14]**

Figure 1.25 – Individual blade control implementation

4.5. Dynamic Systems in Main Gear Box

As detailed in the Introduction, this dissertation argues for a new patented integration **[COI15a]** of the dynamic systems where actuators are placed inside the main gear box with the swashplate. Many advantages come with this new integration: the dynamic systems produce less aerodynamic drag and are protected from bird strike; new high-performance actuators with controlled leakage are introduced; oil is shared between actuators and the MGB, thus reducing the environmental impact of the system; all dynamic systems are lubricated, to name but a few.

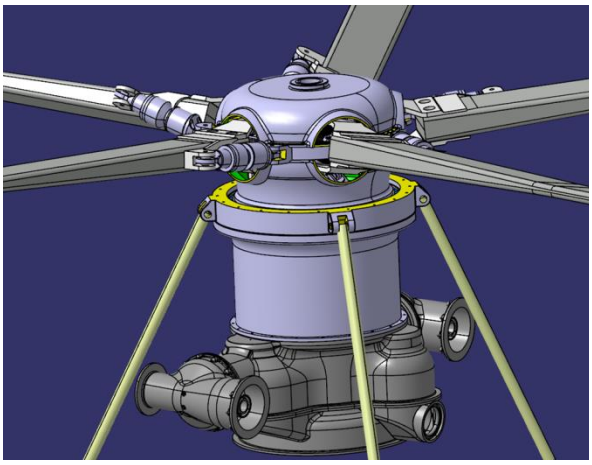

(a) Overview

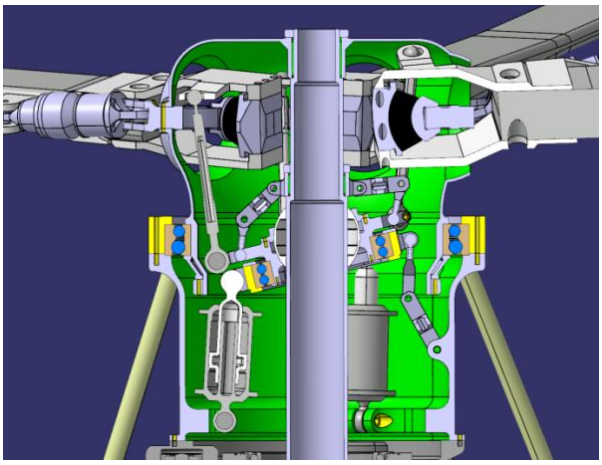

(b) Cross section

Figure 1.26 – Dynamic system in MGB principle [ETM14].

5. CONCLUSION

Helicopter flight controls have evolved incrementally from conventional designs, by progressively adding new functions and components. In contrast, the FbW technology induced a re-engineering of the flight control system architecture, as it required the current components to be replaced instead of simply being upgraded. However, both technologies meet the same main functions with different implementations that impact the level of safety associated to the fulfilment of each function.

Based on this observation, it has been decided to organize the presentation of the evolution of the flight control system in this dissertation by the function each subsystem is aimed to fulfil. A generic architecture and wording has been preferred for detailing the different technologies used for FbW actuators. The recommendation to use DDV for primary flight controls has been addressed and the opportunity to use EHSV for non-critical functions has been pointed out.

The next technological steps impacting the flight control system should be to keep increasing safety and reduce helicopter vibration for passengers' comfort. This should be made possible thanks to new architectures of the Actuation System such as the integration of dynamic systems inside the main gear box.

BIBLIOGRAPHY

[ATT08] ATTAR, B., *Modélisation Réaliste en Conditions Extrêmes des Servovalves Électrohydrauliques Utilisées pour le Guidage et la Navigation Aéronautique et Spatiale*. Toulouse, France, 2008. (in French)

[BOC04] BOCZAR, B. & HULL, B.J., *S-92 Fly-by-Wire Advanced Flight Control System*. AHS 60th Annual Forum, Baltimore, 2004.

[COI14] COÏC, C., ALLIETTA, J.-M., HENG, P. & BIHEL J.-R., *Q670A0901E01 - Requirement Specification for Main Rotor Actuator*. Airbus Helicopters, Marignane, France, 2014. (internal publication)

[COI15a] COÏC, C., BIHEL, J.-R., MARGER, T. & COUDERC, C., *Patent US2015298796 (A1) - Aircraft Hydraulic System Comprising at least one Servo-Control, and an associated Rotor and Aircraft*. Airbus Helicotpers, France, 2015.

[COI15b] COÏC, C. & HENG, P., *Rapport de Synthèse, Choix de Technologie Actionneurs*. Marignane, France, 2015. (internal publication in French)

[COI16a] COÏC, C. & MARÉ, J.-C., *Modeling and Pre-Sizing Process for Hydrostatic Thrust Bearing with Special Consideration to Performance Robustness within a Wide Temperature Range*, International Conference on Hydraulics and Pneumatics, Praha, Czech Republic, 2016.

[COI16b] COÏC, C., FU, J. & MARÉ, J.-C., *Bond Graphs Aided development of Mechanical Power Transmission for Aerospace Electromechanical Actuators*, International Conference on Bond Graph Modelling, Montréal, Canada, 2016.

[DON00] DONES, F., DRYFOOS, J.B., MCCORVEY, D.L. & HINDSON, W.S., *An Advanced Fly-by-Wire Flight Control System Designed for Airborne Research – Concept to Reality*. AHS 56th Annual Forum, Virginia, 2000.

[EAS07] EUROPEAN AVIATION SAFETY AGENCY, *Certification Specifications for Large Rotorcraft, CS-29*. Europe, 2007.

[EST15] ESTIVAL, P., *Concept Innovant d'Actionneur Électromécanique pour la Commande de Vol d'Hélicoptère de Nouvelle Génération*. Paris, France, 2015. (in French)

[ETM14] ETM, *Flight Controls Inside the Rotor Mast*. Airbus Helicopters, France, 2015. (internal publication)

[EUR04] EUROCOPTER, *AS 332/532 "Super Puma", Instruction Manual*. Marignane, France, 2004

[FAA08] FEDERAL AVIATION ADMINISTRATION, *Pilot's Handbook of Aeronautical Knowledge*. U.S. Department of Transportation, 2008.

[FAA12] FEDERAL AVIATION ADMINISTRATION, *Helicopter Flying Handbook*. U.S. Department of Transportation, 2012.

[FAA65] FEDERAL AVIATION ADMINISTRATION, *Federal Aviation Regulations, Part 29, Airworthiness Standards: Transport Category Rotorcraft*. U.S. Department of Transportation, 1965.

[FAI83] FAISANDIER, J., *Mécanismes hydrauliques.* Dunod, Paris, 1983. (in French)

[FOR88] FORMICA, B., KÖNIG, H., BENDER, K. & MANSFELD, G., *A Digital Optical Tail Rotor Control System*. 14th European Rotorcraft Forum, Milano, 1988.

[FUE07] FUERST, D., *Development, Prototype Production and Testing of an Electromechanical Actuator for a Swashplateless Primary and Individual Helicopter Blade Control System*. Aircraft System Technologies, Hamburg, 2007.

[GIA14] GIANFRANCESCHI, M., JACAZIO, G. & WANG, J., *High Bandwidth Electromechanical Actuator for Swashplateless Blade Control System*. International Conference on Recent Advances in Actuation Systems and Components, R3ASC14, Toulouse, France, 2014.

[GLA26] GLAUERT, H., *The Elements of Airfoil and Airscrew Theory*. Cambridge University Press, London, 1926.

[GRO13] GROHMANN, B., CHADUC, C. & TEMPIER C., *Patent US2013168501 (A1) – Primary Flight Controls*, EUROCOPTER, 2013.

[GUI72] GUILLON, M., *L'Asservissement Hydraulique et Élecrohydraulique, Tome 1, Théorie et technique*, Dunod, Paris, 1972. (in French)

[GUI92] GUILLON, M., *Commande et asservissement hydrauliques et électrohydrauliques.* Lavoisier, Paris, 1992. (in French)

[HAB02] HABER, A., JACKLIN, S.A. & DESIMONE, G., *Development, Manufacturing, and Component Testing of an Individual Blade Control System for a UH-60 Helicopter Rotor*. AHS Aerodynamics, Acoustics, and Test and Evaluation Technical Specialists Meeting, San Francisco, 2002.

[HIR04] HIRSCHEL, E.H., *Aeronautical Research in Germany, from Lilienthal until Today*. Springer, 2004.

[JAA99] JOINT AVIATION AUTHORITIES, *Joint Aviation Requirements, JAR-29, Large Rotorcraft*. Westward Digital Limited, United Kingdom 1926.

[KAS14] KASZYCKI, M. & PTACIN, R.R., *Boeing 787-8 Design, Certification, and Manufacturing Systems Review*. Boeing & FAA, 2014.

[KIM14] KIM, S., *The Bell 525 Relentless, The World's First "Next Generation" Fly-by-Wire Commercial Helicopter*. AHS 70th Annual Forum, Montréal, Canada, 2014.

[MAR16] MARÉ, J.-C., *Aerospace Actuators 1 : Needs, Reliability and Hydraulic Power Solutions*. Wiley-ISTE, 2016.

[MARG11] MARGER, T., *Valve Design of Hydro-Mechanical Servoactuator under Cost and Mixability Criteria*. Arts et Métiers ParisTech, 2011.

[MAS78] MASKREY, R.H. & THAYER, W.J., *A Brief History of Electrohydraulic Servomechanisms*. ASME Journal of Dynamic Systems Measurement and Control, 1978.

[MIL93] MILLER, F.G., *Direct Drive Control Valves and their Applications*. Proceedings of the Institution of Mechanical Engineers: Aerospace Hydraulics & Systems, London, 1993.

[MOO87] MOOG, *Type 30 Flow Control Servovalves. U.S.A., 1987.*

[OSD88] OSDER, S.S., *Digital Fly-by-Wire System for Advanced AH-64 Helicopters*. AIAA/IEEE 8th Digital Avionics Systems Conference, San Jose, 1988.

[SAE96] SOCIETY OF AUTOMOTIVE ENGINEERS, *ARP4761, Guidelines and Methods for Conducting the Safety Assessment Process on Civil Airborne Systems and Equipment*. U.S.A., 1996.

[SAE00] SOCIETY OF AUTOMOTIVE ENGINEERS, *AIR 1362 – Aerospace Hydraulic Fluids Physical Properties*. USA, 2000.

[SED89] SEDBON, G., *Aérospatiale flies faster Dauphin*. Flight International, 1989.

[SEE12] SEEMANN, S. & SCHLEGEL, C., *Modeling and Simulation of a Fault-Tolerant Electromechanical Actuation System for Helicopter Swashplates in Modelica*. International Conference on Recent Advances in Actuation Systems and Components, R3ASC12, Toulouse, France, 2012.

[SNC55] SOCIETE NATIONALE DES CONSTRUCTIONS AERONAUTIQUES DU SUD-EST, *SE.3130, Manuel d'instruction*. Marignane, France, 1955. (in French)

[SUD59] SUD-AVIATION, *SA.316, Manuel d'instruction*. Marignane, France, 1959. (in French)

[STI04] STILES, L.R., FREISNER, A.L., LANDIS, K.H. & KOTHMANN, B.D., *"Impossible to Resist", The Development of Rotorcraft Fly-by-Wire Technology*. AHS 60th Annual Forum, Baltimore, 2004.

[VID97] VIDAL, P.A., *NH 90 Helicopter Fly-by-Wire Flight Control System*. Eurocopter, AHS 53th Annual Forum, Virginia, 2000.

[WRI99] WRIGHT, P., *Helicopter Electro-mechanical Actuation Technology*. IEE Colloquium on Electrical Machines and Systems for the More Electric Aircraft, 1999.

Websites:

[webSITEC] www.sitec-aerospace.com/products/hydraulics.html, accessed on 22/07/2016.

CHAPITRE 2

MODELISATION ET SIMULATION DU SYSTEME D'ACTIONNEMENT

Ce chapitre introduit progressivement le besoin relatif à la modélisation de systèmes complexes ainsi que des notions sur les Bond-graphs afin de modéliser chaque composant relatif au système d'actionnement conformément `ce formalisme. Finalement, l'importance de la modélisation du système dans sa globalité est accentuée par quelques scénarios simulés cet effet.

Il convient de rappeler en prélude de ce chapitre un certain nombre de termes relatifs à la modélisation et simulation ainsi que quelques bonnes pratiques (non-exhaustives). La plupart de ces termes sont présentés et développés dans le livre de François E. Cellier **[CEL91]** et il conviendra de se référer à ce livre ou à la version anglaise de ce mémoire pour plus de détails.

Un modèle est une représentation d'un système, presque toujours simplifiée, réalisée dans le but d'obtenir des informations sur ce dernier. En disant cela, il est sous-entendu que l'utilisateur du modèle réalisera des essais sur celui-ci. Il est donc nécessaire de toujours associé à un modèle son domaine de validité.

Un modèle n'est pas exclusivement un ensemble d'équations intégrées dans un logiciel informatique. Un prototype physique d'un système pourra être appelé modèle même si cette appellation est peu employée. À l'inverse, un modèle informatique extrêmement détaillé se verra parfois appelé prototype virtuel afin de mettre l'accent sur sa représentativité.

La modélisation et la simulation d'un système lors de son cycle de vie sont aujourd'hui omniprésentes. La Figure 2.1 présente la place que prennent les modèles lors d'un développement de produit. Les modèles peuvent être utilisés dès la phase de spécification des exigences afin de s'assurer de leur cohérence et compatibilité, lors de la sélection de l'architecture, de la solution technologique, du dimensionnement ainsi que pour les essais unitaires et d'intégration système. Cette figure ne présente pas l'utilité de ces mêmes modèles lorsque le produit est en cours d'utilisation afin de recréer des phénomènes ou comportements observés, à moindre coût et de manière plus sûre. Aussi, nous pourrions citer l'utilisation de modèles complémentaire pour l'optimisation des flux de production de ce système : que ce soit pour la chaîne d'approvisionnement ou d'assemblage.

La version anglaise de ce chapitre détaille chacun de ces termes et essaye de les illustrer avec des exemples relatifs à l'hydraulique. Un ensemble des sources d'erreurs possibles liées à la modélisation et simulation y est aussi présentée.

Le développement d'un modèle doit être mené de la même manière que le développement de tout système. Pour cela, nous avons établi une liste de besoins relatifs au bon fonctionnement et au bon usage des modèles. Cette liste est volontairement scindée en deux grandes familles : les besoins « génériques » intrinsèques à l'ingénierie systèmes basée sur les modèles et les besoins « spécifiques » à l'industrie.

La suite de ce chapitre détaille les solutions choisies pour la modélisation sur la base de ces besoins. Les Bond-graphs sont particulièrement bien adaptés aux critères génériques de par : leur généricité multi-domaine, la représentation de phénomènes physiques facilement incrémentables, la formalisation de l'attribution de causalité si souhaité, etc.

Sur la base du formalisme Bond-graphs, la topologie des modèles est présentée de manière générique en insistant sur la lisibilité de ceux-ci. Pour ce faire, l'accent est porté sur la réticulation des modèles, la différentiation des domaines physiques par des couleurs et la mise en avant des flux de puissance principaux par rapport aux parasites. La Figure 2.4 contient l'ensemble de ces conventions retenues.

Les recherches dans le cadre de cette thèse ont aussi conduit à la standardisation des modèles Bond-graphs représentant le domaine mécanique. Cette standardisation a donné lieu à un article à la « Conférence Internationale sur la Modélisation Bond-graphs » (*International Conference on Bond-Graphs Modeling*) à Montréal en 2016 **[COI16b]**. Cette standardisation s'organise en deux sous-systèmes majeures : les corps (Figure 2.5) et les interfaces mécaniques (Figure 2.6), tous deux modélisés en translation et rotation. Les corps portent les éléments inertiels et s'interfacent avec les forces extérieures ainsi que les interfaces standardisées. Les interfaces standardisées permettent les mouvements relatifs entre corps et décomposent les efforts transmis en efforts normaux et tangentiels. L'interface standardisée se veut générique et donc certains éléments peuvent être supprimés si les effets modélisés ne sont pas souhaités. La généricité de cette standardisation est illustrée par la Figure 2.7, laquelle représente plusieurs liaisons mécaniques types en Bond-graphs s'inscrivant parfaitement dans le patron de l'interface standard.

L'application de l'ensemble des principes évoquées est portée sur la modélisation de système d'actionnement dans la troisième partie de ce chapitre (§2.3). Le modèle de fluide est détaillé, présentant les variables d'intérêt en fonction des phénomènes physiques modélisés, présents dans le formalisme Bond-graph. Ensuite, les composants et leurs modèles sont présentés un par un, en essayant de présenter l'état de l'art et justifiant les choix permettant de retenir une modélisation par composant.

Finalement, la quatrième partie de ce chapitre (§2.4) met en avant l'intérêt de la modélisation du système d'actionnement en présentant les variations de performance du système face à différents

scénarios des phénomènes relatifs aux charges antagonistes des actionneurs, la température de l'huile ou encore les possibles couplages entre plusieurs actionneurs dans un même circuit.

Le modèle d'actionnement complet a été grandement utilisé en entreprise pour le pré-dimensionnement du système d'actionnement d'un nouvel hélicoptère **[COI16c]**, ainsi que pour la modélisation sur simulateur de vol du système d'actionnement d'un hélicoptère existant.

CHAPTER 2:

ACTUATION SYSTEM MODELLING & SIMULATION

1. INTRODUCTION

In order to homogenize the wording, it has been decided to introduce the specific terminology for modelling and simulation in this section. Some terms have been defined in *Continuous System Modeling* by François E. Cellier **[CEL91]**. However, it makes sense to select short extracts from this book, complete them with new definitions and illustrate them with Actuation System examples to give the reader a better understanding.

Once the principal terms have been introduced, the role of modelling and simulation in a new development is presented. In contrast and to finish this introduction, it seems worthy to discuss the main errors that modelling and simulation can bring with it.

1.1. Modelling and Simulation Terminology

Marvin Minsky gives a definition of a model that includes, specific terms needed for modelling and simulation.

> *"A model (M) for a system (S) and an experiment (E) is anything to which E can be applied in order to answer questions about S."* **[MIN65]**

This definition of a model requires a clarification of the terms system and experiment.

1.1.1. System

The term *system* has already been used in this PhD dissertation as it is understood that a system is a set of elements. But even though the term is understandable, most people using it only consider a partial sense of it. The International Council on Systems Engineering (INCOSE) has the legitimacy to provide its own definition of a system:

> *"A system is a construct or collection of different elements that together produce results not obtainable by the elements alone. (…) The value added by the system as a whole, beyond that contributed independently by the parts, is primarily created by the relationship among the parts; that is, how they are interconnected."* **[REC00]**

Following this definition, a hydraulic cylinder includes, but is not limited to, a housing, a piston, a rod, seals and oil. Oil-filled chambers are delimited by the piston and the housing. Sealing devices

prevent the oil to communicate between chambers via the piston-housing clearance. Relative movement between piston and housing is possible. Therefore, the chambers' volume is not necessarily constant. Such relative movement creates an extension or retraction of the rod attached to the piston.

However, such definition does not explicitly include the possibility that a system could have interfaces with other systems. By experience, a good system development consists in first defining its boundaries and corresponding interfaces. In this example, the cylinder could exchange hydraulic power through its ports and provide mechanical power at its mechanical interfaces (housing or rod). Therefore, a more generic definition of a system, provided by Brian Gaines, is preferred.

> *"A system is characterized by the fact that we can say what belongs to it and what does not, and by the fact that we can specify how it interacts with its environment."* **[GAI79]**

The notion of synergy, the interaction between parts or subsystems inside a system, is unfortunately not explicit in Gaines definition. Without knowing the synergies inside a system, it is considered as a black box. Its interest is limited as no internal variable is accessible. It is thus proposed to combine both definitions and to redefine a system as follows: a system is characterized by the interactions with its interfaces and by its synergies between its elements. Both synergies and interactions at interfaces can be either functional or parasitic.

A last definition of a model is introduced by Bernard P. Zeigler and preferred by F.E. Cellier. It could appear quite abstract but receives its meaning in the context of system study and testing.

> *"A system is a potential source of data."* **[ZEI76]**

This sentence fits perfectly with the following definition of an experiment.

1.1.2. Experiment

François E. Cellier provides a definition of the term experiment that seems clear and complete. The term experiment is similar to the term test-case in the particular case of the Verification and Validation (V&V) process.

> *"An experiment is the process of extracting data from a system by exerting it through its inputs."* **[CEL91]**

To the previously defined cylinder, a control valve is added in such a way that its spool position modulates the hydraulic power transmitted to the cylinder chambers. This way, a hydraulic actuator is obtained. A possible experiment could be to position the actuator on a test bench, connected to a hydraulic power supply and without attaching the rod. By piloting a maximum opening of the valve, the

no-load maximum speed[6] of the actuator (for a given pressure supply) would be extracted from this experiment.

It appears relevant to emphasize that this definition does not make any particular reference to the nature of the system or the nature of the experiment.

This definition also allows introducing the terms "controllable" and "observable", which are potential properties of a system. Referring to the system as a source of data implies that it is possible to act on it (through its inputs) and to measure some variables (through its outputs). Selecting the variables that are measured could impact the observability and controllability of variables **[PRU70]** or **[GIL92]**.

1.1.3. Model

Marvin Minsky's definition of a model quoted at the beginning of this chapter should now make more sense. A model of a system is a representation of this system, created by a model architect, in order to process experiments on it. This definition has strong consequences. It implies that the model is sufficiently detailed and correctly implemented, based on the desired experiments so it can be used as a substitution of the real system. This is indeed the correct way to model a system. The model user (who may differ from the model architect) has to keep in mind that models are developed for a certain set of experiments and adding an extra experiment may not be relevant if the model is not adapted. The set of experiments is called the "experimental frame" by Bernard P. Zeigler **[ZEI76]**. The experimental frame shall be accessible from the model to prevent misuse.

A model is a representation of a system and can be of different natures: hardware, software, graphical scheme, etc. In order to be more explicit, it has been decided herein to introduce two subgroups of models: virtual and physical models. The term virtual model is used for software models intended for simulation, whereas hardware models are called physical models. In this PhD dissertation, these terms are preferred as far as possible, as they provide additional information on the model type. Therefore, a Bond-graph model of a hydraulic actuator can be called a virtual model, while a manufactured actuator is a physical model.

1.1.4. Simulation

Granino Korn and John Wait define a simulation using the terms defined above.

"A simulation is an experiment performed on a model." **[KOR78]**

[6] The no-load maximum speed is a characterising value of an actuator.

It is therefore a general term, not only for computer simulation of a mathematical model. As for models, the context should provide the information.

In engineering developments where a system includes both hardware and control, the terms Model In the Loop (MIL), Software In the Loop (SIL) and Hardware In the Loop (HIL[7]) are used to precise which real and simulated parts are combined during simulation. MIL refers to computer simulation of virtual models that include both a multi-physics system and an associated controller. SIL consists in generating the real code of the control loop and implementing it in a Real Time platform coupled with the virtual model of the multi-physics system. Finally, HIL implies that physical models are used coupled with virtual models.

1.2. Role of Modelling and Simulation in a New Development

Models and their simulations are widely used for new developments. The RFLP (Requirement, Function, Logical solution element and Physical element) diagram presented in Figure 2.1, based on the VDI 2206 standard **[VDI04]**, shows the importance of modelling in the design process. Modelling and simulation are used in the design phase – the requirement definition and validation, the study of candidate architectures and solution selection, the solution definition and design – and in the verification phase – virtual unitary and integration tests. Virtual verification enables detecting non-compliance with the specification early in the development and at low cost. The modelling and simulation cycle is indeed much faster than the manufacturing and testing cycle.

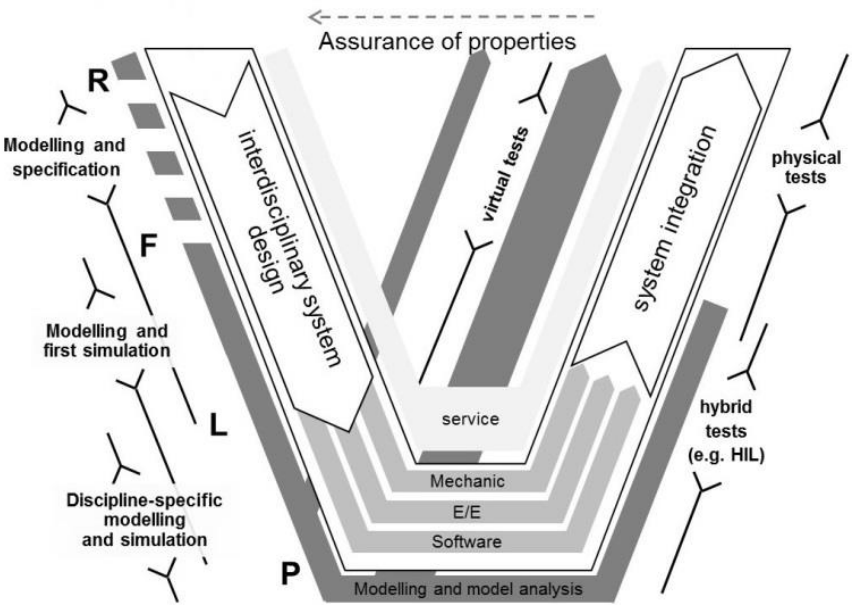

Figure 2.1 – The place of modelling in a new development [EIG12].

[7] HIL might also mean "Human In the Loop". However, this meaning is not used in this dissertation.

In the descending part of the double V-cycle, the model becomes more and more detailed and, simultaneously, the complexity usually increases. At the beginning of ascending part, the test environment shall be ideal for characterizing the tested subsystem only, without coupling it with the real environment. As the integration advances, the test environment realism increases to allow for a better assessment of the entire system behaviour.

Therefore, the required models could be different for each phase of the RFLP process even if the modelled system remains unchanged. This could be a cause of error in modelling and simulation practices, but it is not the only one. It seems important to list the major errors that modelling and simulation can bring with it if no particular care is taken.

1.3. Modelling and Simulation Errors

Virtual model simulation can support the development of new complex systems. It is a tool that enables the prediction of the system's behaviour. However, it must be kept in mind that the results obtained always contain errors. These have to be defined and understood so that the model architect can contain them and keep the simulation error at an acceptable level. Main errors come from:

- **Model representativeness.** The virtual model of a system shall represent the relevant phenomena of this system. However, it cannot reproduce the complete system. There are always more external interactions and synergies than those that are modelled. For example, in fluid power modelling, it is not usual to define the movement of each fluid particle but rather to define volumes with the associated behaviour. Therefore, the molecular flow pattern on a porous filter is not modelled in fluid power modelling. It is often a choice not to model certain phenomena. When a load of several thousand newtons is applied to an actuator, maybe the gravity can be neglected. The model architect shall ensure that the virtual model realized is representative of the experiments to be simulated on it (each relevant phenomenon is present and correctly implemented). On his side, the model user shall only run simulations for which the virtual model has been conceived.
- **Data correctness.** It could appear obvious that the data used for the virtual model shall be entered correctly. However, many errors at first simulations come from data provided with wrong units, sign convention errors or erroneous initialization of state variables, etc.
- **Numerical robustness.** Virtual models usually include state variables (if not, a virtual model may not be needed but an algebraic model may be sufficient). A solver is used for the integration of the state variables. The choice of the solver and the associated step size determines the numerical stability and robustness of the simulation. For example, a stiff variable step solver would be preferred for hydraulic systems due to high frequency modes (letting little space for numerical error), whereas for Real Time simulation a fixed step solver is required (the step size shall be chosen with caution).

- **Observation errors.** It is common to plot simulation results. Caution should be exercised as plots only present partial information (e.g. aliasing effect affecting sampled data). Also, solvers calculate a finite number of points. Interpolations are performed between points in order to smooth the shape of the plot. The model user has to ensure that these interpolations are legitimate.
- **Software constraints.** Implementing a model in a software usually adds new constraints imposed by software limitations. For example, generic models can require parameter values that are unknown at this step of the development. Also, if the software is causal, it may require the addition of elements for model interfacing even if the model architect would have neglected their effects, e.g. a capacitance between two resistances or inertia between two compliances. These constraints tend to decrease with software improvement: basic elements are usually available and combined with hierarchical modelling; acausal languages such as Modelica are more and more used; tearing is a solution for solving algebraic loops…

These sources of error are similar when dealing with physical models. The experimental frame shall be defined. When testing a hydraulic actuator physical model, examples of each listed item could be:

- Model representativeness: either if the physical model is complete and in final configuration for the desired experimental frame, or the representativeness of its interfaces including the environment (loads, vibration, temperature, etc.), the power supply (hydraulic pump, etc.), etc.
- Data correctness: is the manufacturing of the actuator within its tolerances? Is the nominal pressure of the hydraulic power source well set?
- Numerical robustness: in case of electronic hardware or HIL testing, errors can arise from numerical integrations.
- Observation errors: for physical models, this could be for example sensor linearity, accuracy or error and dynamics.
- Software constraints: software is usually needed for HIL such as SIMULINK© for control design and ControlDesk© for the Human Machine Interface (HMI).

In order to reduce possible representativeness errors, modelling needs are established. Model architecting and development shall focus on meeting these needs.

2. MODEL ARCHITECTURE

Model architecture is probably the key for success in a virtual model development. It provides a common structure to the models, leaving less room for the errors listed above.

This PhD dissertation first details the main modelling needs that have been identified by experience and then the recommendations that can be derived from these needs. Bond-graphs are selected as a modelling language and are thus introduced here. The main principles presented in this section are

already available in **[COI16b]**. In this paper, we detailed the development of a nut-screw for aerospace EMA[8] based on the engineering needs. In contrast, examples provided in this dissertation are more oriented towards electro-hydraulic actuators. Also, modelling fluid power and electrical domains with Bond-graphs is covered in this section.

2.1. Selected Modelling Needs

In order to focus on the engineering needs, engineering and industrial requirements are listed in this section. It has been chosen to separate both kinds of requirements as the first kind involves good practices that fit to the System Engineering process while the second kind could vary from one company to another.

2.1.1. Engineering Requirements for Model Development

With reference to **[MAR16]**, engineering requirements have been identified and are listed below. In addition to this communication, it has been decided herein to provide the rationale associated with each requirement so that the applicability can be discussed for each new development.

R1 Realism. The model architecture shall enable incremental modelling to progressively increase realism regarding the key physical effects that impact performance. Models are a part of any step of a complete development process, as detailed in section 1.2 and shown for RFLP in Figure 2.1. However, the representativeness of the model can vary during the process depending on its aim.

R2 Genericity. As far as possible, the model shall be made up of a combination of generic sub-models that can be re-used for other modelling purposes. This facilitates comprehension and maintenance of the model (or library of models).

R3 Interfacing. The model shall have standard interfaces that are conserved throughout all modelling levels. Defining standardized interfaces ensures the model's connectivity and replaceability.

R4 Balancing. The model shall be balanced (mechanically, energetically, etc.). This reduces the number of result misinterpretations by reproducing, for example, action and reaction forces (mechanical balance). When thermal balance plays a key role in a system sizing, it is of particular interest to address thermal power flows (energetic balance).

R5 Ageing and faults. The model shall enable ageing effects or faults to be simulated. This allows representing the system's behaviour over its entire lifespan as well as its response to faults. Transients after a failure and degraded performance are usually sizing parameters for helicopter actuators.

[8] Electro-Mechanical Actuators are introduced in Chapter 1 section 4.3, which is dedicated to PbW flight controls.

R6 Causality. The model shall be developed to admit various causalities. For example, inverse simulation is of great help for system sizing and integral causality on storage elements is preferred for model simulation.

2.1.2. Industrial Requirements for Model Development

In addition to the engineering needs, industrial needs are defined. The industrial requirements listed below are specific to this work and to the fact that the modelled system (the actuation system in our case) is, indeed, a contributor to the global function performed by the Flight Control System. The flight control system is modelled by another engineering team, using a simplified Actuation System model. As both models are intended to interact, the simplified Actuation System model can be replaced by the one developed within the scope of this PhD research.

R7 Workshare. The model shall correspond to the industrial workshare. The global interfaces of the model shall thus be the real physical interfaces of the system as defined by the responsible Airbus Helicopters department.

R8 Engineering. Model parameters shall be those which engineers are able to provide. They could be specific to industrial experience or come from datasheet.

R9 Units. The data units provided to and extracted from the model parameters shall be the industrial units.

R10 Export. The model shall have export capability to be interfaced with other models within the interfacing standard of Airbus Helicopters.

R11 Documentation. The model shall include the information needed for its use and development, including test cases.

R12 Capitalization. The model shall be a tool that facilitates further developments, easy to use by simulation non-experts.

The last requirement needs to be detailed. It makes sense that a model is developed not only for the model architect but for use by interested colleagues inside the company. They may not be familiar with the overall system modelled and the complexity of the simulation environment shall be adapted accordingly. However, these users shall be aware of simulation and the associated risks.

It is important to note that requirement R9 is not incompatible with using international system units for calculation, which is a good basis to avoid errors in equations. Requirements R10 and R11 contribute to requirement R12.

2.2. Bond-graph Formalism

As detailed in the first chapter, recent Flight Control System of helicopters involves many physical domains including: mechanics, fluid power, electromagnetics and heat transfer. Bond-graphs are well suited for dealing with multi-physical domain modelling and are thus used for modelling purpose in this thesis.

The Bond-graph formalism is well established and presented in many books such as **[THO75]**, **[DAU00]**, **[BOR10]** and **[KAR12]**. Therefore, this simple introduction to Bond-graphs presents only the basic concept and elements.

Bond-graphs allow having a uniform terminology and graphical representation for all physical domains (requirement R2). Each bond, represented by a half-arrow, associates an effort (e) and a flow (f) variable, the product of which corresponds to the transmitted power (an exception is made for pseudo Bond-graphs). By convention, the flow variable is on the half arrow side of the bond and the effort variable on the other side. The time integral of the effort is the momentum (p), while the time integral of flow is the displacement (q). Bond-graphs emphasize the nature of the physical phenomena a system can contain. Therefore, dissipative, capacitive and inertial effects are modelled using R, C or I elements respectively. The relation between these elements is usually represented by a tetrahedron **[PAY61]** or a carousel **[THO75]**. Figure 2.2 shows the carousel with both integral and derivative links between the variables and the effects. It represents the possible transfer of energy in a free system (without interfaces).

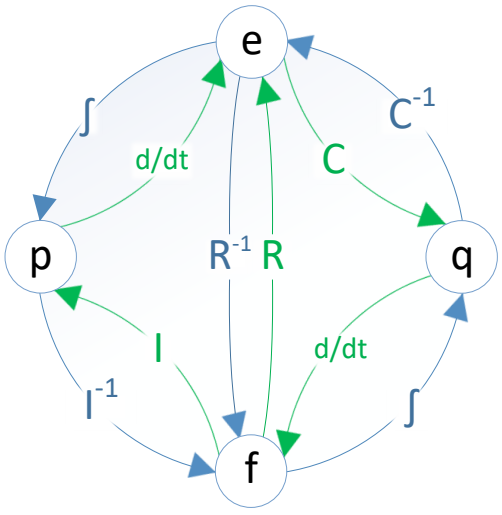

Figure 2.2 – Bond-graph carousel.

In order to show the multi-disciplinarity of the Bond-graphs, these examples make use of the three R, C and I elements in three different physical domains. However, it is important to emphasize that these three phenomena can be present in each physical domain.

1 In the linear mechanical domain, the flow and effort variables are, respectively, linear speed *v* and force *F*, the inertia is mass *m*. Newton's second law can be obtained with the Bond-graph carousel: the force (effort) is equal to the derivative of the momentum, which can be calculated by multiplying the mass (inertia) and the speed (flow).
2 In the electrical domain, the flow and effort variables are, respectively, current *i* and voltage *U*. The constitutive law of a capacitor can be found as follows: the current (flow) is the derivative of the charge (displacement), which is equal to the voltage (effort) times the capacitance.
3 In the hydraulic domain, the flow and effort variables are, respectively, volume flow rate Q and pressure drop P. Pressure losses in a hydraulic restriction are resistive functions of the flow rate.

The carousel can thus be read through the derivative form (green, usual formulation of the equation) or integral form (blue, preferred way for implementation on computers). The last example shows that elements can be either linear (e.g. laminar flow) or non-linear (e.g. turbulent flow).

In addition to the carousel elements, two junctions model the Kirchhoff laws: the 0 junction for flow summing (i.e. current law in electrical domain) and the 1 junction for effort summing (i.e. voltage law in electrical domain). Effort and flow sources are symbolized by Se or Sf elements. Transformers (TF) and Gyrators (GY) are two-port components that conserve power and are reversible. Transformers provide a proportional relation between both efforts and both flows of the two-ports. Gyrators provide a proportional relation between the effort of one bond and the flow of the other one.

It is important to note that the characteristics of the Bond-graph elements can be modulated. In that case, an "M" is added at the beginning of the element to indicate this modulation. For example, a variable restriction in fluid power is represented by an MR element. Caution should be exercised when modulating elements which store energy, as the energy conservation law may not be satisfied. This has been shown by Serge Scavarda in **[DAU00]** or by Belkacem Ould Bouamama and Geneviève Dauphin-Tangy in **[OUL06]**.

In the Bond-graph formalism, in contrast to half arrows (bonds) that transmit power, complete arrows stand for signals. Causality provides the "cause-to-effect" relation for mathematical calculation of the modelled phenomena. Causality can be represented on bonds by a line, perpendicular to the bond, on the side of the element that imposes the flow and receives the effort. For special uses, such as model inversion **[MARQ11]**, elements can provide both effort and flux: this is called bi-causality. It is represented by a bi-causal line which consists indeed of two causal half-lines. Figure 2.3 shows the different arrows and causalities involved in our Bond-graph models.

(a) – Signal arrow (b) – Acausal bond (c) – Causal bonds (d) – Bi-causal bonds

Figure 2.3 – Different arrows and causalities involved in our models.

The Bond-graph formalism is independent of the software implementation. To name but a few, models detailed in this chapter could either be simulated on:

- Bond-graph software such as 20-SIM©, **[web20Sim]**
- a C++ code,
- causal software with signal representation of the model such as MATLAB©/SIMULINK©, **[webMAT]**
- causal software with power representation of the model such as AMESim©, **[webAME]**
- acausal software with power representation of the model such as DYMOLA©. **[webDYM]**[9]

This fact promotes the use of Bond-graph for modelling purposes as the model remains independent of simulation software (requirement R12). Of course an adaptation is needed, but the desired physical effects modelled are preserved.

It is important to emphasize that Bond-graphs can be used for several purposes, such as defining the causal paths on a model **[DAU00]**, studying the main natural frequencies **[THO99]**, evaluating the detectability of faults and where to place new sensors for isolation of such faults **[BOR11]**, etc. However, in this PhD dissertation, Bond-graphs are mainly used to structure the models, define standard interfaces and ensure that the model parameters are those used by engineers or provided in datasheets. These other assets of Bond-graphs are thus left as perspectives to this work.

2.3. Proposed Concepts Defined by Modelling Needs

2.3.1. Model Readability Improvement

As suggested in **[KAR06]** and in agreement with the author's experience, model readability is increased when the functional power flow is emphasized, e.g. by bolding the relevant power bonds. This also helps highlighting the parasitic effects that are considered.

Optional power paths or elements are differentiated by dotted bonds **[COI16b]**. This provides the model architect with a better view of model realism improvements (requirement R1).

Finally, physical domains are associated to colours. Most simulation software already uses a colour code for the domain but it is not unified. In this dissertation, it has been decided to use the following

[9] It is also possible to use the BondLib 3.0 Modelica library **[CEL13]** on Dymola© for Bond-graph simulation.

colours and domains: green for the mechanical domain, blue for hydraulics, purple for the electrical domain and brown for the thermal domain.

2.3.2. Model Topology

As far as possible, it is interesting to make the model's architecture consistent with the topology of the system to be simulated. This approach, proposed in **[MAR12]**, is extended to our work. It facilitates the model decomposition into generic submodels (requirement R2) which can have several levels of detail (requirement R1).

For example, a Direct Drive Valve control module has two mechanical degrees of freedom: the axis of translation of the housing and the axis of rotation of the shaft, both in-lined. A word Bond-graph of such a DDV is presented in Figure 2.4. The control module has been decomposed, from a mechanical point of view, into bodies (the housing, the rotor and the rod) that are interconnected by joints (cylinder pair and hinge that are not represented in the cross view for readability) and power transformations (electric motors, valves).

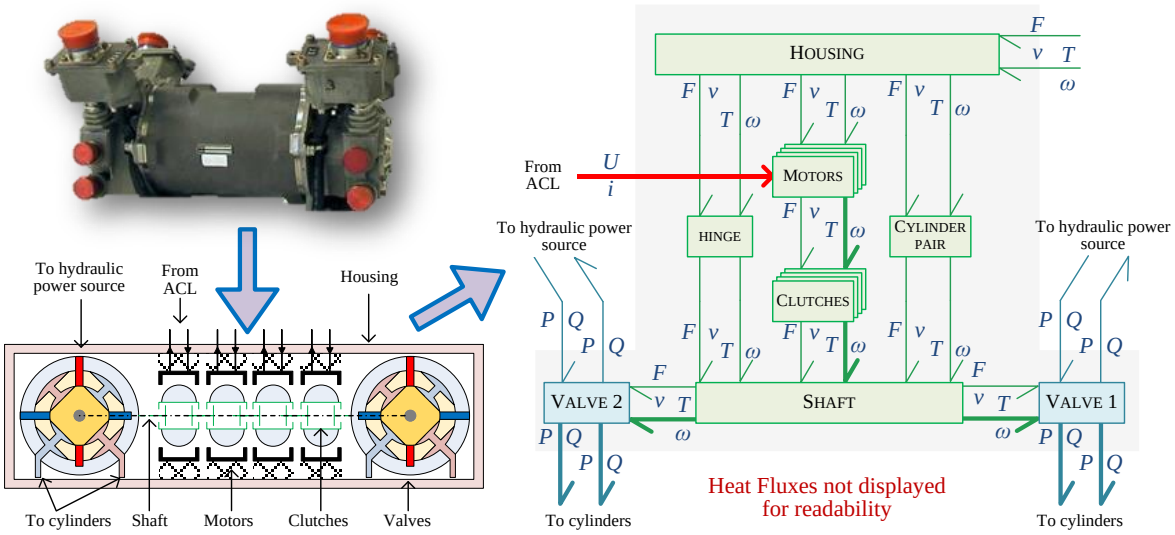

Figure 2.4 – Linking the model architecture to the system topology.

Note 2.1: The pair of variables P / Q and F / v, already introduced previously, are respectively the effort and flow variables of the hydraulic and linear mechanical domains. In addition, U / i and T / ω are the variables from the electrical and rotational mechanical domains.

It has been decided to emphasize the functional power flow from a control point of view, i.e. from the ACL command to the hydraulic flow towards the cylinder chambers. This is not the only possibility. For example, once this model has been interfaced with the cylinder model, it could be interesting to follow the fluid power path to evaluate the consumption of the hydraulic power network.

2.3.3. Mechanical Balance

In the former example, both rotation and translation along the same axis are involved. Mechanical balance (requirement R4) is thus reached by modelling each sub-model with mechanical quadriports (linear and rotational power bonds for each body or interface). Indeed, to reach mechanical balance, the number of ports should be an even number to reproduce action and reaction forces. In our application, it is sufficient to consider one linear and one rotation axes, therefore four ports are needed. A particular focus is laid on modelling mechanical elements in section 2.4, taking into account the quadriports concept.

2.3.4. Energy Balance

As thermal balance plays a key role in the sizing and lifespan of a DDV's motors, it is of particular importance to enable the designers to address not only mechanical but also thermal power flows. For this purpose, any energy loss (R element) is transformed into an RS field in order to output the heat power $\mathcal{P}_h$ that is generated by the loss effect (e.g. friction or even structural damping for mechanics). As a very beneficial effect for embedded systems operating over a wide temperature range, using a pseudo thermal bond enables the loss effect to be made sensitive to the temperature prevailing at the thermal bond (e.g. influence of temperature on wire resistance and on friction). The objective of getting energy-balanced models (requirement R4) has been applied to the following models unless it is explicitly mentioned. However, for reasons of readability, thermal bonds are not represented except for direct thermal coupling.

2.3.5. Fault Injection

During the development of safety-critical applications, it is important to assess the fault-to-failure mechanism and the response to faults in case of progressive or sudden degradation. Simulation is generally the only way to investigate the response to faults without danger (requirement R5). It is also helpful for assessing fault signature and detectability during the design of health and usage monitoring (HUM) features. In FbW systems, these features can be implemented at low cost thanks to the availability of numerous sensor signals.

In the case of Figure 2.4, the model must be increased with fault triggering inputs to force either progressive degradations (e.g. through real signals) or sudden faults (e.g. through Boolean inputs), as suggested in **[LIN14]**. This is addressed in the following sections, dedicated to each domain modelling.

2.4. Proposed Standardization of the Mechanical Domain

When progressing from the preliminary to the detailed design phases, model complexity increases versus realism. In this dissertation, standardized mechanical components are proposed to ensure

modularity and to simplify the model's interfacing. It is proposed herein to split the mechanical power transmission into two main classes: bodies and interfaces. The body is assumed to be infinitely rigid. It can be either a single solid or and assembly of solids. The interfaces can be either functional (e.g. joints, motion transformations) or parasitic (e.g. compliance).

This proposed standardization on mechanical Bond-graph models was presented, as part of an article **[COI16b]**, at the *International Conference on Bond-Graphs Modeling* in Montréal, 2016. At this conference, the aim was to submit the proposed standardization to both Bond-graph and simulation experts.

2.4.1. Standardized Mechanical Body

The standardized mechanical body shall include standard interfaces (requirement R3). Based on previous discussions, the components are modelled as mechanical multi-ports. The proposed standardized mechanical body thus includes two 1 junctions (rotation and translation) in the absolute reference frame. To the sum of these efforts can be added, if relevant and of interest: the inertia (J in the rotational domain), any other external torques or forces (with subscript *ext* – e.g. airload or gravity force) and interfaces (e.g. with other mechanical solids or transformations to other physical domains like fluid power, or electromagnetics). According to a standard vision, it is important to allow the user to select the right level of modelling as well as the number of interfaces.

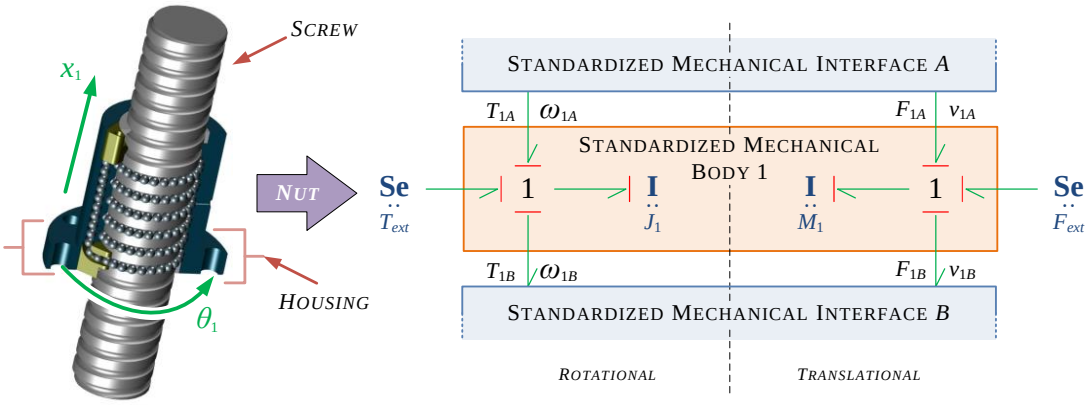

Figure 2.5 – Standardized mechanical body with preferred causalities at interfaces [COI16b].

Figure 2.5 shows the representation of a nut from a nut-screw[10] (3D-view from **[webBAR]**) with a standardized mechanical body. It has two degrees of freedom: the translation in and the rotation around the screw axis. In this case, it is connected to two standardized mechanical interfaces (presented below).

[10] The study of a nut-screw is at the origin of both the standardized mechanical body and interfaces. Therefore, this dissertation uses the nut-screw to illustrate these standardized components, but they fit with all mechanical parts.

Interfaces *A* and *B* model its interfaces with the screw and with a schematic housing impeding translational motion.

The choice of causality for simulation purpose is direct if the model architect decides to consider component inertia. Otherwise, the model architect should define the causality in order to meet the modularity requirement, as far as possible. This means that the causality on the interfaces should remain unchanged. For example, in inverse simulation (requirement R6), a flow (speed) source can be added to satisfy this need when no inertia is considered.

2.4.2. Standardized Mechanical Interface

The main idea behind the standard interface is to represent the power transmission between two mechanical components as a combination of effort and flow losses in the plane tangent to contact (e.g. between screw and nut threads). The proposed model makes causalities consistent with those of standardized mechanical components. In that manner, it can be implemented in any causal simulation environment.

In continuity with the standardized mechanical body, the interface in Figure 2.6 is illustrated in analogy with a nut-screw interface. In this application, the plane of contact is the thread.

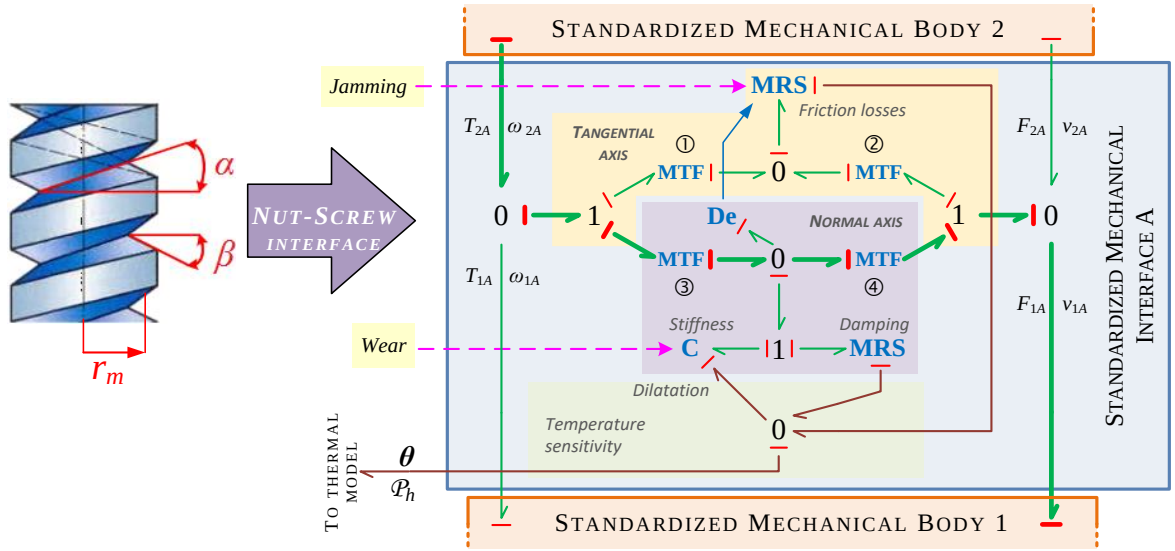

Figure 2.6 – Standardized mechanical interface with the preferred causality [COI16b].

In the normal axis of the plane of contact, the flow losses are placed on a 0 junction which receives flow variables from the mechanical solids through transformers ③ and ④. In the particular case of nut-screws, transformer ratios ③ and ④ equal respectively ($r_m cos\beta sin\alpha$) and $1/(cos\beta cos\alpha)$, where α is the helix angle, β the thread angle and r_m the mean radius. Relative velocity is computed and transmitted to

the optional compliance (C field) and dissipative (MRS field) for effort calculation. In the C field, preload or play can be considered and rupture can be triggered.

The effort losses, which are mainly due to sliding friction, are calculated in the plane of contact and receive the sign for relative velocity between the two component surfaces. Therefore, frictional loss is represented as an MRS field connected to a 0 junction. It is modulated by the effort component acting perpendicularly on the contact point. This simply denotes that due to friction, the tangent force is directly dependent on the normal force applied at contact. Effort losses are transmitted to the mechanical solids through transformers ① and ②, which respectively equal ($r_m cos\alpha$) and ($sin\alpha$) for a nut-screw interface. Jamming can be easily triggered by increasing the amount of friction in the MRS element implementation and friction can be made dependent on the transmitted force and temperature (in addition to the dependency on velocity induced by the constitutive law of an R element).

Note 2.2: Modulated transformers are used in the standardized mechanical interface for generalization purposes. In the particular case of nut-screws, the transformers have constant ratios. However, in many applications the ratio varies, e.g. the swashplate angle of a variable displacement pump.

Both flow and effort losses apply to relative motion. To keep it as general as possible, this model structure includes four transformation elements for each projection in the normal and tangential directions of the contact interface plane. However, if a transformation is not relevant, it can be withdrawn or affected by a unity ratio. In the same modular approach, compliance and resistance elements are placed in the normal axis that the modeller can remove if it is not relevant. In this drawing, the thermal power bonds are represented in order to fulfil the thermal balance (requirement R4).

The modularity and genericity is the strength of the proposed standardized mechanical interface. It covers any mechanical interface. This is highlighted by addressing the Bond-graph models of several functional interfaces, as illustrated in Figure 2.7 for hinge pair, prism pair, cylinder pair, nut/screw and dog-teeth.

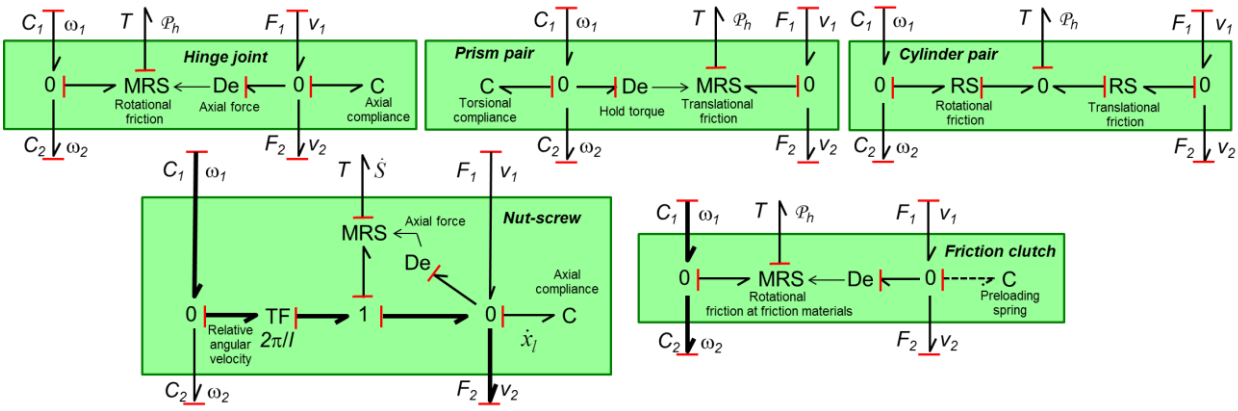

Figure 2.7 – Functional interfaces based on the proposed standardized interface from [MAR12].

For example, a hinge joint (top left of Figure 2.7) functionally enables one degree of freedom in rotation (relative angular velocity) between two bodies. The required axial force is transmitted from one body to the other in order to avoid any axial relative motion. A real hinge displays rotational friction and translational compliance. Moreover, the parasitic torque opposed to rotation increases with the axial force. Therefore, transformations ① and ④ have a unity ratio and transformations ② and ③ are removed.

2.4.3. Benefits of the Proposed Standardization

The standardized mechanical body and interface meet all the engineering requirements (R1 to R6) and facilitate workshare decomposition (R7) – as the interfaces are well defined – as well as capitalization (R12) – with an "object-oriented" Bond-graph model. Together, they facilitate the creation of mechanical models by combining these standardized components with the right level of realism for each element.

2.5. Modelling Fluid Power Systems with Bond-graphs

In fluid power applications, energy is given to the fluid in terms of pressure. The hydraulic power is then usually intended to be transformed into mechanical power. Typical applications on helicopters are primary flight controls – in particular, the (electro-) hydraulic actuators – or hydraulic equipment – used for example in landing gears, hoists or sonars.

Fluid power modelling focuses on the macroscopic evolution of the fluid effort and flow variables, i.e. pressure and volume flow rate, respectively. Usually, reference volumes are defined with the associated flow pattern, which is modelled once for the entire volume. For example, in a hydraulic circuit, a pipe can be identified as a reference volume in which the flow pattern – characterized by the Reynolds number – can be laminar, in the transition domain or turbulent. It is also possible to consider an establishment length[11] due to possible disturbance at the pipe entrance. This example emphasizes the

[11] In this dissertation, the term "establishment length" is preferred to "transition length" often found in the literature, which could wrongly refer to the laminar-turbulent transition.

possibility to change flow patterns (or even have two of them at the same time) for a given volume, but it is modelled only once for the entire volume. For a more detailed view of the flow pattern, it could be interesting to model the evolution of each fluid particle, but then the simulation would have to be carried out with another detailed CFD model.

2.5.1. Energetic Balance in Fluid Power Modelling

Energetic balance (R4) requires a thermo-hydraulic model of the internal energy of the fluid. However, this is not addressed in this fluid model for two main reasons:

- The complexity added by thermo-hydraulic modelling counters requirements R8 (engineering parameters) and R9 (industrial units). Fluid power engineers usually are more comfortable with "Bar" and L"/min" than with "Pa", "kg/s" and "kJ".
- Precise modelling of the thermal properties of the fluid is useless without a detailed model of the hydraulic system environment for thermal exchanges. Unfortunately, such an environment model is highly dependent on each helicopter and is therefore not available at the beginning of a new development. At Airbus Helicopters, the thermo-hydraulic model is developed at the end of the rotorcraft development (after cold and hot flight test campaign) to investigate specific behaviours under harsh conditions.

Therefore, the thermal effect is partially addressed in this dissertation. The fluid temperature – and with it its intrinsic properties – can be imposed (by an input variable in the model) but is considered constant all along the virtual model at a given simulation time. This hypothesis is made when dealing with hydraulic power Bond-graphs (using pressure and flow rate as effort and flow variables).

Local dissipation is computed (RS element), which provides a good approximation of the resulting created heat. It makes the model ready for interfacing with the environment model for a first estimation.

2.5.2. Volume Computation

In this dissertation, Bond-graph models are used to structure the virtual model. The lack of a Bond-graph simulation environment at Airbus Helicopters forces the implementation with another simulation software, usually causing the engineer to convert the Bond-graphs into equations. But the equations obtained from Bond-graphs may slightly differ from one engineer to another.

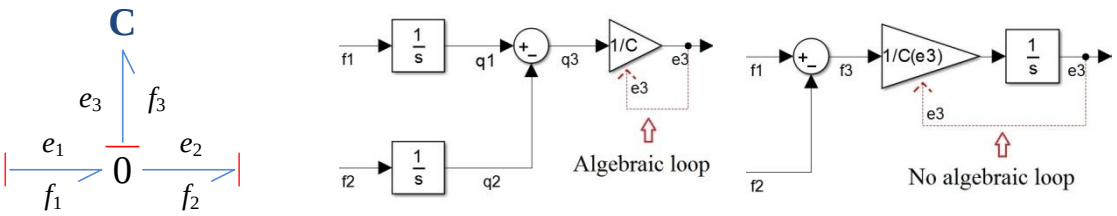

(a) – Causal Bond-graph (b) – Volume computation (c) – Continuity equation

Figure 2.8 – Bond-graph of a hydraulic capacitive effect and two possible implementations.

Note 2.3: In Figure 2.8, the C element is represented as a gain. It is a simplification to illustrate this point. The result would have been the same considering C as a function of displacement q.

As an example, a capacitive effect is considered as pictured by the causal Bond-graph in Figure 2.8-(a). In the hydraulic domain, this corresponds to the compression (or decompression) of a fluid in a volume, thus converting flow rate into pressure (or vice-versa). Integral causalities are shown in order to support the implementation in simulation software.

To continue with the hydraulic example, one engineer could apply strictly the rules of Bond-graphs stating that:

$$\begin{cases} f_3 = f_1 - f_2 \\ e_3 = \dfrac{1}{C}\int f_3 dt \\ e_1 = e_3 \\ e_2 = e_3 \end{cases}$$

Equation 2.1

It is possible to see that, in the second member of Equation 2.1, the computation of the generalized displacement (volume for hydraulics) is performed first and is then affected by the inverse of the capacitance (the stiffness). This is convenient as volumes are the state variable of fluid power systems. It is even more convenient to make appear volumes V_1 and V_2, which is possible as the time integral of the volume flow rate is a first order homogeneous function. Thus, it is possible to assess the filling of a chamber with oil or, in other words, the quantity of air in the chamber. Unfortunately, negative values of volume 3 lead to negative values of pressure in the 0 junction. It is then necessary to either stop the simulation or impose a zero low limit to the pressure values. Also, if the compressibility is dependent on the effort, as is usually the case in hydraulics, where the Bulk modulus is a function of the pressure, an algebraic loop appears. The corresponding block diagram is shown in Figure 2.8-(b).

In fluid power, engineers usually apply the continuity equation to volumes **[GUI92]**. This equation first divides volume flow rate Q_3 by the capacitance, and then integrates the result with respect to the time (Equation 2.2). The corresponding block diagram is shown in Figure 2.8-(c).

$$e_3 = \int \frac{1}{C} f_3 dt$$ **Equation 2.2**

In this case, it is not possible to perceive the volume values. However, this solution has the advantage that the Bulk modulus (included in the capacitance) can be made dependent on the pressure without creating an algebraic loop.

Note 2.4: It is important to note that the continuity equation is equivalent to the equation derived from Bond-graphs only if the C element is constant with time and can thus be introduced in the time integral. However, the continuity equation is usually applied to time variable volumes such as cylinder chambers. On the contrary, in Bond-graphs, C elements modulated with signal inputs should not exist ***[BEA88]****.*

2.6. Electrical Systems with Bond-graphs

Electrical models are developed in analogy with hydraulic models. The temperature is made accessible with an input variable but is considered constant in the entire electrical circuit. For example, a resistance is the function of the temperature. Herein, it is modelled with an RS element, the characteristic of which is temperature-dependent and from which the Joule losses are computed. But no coupling is performed at this level, so the Joule losses do not affect the resistance temperature.

Bond-graph modelling of electrical systems has been studied in more detail at the Institut Clément Ader laboratory. For example, Jian Fu **[FU15]** modelled EMAs and their power electronics with Bond-graphs. This is why this subject is not studied more thoroughly in this dissertation.

3. ACTUATION SYSTEM VIRTUAL MODEL

In this section, the purpose of actuation system modelling is detailed with its interfaces. Then each subsystem is modelled with Bond-graphs in a component-oriented manner.

3.1. Purpose of Actuation System modelling

In this PhD dissertation, an Actuation System covers hydraulic power generation and distribution, and main and tail rotors actuators (Figure 2.9).

The Actuation System is a dominant contributor to the Flight Control System's overall performance. Actuation system design shall take into account severe environmental and hydraulic power consumption constraints. If managed independently, these two levels of constraints – functional needs (piloting) and environmental constraints (oil temperature, failures, etc.) – could lead to oversizing or undersizing of the Actuation System design. Incorrect sizing generates undue costs and weight increases (oversizing) or operational limitations (undersizing), which negatively impact helicopter final design or performance.

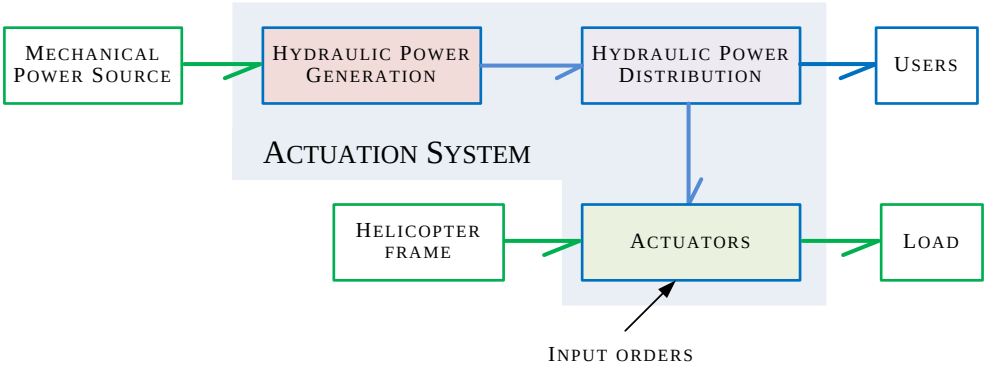

Figure 2.9 – Actuation System word Bond-graph.

In order to facilitate Actuation System sizing, a specific modelling is proposed, based on Airbus Helicopters' experience that enables optimization. The aim is to design the Actuation System with the right level of performance regardless of the environmental condition by identifying the right constraints at the right time.

The virtual model of the Actuation Systems reproduces the static and dynamic responses with the associated saturations, considering the hydraulic, mechanical, thermal and electrical domains. This virtual model is validated using real flight data taken from representative flight test campaigns.

A main point to be highlighted is the capacity of the Actuation System virtual model to be interfaced with the full helicopter flight loop modelling, which integrates:

- Pilot inputs
- Flight Control System model
- Flight mechanics model (helicopter evolutions during manoeuvres including wind effect)
- Load model (aerodynamic loads generated by helicopter evolutions during manoeuvres)
- Actuation system configuration (failures: loss of one hydraulic circuit; architecture: addition of an accumulator; parameters: maximum pump flow capacity)
- Environmental conditions (oil temperature).

The helicopter flight loop modelling allows Airbus Helicopters to simulate representative manoeuvres. The aim of integrating the proposed Actuation System virtual model into the flight loop modelling is to ensure that the studied Actuation System design satisfies the specified dynamics response from the Flight Control System and does not induce static or dynamic limitations in any flight condition.

3.2. Fluid Modelling

3.2.1. Needs of a Fluid Model

In this dissertation, the reference fluid used is the MIL-PRF-83282 **[SAE00]**. The performance variations of the Actuation System with the pressure (P) and temperature (T) are mainly due to the change of oil intrinsic properties. The fluid model shall thus provide the intrinsic properties needed by the Bond-graph elements:

- The I element requires the mass density: ρ in [kg/m^3]. It represents the mass of fluid per unitary volume. It is necessary to compute inertial forces involved in transients such as the "water hammer" effect or line dynamics, to name but a few.
- The R element requires:
  - the absolute viscosity: μ in [Pa.s]. It characterizes the fluid resistance to flow. It is the principal contributor to performance evolution with temperature: it creates high pressure drops at low temperatures and increases the leakage at high temperatures.
  - the mass density for several calculations such as the Reynolds number (through the link between kinematic and absolute viscosity), or for pressure losses under turbulent flow.
- The C element requires the Bulk modulus: β in [Pa]. It provides the relation between pressure and volume variations. It is thus mandatory for modelling the oil compressibility. Four Bulk moduli can be defined: adiabatic tangent or secant and isothermal tangent or secant. The SAE **[SAE00]** states that system sizing in fluid power applications requires adiabatic Bulk moduli. Tangent is used for small variations of pressure (e.g. pipe, actuator…) while secant is for large variations (e.g. pumps…). In practice, a single Bulk modulus is measured by tests and used for all applications.

The evolution of these properties is thus presented regarding pressure and temperature, based on **[SAE00]** for the fluid MIL-PRF-83282. Note that the operating temperature range defined in table 2 of this information report for this fluid is $[T_{min};T_{max}]$=[-40;+205]°C. This range is the basis for temperature normalization in this dissertation (e.g. in Chapter 3 for the dimensionless design of fluid bearings).

According to Figure 2.10-(a), the density varies by less than 20 % of its maximum value over the total range of the operating temperature. On its side, the kinematic viscosity is affected by a factor of nearly 3000 from -40°C to +195°C, according to Figure 2.10-(b). With this comparison, it is already possible to anticipate that the viscosity will play a major role in fluid power applications operating in a wide temperature range. Change of density and viscosity with pressure should be modelled but should have a limited impact on the simulation results, except for the transient effect in hydraulic capacitances.

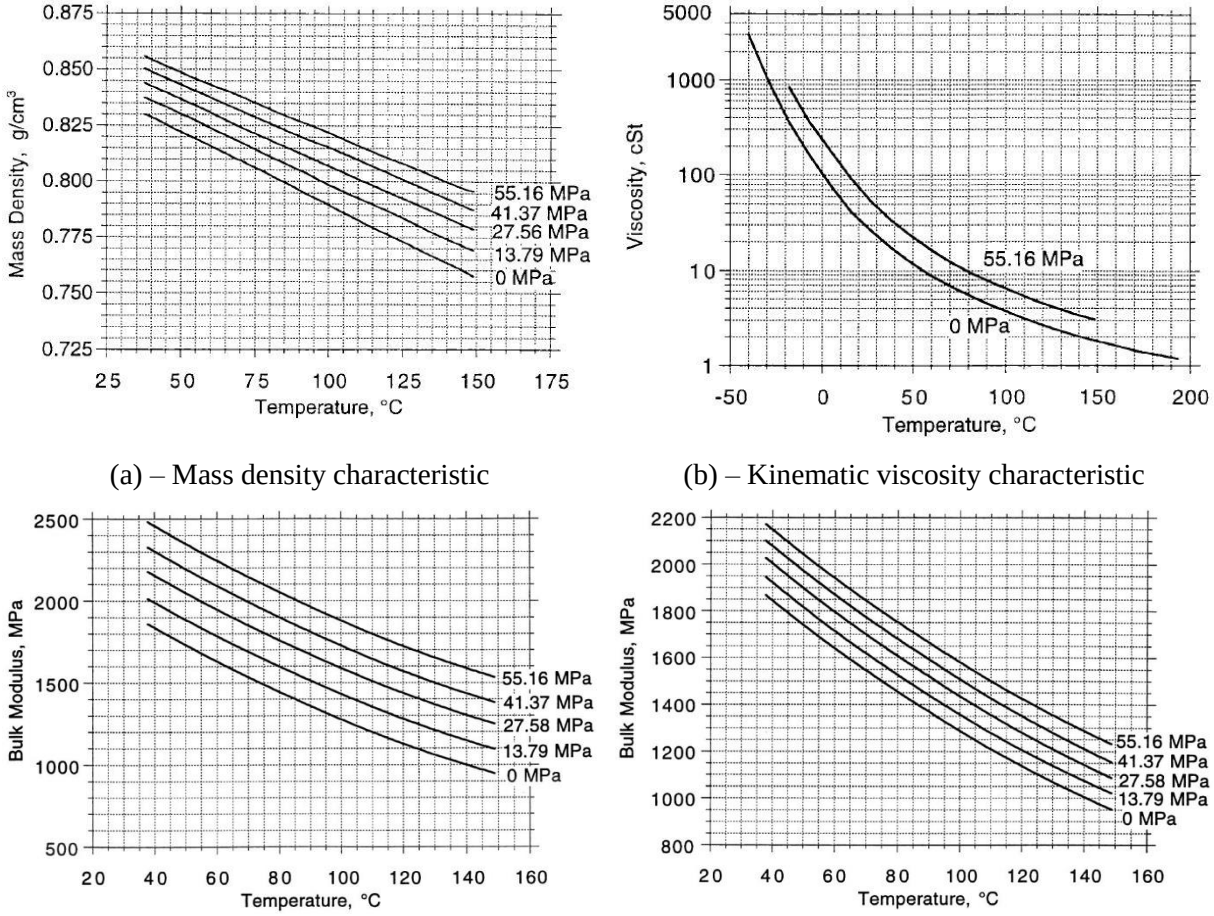

(a) – Mass density characteristic

(b) – Kinematic viscosity characteristic

(c) – Adiabatic tangent Bulk modulus

(d) – Adiabatic secant Bulk modulus

Figure 2.10 – MIL-PRF-83282 properties, oil sensitivity to temperature and pressure taken from [SAE00].

3.2.2. Mass Density

A first order Taylor expansion can be used to model a linear dependency of the fluid density on temperature and pressure **[ATT08]**. These assumptions from -40°C to +205°C and from 0 Bar to 275.6 Bar, combined with a good identification of partial derivatives, lead to a maximum error of 2 % compared to values extracted from Figure 2.10-(a). Subscript "0" corresponds to the reference point.

$$\rho_{(T,P)} = \rho_0 + \left(\frac{\partial \rho}{\partial T}\right)_P (T - T_0) + \left(\frac{\partial \rho}{\partial P}\right)_T (P - P_0) \qquad \textbf{Equation 2.3}$$

It is relevant to emphasize the meaning of the partial derivatives involved in Equation 2.3:

– $\alpha_P = -\frac{1}{\rho_0}\left(\frac{\partial \rho}{\partial T}\right)_P$ is the coefficient of thermal expansion expressed in [°C^{-1}]. It represents the relation between the variation of density and temperature. Fortunately for our fluid model, it can be considered constant regarding pressure and temperature for the operating range. It equals 8.2x10^{-4}°C^{-1} for MIL-PRF-83282 **[SAE00]**.

– $\beta_{t,i} = -\rho_0 \left(\frac{\partial P}{\partial \rho} \right)_T$ is the tangent isothermal Bulk modulus.

These remarks have strong implications for the fluid model. Interrelations exist between the mass density, the coefficient of thermal expansion and the Bulk modulus. In this dissertation, it has been decided to model the mass density as a function of both α_p and β (and T_0 and P_0). Therefore, in addition to the three initial intrinsic properties required by the Bond-graph elements listed above, the coefficient of thermal expansion is added.

3.2.3. Absolute Viscosity

Fluid viscosity is often approximated by an exponential decrease with the increase of temperature **[SAE00] [ATT08]**. However, different fittings exist for temperature dependency, e.g. the one provided by Faisandier **[FAI83]**, which uses the Barus equation **[BAR93]** for the pressure dependency.

$$\mu_{(T,P)} = \exp\left[\ln(\mu_0) * (T / T_0)^a + k(P - P_0) \right]$$ **Equation 2.4**

where:

– a is the fluid viscosity index [-]

– k is a pressure-viscosity coefficient, which varies with temperature [Pa^{-1}]

In this dissertation, tables are preferred to model the fluid properties. Indeed, most of the data are taken from tables of the AIR 1362 **[SAE00]**. Trying to fit equations to these points is an additional source of error which is not desirable.

3.2.4. Bulk Modulus

Figure 2.10-(c) and Figure 2.10-(d) show the adiabatic tangent and secant Bulk moduli. Their values for a relative pressure of 0 MPa is quite similar. The adiabatic tangent Bulk modulus appears more strongly influenced by pressure increase than the secant Bulk modulus. In practice, once the effect of entrained air and the compression of mechanical parts are taken into account, it is possible to consider a single equivalent Bulk modulus as a function of both the pressure and the temperature. In our application, simulation results are sufficiently accurate with this approach. In practice, the equivalent Bulk modulus also includes the elasticity of the fluid envelope (e.g. pipe, actuator housing…), as detailed for example in **[MER67]** or **[GUI92]**.

Several models exist to fit the Bulk modulus evolution with temperature and pressure, such as **[BOE95]**, **[EGG80]**, **[HOF81]**, **[JIN94]** or **[LEE77]**. However, as for the absolute viscosity, tables have been preferred to model a single Bulk modulus.

3.3. Hydraulic System Virtual Model

The hydraulic system virtual model includes the hydraulic reservoirs, power generation and distribution.

As presented in Chapter 1, the flight control system – and thus the Actuation System – ensures a safety-critical function. Therefore, it is necessary to design the hydraulic system including redundancies to meet the flight control system reliability requirement.

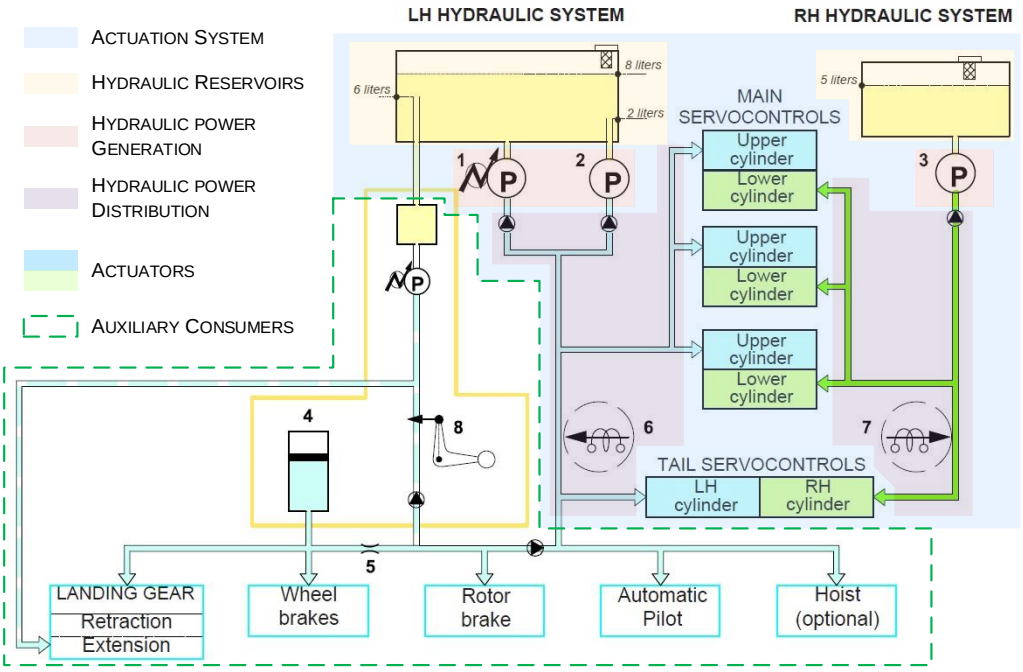

Figure 2.11 – H225 Hydraulic System with the main users identified from [EUR04].

In our helicopter, usually one "clean" circuit only generates and distributes hydraulic power to the lower cylinders of the main and tail rotor actuators; another hydraulic circuit is connected to the upper actuator cylinders and to the other auxiliary consumers (landing gear, wheel and rotor brakes, automatic pilot and hoist).

Figure 2.11 shows a representation of the two hydraulic systems of an AS332 with the main consumers identified. The Actuation System and its main subsystem are highlighted.

In this PhD dissertation, an effort is made to accurately model the Hydraulic System in terms of pressure losses, fluid dynamics, generated heat, etc. At this level, actuators are considered as power consumers. They are modelled in section 3.3. Auxiliary consumers are also considered as power consumers but are not modelled in more detail as they are under the responsibility of another Airbus Helicopters department (requirement R7). However, model interfaces are created and enable further connection with auxiliary consumer models.

3.3.1. Hydraulic Reservoir Virtual Model

In most Airbus Helicopters simulations, the hydraulic reservoir is not modelled. It mainly influences the thermal cooling of the fluid, which is, as justified before, not considered in this dissertation. However, it may be of interest for a first study to assess the fluid level remaining in the reservoir when the maximum volume is requested by the hydraulic consumers. Therefore, a simplified reservoir virtual model is built (Figure 2.12).

Left Hand (LH) and Right Hand (RH) reservoirs in Figure 2.11 differ in the number of exits. The virtual model presented below is compatible with both designs due to optional output that the model user is free to consider or not. Reservoirs can be pressurized or not. The pressurization solution is not unique. Therefore, a pressurized reservoir model would depend on the technology used. In the presented model, the reservoir is not pressurized, as is the case for most of the Airbus Helicopters France fleet.

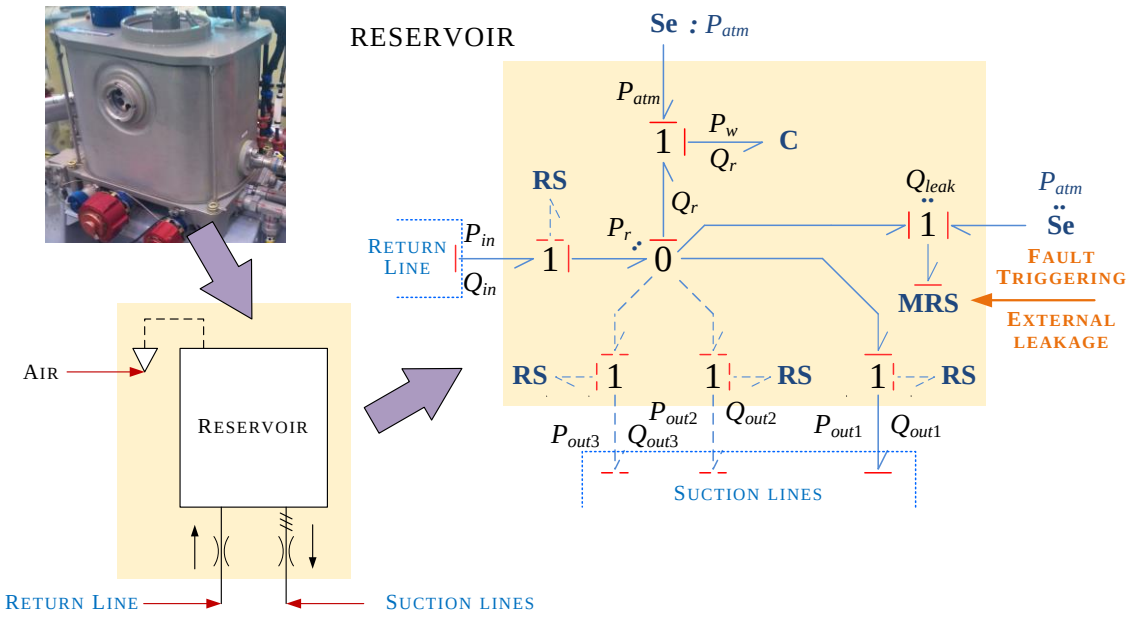

Figure 2.12 – Non-pressurized reservoir virtual model.

In terms of fluid levels, the virtual model is divided into two parts. The upper part is the fluid layer in contact with atmospheric pressure (P_{atm}) and the lower part is where the inlets and outlet meet. The variation of reservoir volume (Q_r) is computed from the input flows (Q_{in}) and output flows (Q_{out}) on a 0 junction. The upper part is modelled as a source of effort which equals the atmospheric pressure. It is connected to a 1 junction with a C element that models the pressure induced by the weight of the fluid column.

Note 2.5: The pressure induced by the fluid column weight is a function of the remaining height of fluid in the reservoir (P_r-P_{atm}=$\rho g h_r$, with g being the gravitational acceleration and h_r the fluid height

in the reservoir). It is thus dependent on the fluid volume (divided by the reservoir section) and therefore modelled with a C element.

Therefore, the pressure in the lower part (P_r) is made dependent on the remaining fluid in the reservoir. Cavitation phenomena can be assessed with more accuracy considering this weight-related pressure increase. Also, the reservoir volume (the state variable of interest) is provided by the constitutive law of the C element.

The displayed causalities of the reservoir virtual model are induced by the effort source and the choice to have integral causality on the C element. However, it is possible to adapt the causalities of the interfaces thanks to dissipative phenomena at inlet and outlet lines that are optionally modelled with RS elements. Their causalities are not constrained as the restriction they model is constant.[12]

Finally, a signal port enables triggering an external leakage from the reservoir. It acts on a modulated RS element. It is important to note that the leakage appears at the lower part of the reservoir. In order to model a different height for the leakage point, the reservoir volume shall be decomposed into at least two C elements – before and after the leakage point. Another option could be to replace the MRS element with an effort source which is modulated by the fluid level.

No particular power path is emphasized on this Bond-graph model as it is highly dependent on what the model user wants to simulate. The scope could either be to assess the minimum volume on the reservoir in a nominal operation or to determine the evolution of the actuation performances after the triggering of an external leakage on the reservoir.

3.3.2. Hydraulic Power Generation Virtual Model

Typically, on helicopters, either constant or variable displacement pumps generate hydraulic power that is intended to be distributed at constant pressure. Usually on new developments, variable displacement pressure-compensated pumps are preferred over fixed cylinder pumps in order to reduce hydraulic thermal dissipation. Therefore, the virtual models developed are based on this technology. Two levels of pump modelling are presented: an ideal pump and a pump modelled for equipment integrators (such as Airbus Helicopters). Reference for a detailed model intended to facilitate the development of a pump is given.

In a first approach, the pump can be considered as a constant source of effort. It is a strongly simplifying hypothesis but it is justified for the ascending part of the V-cycle as detailed in section 1.2. For example, the pressure source is almost ideal on test benches where the hydraulic power generation

[12] Causality of R elements cannot always be chosen freely. This point is addressed in more detail in the following sections.

of the laboratory is highly oversized regarding the consumer needs. In a second step, the constant source of effort can be incremented to a modulated source of effort combined with a dissipative effect. The modulation enables introducing variation on the pump power supply (mechanical or electrical), whereas the RS field reproduces the pump characteristic as a function of the flow, see Figure 2.13.

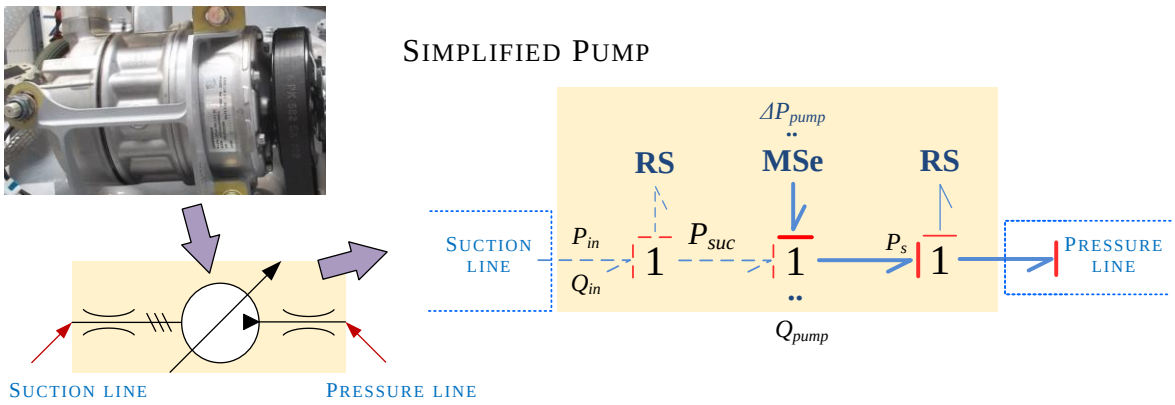

Figure 2.13 – Variable displacement pump modelled as a combined effort source.

The pump provides an augmentation of pressure (ΔP_{pump}) through a 1 junction. If the reservoir virtual model is not needed, the Bond-graph is reduced to a source of pressure which directly equals the supply pressure (P_s). Similarly to the hydraulic reservoir virtual model, the interface causalities can be managed by reversing the line dissipations causality (RS elements).

This simplified model is not suitable for modelling the Actuation System of a helicopter. Indeed, the pump dynamics and limitations influence actuator responses **[COI16c]**. Therefore, a more detailed virtual model is developed. This new modelling is based on a pump architecture similar to Figure 2.14.

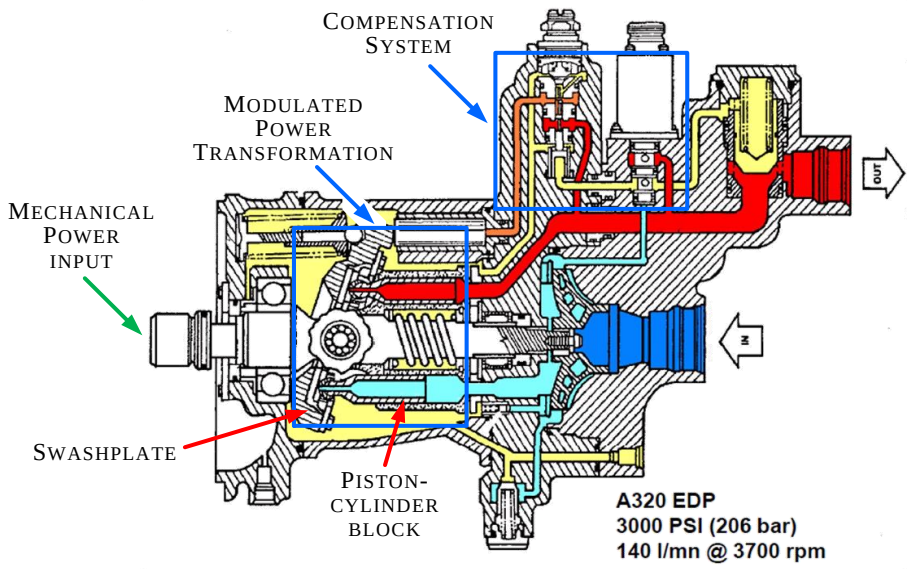

Figure 2.14 – Axial piston, variable displacement, pressure regulated pump from [MAR01].

In such a pump architecture, mechanical power drives a shaft that rotates a cylinder block. In this block, several pistons are guided in a parallel direction with regard to the drive shaft. All pistons are linked to a swashplate by a spherical fluid bearing connection called piston shoe. Piloting the swashplate angle allows modulating the piston strokes inside the cylinder block. Fluid is sucked from the inlet with a flowrate function of the rotation speed and the swashplate angle (and thus the cylinder displacements). In one block rotation, the reduction of piston-cylinder volumes, due to the piston displacement, compresses the contained fluid, thus providing a pressurized flow rate to the hydraulic system. The compensation system is composed of a regulator valve and a displacement actuator. The regulator valve compares the output pressure with a reference pressure (usually set by a spring) and modulates hydraulic power to the displacement actuator, which acts on the swashplate angle.

One way to model this pump is to consider that the piston-cylinders act as several modulated power transformers (MTF element) from the mechanical to the hydraulic domain, the transformation ratios of which equal the cylinder displacements relative to the shaft rotation. The flow source in the mechanical domain, the angular speed ω_{shaft}, becomes a volume flow rate Q_{pump} that is propagated to the suction and delivering lines through a 1 junction. In the delivering line, the flow is compressed by a C element. The compensation system is modelled as a simple first order dynamic with saturations which modulates the MTF elements.

Note 2.6: The compensation saturation shall be placed on the integral itself (and not after) in order to avoid unrealistic delays when leaving the saturation. To do so, it is necessary to write the first order in its canonical form. This also allows introducing speed saturation before the integral.

In nominal operation, the internal leakage is functional. It allows the generated heat and pollution[13] to be evacuated and is used as a fluid bearing in some parts such as piston shoes. Usually, the internal leakage outlet is the drain. Therefore, the internal leakage is herein modelled as an MRS-field dissipating hydraulic power to the drain, seen as a pump interface. With the increase of wear, the internal leakage also increases. It is herein optionally modelled as a single, entirely dissipated, loss of flow at the pump high pressure. Leakage evolution is controllable through the triggering input, as an extension of the model from **[MAR01]**.

[13] Quantification of the fluid pollution is not addressed in this model.

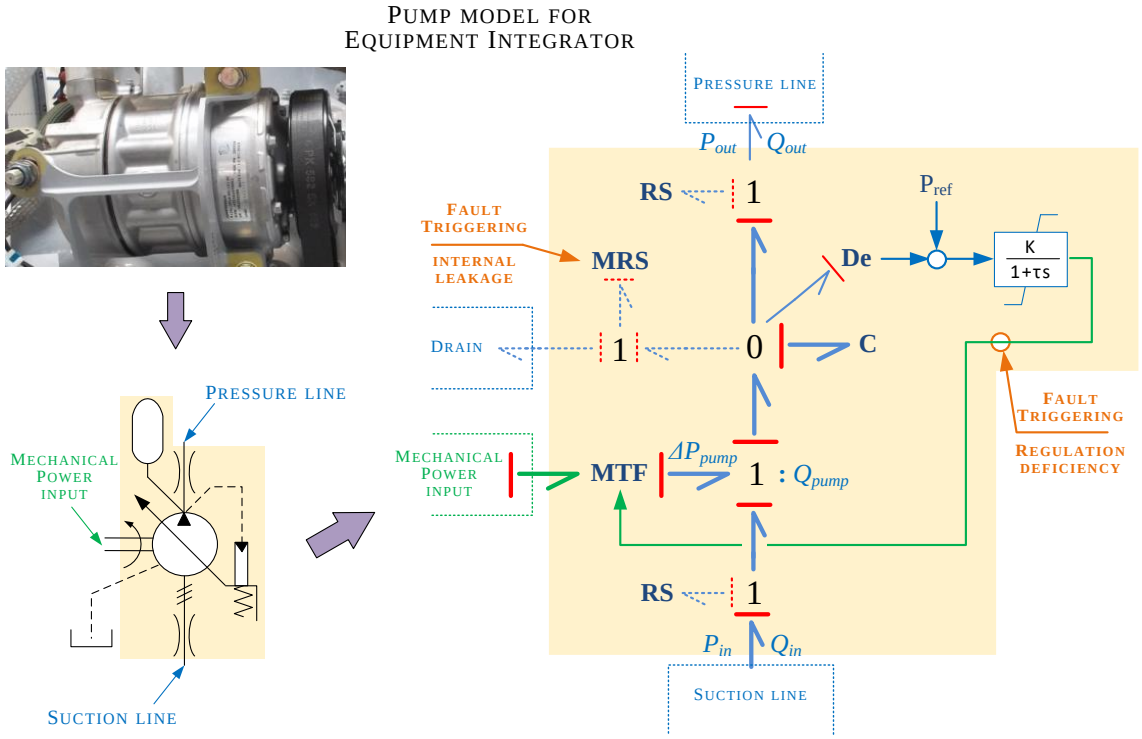

Figure 2.15 – Virtual Model: axial piston, variable displacement, pressure-regulated pump.

Another possible fault that has been modelled is regulation system deficiency. It can be either progressive, leading to a slower regulation dynamic, or instantaneous. It usually ends with a constant angle of the swashplate (the pump becomes thus a fixed displacement pump). Both cases can be triggered with the signal arrows using real or Boolean input respectively.

The pump virtual model developed in this PhD dissertation for virtual integration of the Actuation System is presented in Figure 2.15. As a simplification, a single modulated transformer is used to represent an equivalent cylinder block which compresses the fluid in an equivalent chamber. Consequently, this model does not allow simulating the dynamic of each piston and the associated pressure and flow ripples.

It is relevant to note that such a model is detailed enough for most Airbus Helicopters simulations, but too simplified for pump manufacturers. It is then important to know that more detailed models exist, for example **[VEL03]** modelled vane pumps using multi-Bonds. These models could be used for our simulation needs, but the dynamics involved would dramatically slow down the simulation and the parameters needed by the models are usually not available for integrators at early phases of the development.

3.3.3. Hydraulic Power Distribution Virtual Model

Hydraulic power coming from the power generation is distributed to the consumers through a sophisticated hydraulic circuit which was designed based on the safety requirements and includes several by-pass valves, check valves, filters, pipes…

In an early development phase, the architecture of the hydraulic power distribution and the routing of the pipe are not known. But a good estimation of the pressure losses (ΔP) – which depend on the volume flow rate (Q) – is needed to assess the impact on actuator performance. The overall Actuation System virtual model shall be accurate but conservative in terms of performance. This means that the physical model shall at least have the same performances as the one simulated. The consequence for the hydraulic power distribution virtual model is that the pressure losses shall not be underestimated.

Therefore, it is suggested herein to design a simplified hydraulic power distribution network which represents the main pressure losses. These are considered as local or distributed (but modelled as lumped effect) pressure losses. Both dissipative effects are modelled in Bond-graphs with an RS element, but the equations linking the effort and the flow variables depend on the flow pattern and the type of hydraulic restriction.

3.3.3.1. Flow Patterns

Flow patterns can be either laminar, turbulent or in transition. In a laminar flow pattern, the flow rate is mainly constrained by the viscous friction of the fluid. Speed vectors of neighbourhood fluid particles tend to be parallel and oriented in the flow direction **[FAI83]**. By contrast, a turbulent flow pattern is characterized by the inertia forces of the fluid. Speed vectors of all particles tend to diverge from the flow direction **[GUI92]**.

The transition domain is still neither well-known nor well-defined in the literature. This can be explained as it has been experimentally shown that the restriction shape highly impacts the value of the transition. However, the transition range is quite small relative to the Reynolds number values that can be reached. Therefore, the transition is usually considered as a point (and no longer a range) called the critical Reynolds number. The hysteresis effect in the transition domain is thus neglected.

The Reynolds number (R_e) **[REY86]** characterizes the type of flow pattern. It is given by Equation 2.5 for circular[14] flow sections.

$$R_e = \frac{vD}{\upsilon} = \frac{\rho}{\mu}\frac{4}{\pi D}Q \qquad \textbf{Equation 2.5}$$

[14] If the flow section is not circular, the "hydraulic diameter" provides genericity to this formula by defining an equivalent diameter regardless of the shape of the flow section. It is not used in this dissertation.

where:

- v is the fluid velocity, [m/s]
- υ is the kinematic viscosity, [m²/s]
- D is the pipe or orifice diameter, [m]

Equation 2.5 is applied to pipes or orifices, which are the main components used in the Actuation Systems that require Reynolds number calculation. The Reynolds number is a positive[15] dimensionless relation that represents the ration between the inertial forces and viscous forces. Sufficiently low Reynolds numbers correspond to a laminar flow, while sufficiently high values are for a turbulent flow pattern.

It is important to note that calculating the Reynolds number requires the volume flow rate. It is then convenient to express the pressure losses as a function of the volume flow rate:

$$\Delta P = \xi_{(R_e)} \frac{\rho}{2} \frac{Q^2}{\sigma^2} sign(Q) = \xi_{(R_e)} \rho \frac{v^2}{2} sign(v) \qquad \textbf{Equation 2.6}$$

Even if a square root appears in Equation 2.6, the flow pattern is not necessarily turbulent. Indeed, the pressure drop coefficient[16] ξ is dependent on the flow pattern and thus on the Reynolds number. In case of a laminar flow, the pressure drop coefficient has the Reynolds number at the denominator, leading thus to a linear relation between the volume flow rate and the pressure losses. Expressions of this coefficient are given in the two following sections.

Respecting this causality of the equation constrains the causality of the bond linked to the R element in order to avoid an algebraic loop. The flow number (λ) has been created conveniently **[CLO80]** to permit the other causality without generating an algebraic loop.

$$\lambda = \frac{D}{\upsilon} \sqrt{\frac{2|\Delta P|}{\rho}} \qquad \textbf{Equation 2.7}$$

The flow number is obtained by substituting the expression of the flow rate in the Reynolds number expression. This leads to a new equation linking the Reynolds number, the flow number and the restriction coefficient. The flow coefficient (c_q) is an image of the pressure drop coefficient in the inverse causality, i.e. volume flow rate function of pressure losses. It is a conductance coefficient.

$$R_e = \frac{\lambda}{\sqrt{\xi}} = c_q \lambda \qquad \textbf{Equation 2.8}$$

[15] Even if the well-known expression of the Reynolds number does not include the absolute value of the speed or volume flow rate, it is usual to plot its values in a logarithmic scale, requiring a positive flow or speed.
[16] The pressure drop coefficient is also called “resistance coefficient” in the literature, e.g. **[IDE66]**.

Once the flow number has been introduced, it is possible to select the right flow coefficient without any algebraic loop and thus compute the volume flow rate using Equation 2.9.

$$Q = c_q \sigma \sqrt{\frac{2}{\rho}|\Delta P|} sign(\Delta P) \qquad \textbf{Equation 2.9}$$

These principles have been presented herein with a focus on causality aspects in order to facilitate further software implementation for simulation. This is not necessarily done in a chronological order. In fact, it depends on regional conventions if Equation 2.6 or Equation 2.9 is used.

3.3.3.2. Local Pressure Losses

Local pressure losses occur in almost any change of shape in the hydraulic line: hydraulic fittings, pipe bend angles, valves, etc. These restrictions can be classified into fixed and variable restrictions.

On one side, the causality on fixed restrictions is "free". However, the literature usually presents the parameters characterizing many local restrictions using the pressure drop coefficient (ξ), e.g. **[IDE66] [GUI92]**. Therefore, Equation 2.6 would be preferred as it becomes easier to provide the parameters (requirement R8).

On the other side, some variable restrictions can be fully closed, which leads to a zero flow section, e.g. a poppet valve. In order to avoid division by zero, it is preferable to reverse the causality using the flow coefficient and thus Equation 2.9.

Figure 2.16 synthesizes the preferred causalities for each type of restriction based on equations found in the literature and implementation constraints as detailed above.

(a) – Fixed restrictions (b) – Variable restrictions

Figure 2.16 – Preferred restriction causalities based on equations found in literature.

Any change of shape in the distribution system disturbs the flow lines. As a consequence, a flow pattern in singularities becomes rapidly turbulent. This is equivalent to low transition Reynolds numbers or flow numbers. For example, in case of an orifice (small length compared to its diameter), transition can occur for Reynolds numbers between 15 and 240 **[GUI92]**. The critical Reynolds number is usually considered equal to 100 in our application. In the next section, values of critical Reynolds numbers are given for pipes.

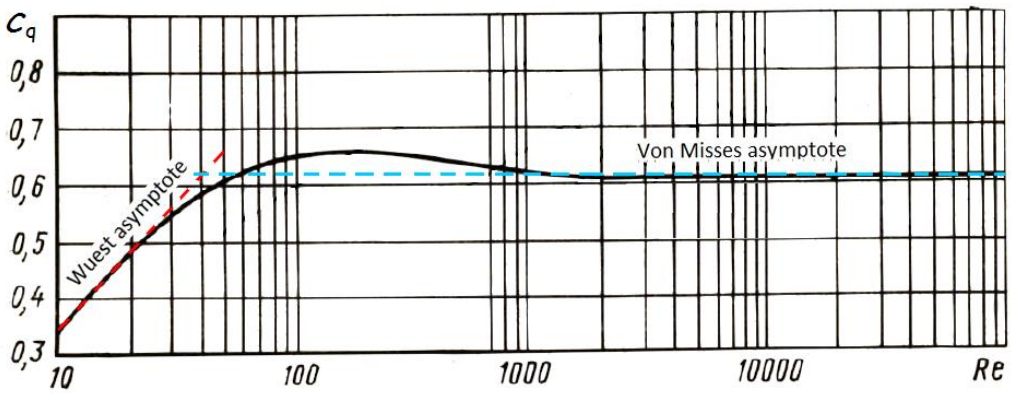

Figure 2.17 – Flow coefficient evolution with the Reynolds number, from [TCH79].

Sensitivity of the volume flow rate to temperature through orifices is studied in section 3.4.4 dedicated to valve modelling. A particular case of restriction, where the transition from laminar to turbulent is functional and managed by design, is presented in Chapter 3: the short tube orifice. This has also been presented in a paper **[COI16a]** at the International Conference on Hydraulics and Pneumatics (Praha, Czech Republic). This paper had been selected as the opening keynote of the conference.

3.3.3.3. Distributed Pressure Losses

Distributed pressure losses occur when the flow goes through a hydraulic line with a length (without any major change of shape) that is much higher than its diameter. This is mainly the case for rigid pipes and hoses with low curving in the hydraulic power distribution. Both will be referred to as pipes or hydraulic lines in this dissertation, unless otherwise specified. However, the parameters provided to the virtual models will depend on the nature of the hydraulic line.

Equation 2.6 models these flow patterns in a lumped parameter manner, taking into account that the pressure drop coefficient equals a friction factor times the length to diameter ratio of the pipe:

$$\xi = f\frac{L}{D} \qquad \textbf{Equation 2.10}$$

where:

- f is the friction factor, [-]
- L is the pipe length, [m]

In pipes, the pressure losses are modelled by the Hagen-Poiseuille equation for laminar flow patterns. However, this modelling does not include the perturbations at the pipe entrance and exit or the length needed to establish the laminar flow after such perturbations. Therefore, a general expression is used for pipes that are longer than the establishment length:

$$\xi = \frac{64}{R_e}\frac{L}{D} + \xi_{in} + \xi_{est} + \xi_{out} \qquad \textbf{Equation 2.11}$$

where:

– $64/R_e$ is the friction factor providing the Hagen-Poiseuille equation, [-]
– ξ_{in} is the pressure drop coefficient representing local entrance losses, [-]
– ξ_{est} is the pressure drop coefficient representing the establishment length, [-]
– ξ_{out} is the pressure drop coefficient representing local output losses. [-]

Typical values for ξ_{in}, ξ_{est} and ξ_{out} can be found for example in **[IDE66] [MER67] [GUI92]**.

For turbulent flow patterns, input and output perturbation and establishment length are negligible. Blasius experimentally defined the friction factor for turbulent flow patterns with Reynolds numbers below 10^5 and Prandtl's determined a universal law that is difficult to manage mathematically **[MER67]**. Nikuradse linked the friction factor with the pipe roughness for turbulent flow patterns **[NIK33]**.

Based on a study conducted with Airbus Helicopters data, it is affirmed herein that in pipes of our hydraulic power distribution network, admissible velocities correspond to a Reynolds number for which the Blasius equation is always applicable in case of turbulent flow. As listed in **[SAE12]**, fluid velocity limitations should be identified taking into account:

– "Allowable pressure drop at minimum required operating temperatures.
– Pressure surges caused by high fluid velocity and fast response valves.
– Back pressure in return lines, as it may affect brakes and pump case drain lines.
– Pump inlet pressure, as affected by long suction lines and a high response rate variable volume pump."

Regarding the laminar to turbulent transition, Osborne Reynolds wrote in **[REY86]** that a laminar flow pattern occurs for Reynolds numbers below 1400. Herbert E. Merritt defined a transition range from 2000 to 4000 **[MER67]**. Jacques Faisandier considered that this range could be from 1000 to 2300 **[FAI83]**.

With the aim of being conservative on the pressure loss calculation, the critical Reynolds number for pipes has been determined as the intersection between the Hagen-Poiseuille and Blasius asymptotes. Such intersection occurs when the Reynolds number equals 1187, which gives a friction factor f of 0.054. With this value for the critical Reynolds number, it is ensured that the friction factor considered is always the highest value of those given by the Hagen-Poiseuille and Blasius equations. Figure 2.18 synthesizes the previously detailed information.

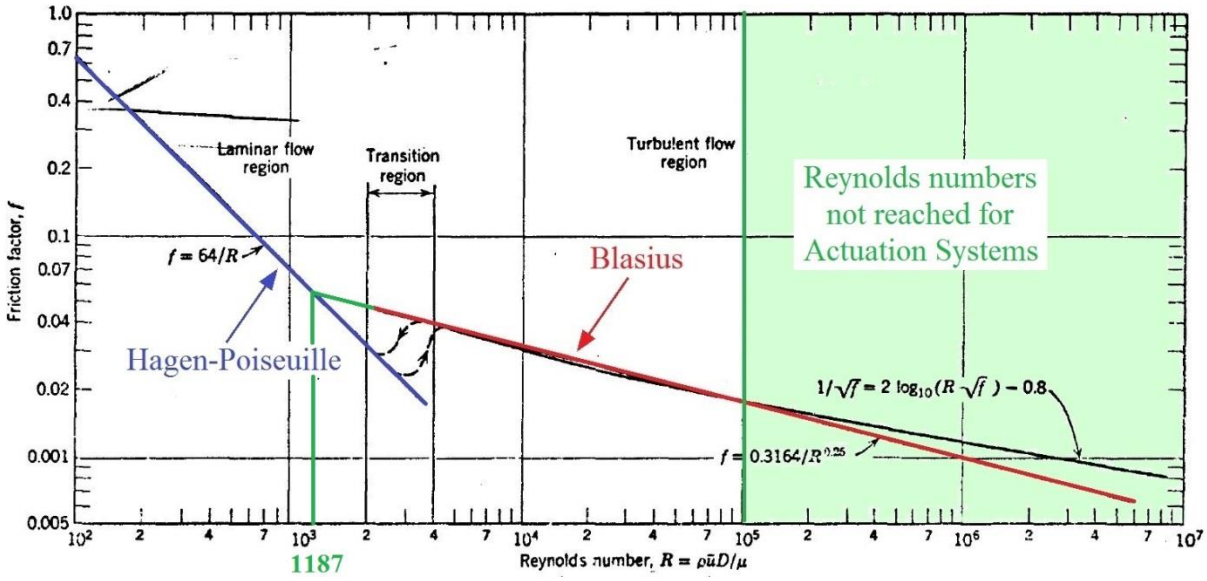

Figure 2.18 – Flow pattern in hydraulic lines from [MER67].

3.3.3.4. Hydraulic Lines Virtual Model

Several hydraulic line models are available in the literature. Lebrun **[LEB84]** defined Bond-graph models of the hydraulic lines obtained from the modal analysis of the wave equation. Pršić et al. **[PRS13]** divide the hydraulic line into segments (finite difference) that can be connected together, inducing then an approximation of wave equation. These two models, which have been taken from these articles, are shown in Figure 2.19. Sjölund et al. **[SJO10]** address the problem of simulation efficiency once the model has been implemented on computers. These models are only a selection of the existing ones in order to show the diversity of research axes for hydraulic line modelling.

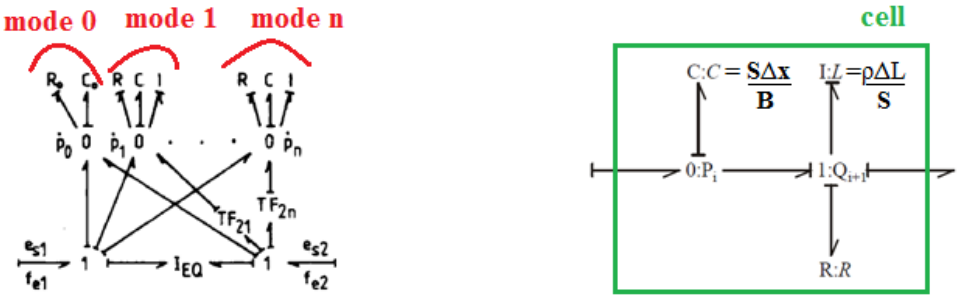

(a) – Obtained from modal analysis **[LEB84]** (b) – Segment to be repeated **[PRS13]**

Figure 2.19 – Existing virtual models of Hydraulic lines.

For helicopter Actuation Systems, the need is more basic. Hydraulic lines are short but dissipate energy at low temperatures, thus decreasing the pressure available at actuator interfaces. This has to be considered for section cylinder sizing. Therefore, the main effect to be modelled is the dissipative effect. It can optionally be combined with a capacitive effect and fluid inertia. Even if it may be interesting not to model the capacitive effect in some cases (e.g. small volume tubes that generate high natural

frequencies), in most applications, the capacitance is used to add a state variable and thus to compute the pipe pressure. According to the needs of Airbus Helicopters, inertia is rarely modelled. However, it is required when modelling the line dynamics (for other applications such as fluid injection or investigation of the "water hammer effect").

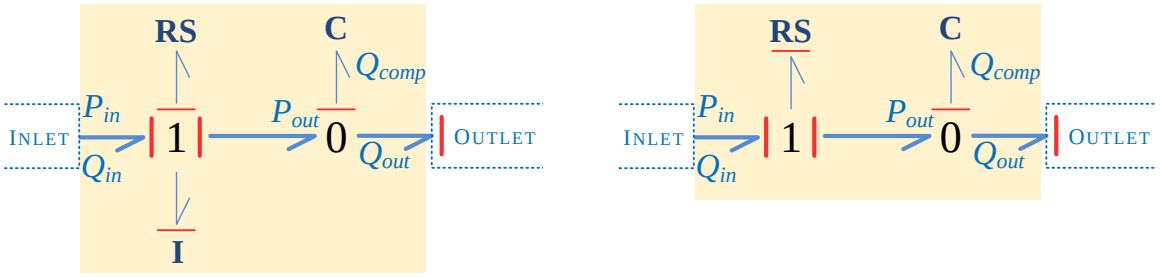

(a) – RIC model (b) – RC model requiring the use of the flow number

Figure 2.20 – Pipe virtual model used in our Actuation System modelling.

Causality on the RS element is dependent on the modelled effects. As detailed above, it is convenient to use the pressure drop coefficient in the pipe model. Therefore, causality on the RS-element is preferable to receive the flow variable and provide the pressure losses to the 1 junction. However, if inertial forces are not modelled, the causality on the dissipative effect must be modified in order to keep the same interfaces and to conserve the integral causality on the capacitive effect (preferred for simulation). Then the flow number is used in combination with Equation 2.9.

Note 2.7: The volume flow rate calculation from the "enriched" Hagen-Poiseuille equation – as defined in Equation 2.11 – would need polynomial solving if the establishment length were considered.

This concludes the hydraulic power distribution virtual model. The next section is dedicated to the main consumers of interest for the Actuation System: the primary flight control actuator virtual model.

3.4. FbW Actuator Virtual Model

There are many actuators on helicopters, but within the scope of this thesis they can all be neglected except for hydraulically powered actuators. Therefore, in this dissertation, the term actuator refers exclusively to hydraulic actuators (including electro-hydraulic and hydro-mechanical actuators).

FbW actuators are considered as main consumers of the hydraulic power generation and distribution systems. This does not mean that they consume more power than other equipment. Indeed, on many helicopters, landing gears or military equipment such as harpoons or sonars are more demanding in terms of instantaneous volume flow rate. But these demands are limited to a short period of time and associated with lower criticality. In contrast, actuators are in permanent motion to satisfy pilot and autopilot orders.

The actuator virtual model is divided into the same subsystems that have been suggested in Figure 1.15 of Chapter 1. This coherence satisfies requirement R1 of the modelling needs, thus facilitating incremental modelling.

It has been preferred to first detail the cylinder virtual model as it can be used for the EHSV virtual model for example. Then, as part of the control module, the interface, pilot and power modulation stages are described. Finally, the closed loop virtual model is presented.

3.4.1. Cylinder Virtual Model

In this dissertation, the cylinder, also called piston-cylinder assembly in the literature, refers to double effect cylinders. As mentioned above, primary flight control actuators are redundant and thus usually include two cylinders which are geometrically associated in series or in parallel. Only one cylinder is detailed in this section as the second one would be identical.

From a mechanical point of view, only two degrees of freedom are relevant: the axial displacement along the rod axis and the rotation around the eye-end necessary for the swashplate kinematic. The standardized mechanical components are then used to connect bodies and interface as "plug and play" components. The mechanical quadriport provides a high added value as both degrees of freedom are modelled in it.

With regard to the hydraulic interfaces, the cylinder has two connections with the control module in order to receive the fluid going to one chamber or deliver the fluid ejected by the other chamber. By convention, the positive volume flow is the flow entering the chambers.

The cylinder is virtually split into two parts: the extension side, relative to the extension chamber, and analogically the retraction side. Subscripts "*ext*" and "*ret*" respectively refer to the extension and retraction sides.

In each chamber, the flow coming from the EHSV valve is either compressed (subscript "*c*"), as required for piston displacement (subscript "*d*"), or optionally leaked (subscript "*L*") from the chambers to the atmosphere or between chambers through the piston (subscript "*pist*").

Note 2.8: The leakage can be dependent on the piston-rod/housing cylinder assembly. This dependence is not shown in Figure 2.21 for readability reasons but is necessary for modelling fluid bearings (see Chapter 3).

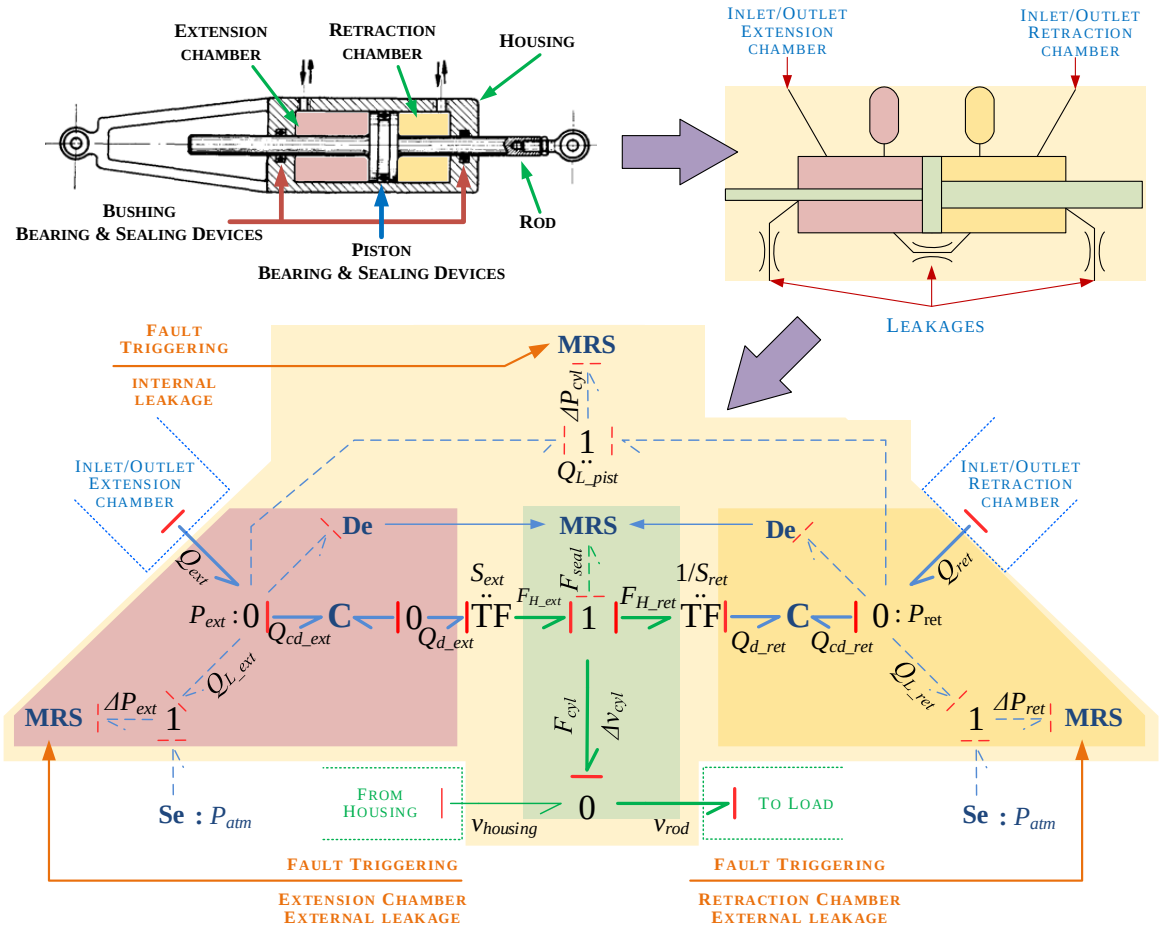

Figure 2.21 – Cylinder virtual model.

The piston has a section *S*, which transforms the hydraulic power into hydrostatic force (subscript "*H*"). Both chambers, which are mechanically linked, sum their forces in the 1 junction, the speed of which is relative to both the piston-rod assembly and the housing.

The dissipation effect between the piston and the cylinder has been modulated by the pressure of both chambers as it could occur in practice. In this example, the seal frictions (subscript "*seal*") depend on the compression of the seals generated by pressures on their ends. It is also made dependent of the piston-rod assembly relative speed with respect to the housing

An alternative could have been to model the cylinder chambers as introduced by Peter C. Breedveld in **[BRE82]**. This model is rigorous in terms of energy balance; however, it is more complex to deal with. It is often less convenient to use thermodynamics units and variables than fluid power ones. Also, Peter C. Breedveld highlighted in **[BRE13]** a mechanical port on each chamber in order to represent the potential motion of the piston. Another representation of the same effect has been presented for a double acting hydraulic cylinder by Wolfgang Borutzky in **[BOR10]**. The C-field thus includes both potential motion and displacement flow of the piston.

However, it is more usual to use a capacitive effect modulated by the chamber length (integral of the piston-housing relative speed) **[MUV10]** or **[ATT08]**. This can be justified as in normal operating conditions the maximum value of the potential motion of the piston only represents 1.5 % of the total force of the chamber. But as in Bond-graphs, modulation of storage elements is not energetically consistent, a C-field is used in our chamber models (see Figure 2.21) as, for example, used by **[XU13]**.

3.4.2. Interface Stage Virtual Model

As a reminder of Chapter 1, the interface stage receives the input signals and transmits them to the pilot stage. This section describes how to model the interface stage for each technology considered.

It is important to recall that the best model is not necessarily the most complex one. Interface stages impact the Actuation System response and stability mostly due to their dynamics. Therefore, the models presented in this section focus on reproducing main dynamics, generated heat (requirement R4) and fault generation (requirement R5).

3.4.2.1. Mechanical Lever – Hydro-Mechanical Actuator

The interface stage is usually a mechanical lever on hydro-mechanical actuators. While the virtual model of the interface stage does not reach any saturation (i.e. the end stops), it is convenient to model the inputs with position command signals (complete arrows).

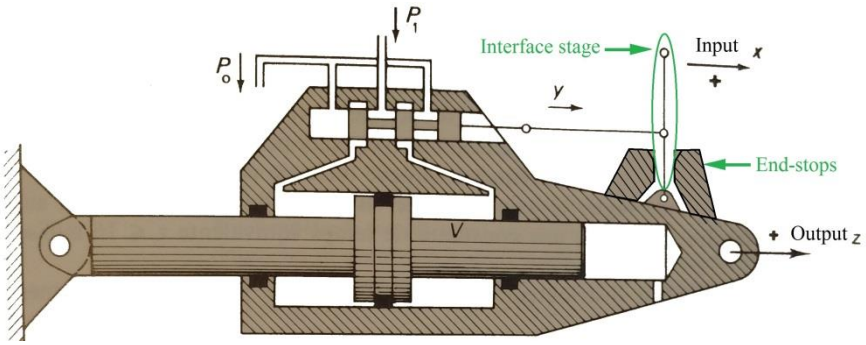

Figure 2.22 – Interface stage shown on a hydro-mechanical actuator adapted from [GUI92].

However, this simple model is no longer valid if:

- The rate of the input signal is higher than the actuator speed.
- The hydraulic circuit is lost on single hydraulic helicopters[17].
- The external load exceeds actuator reversibility (see definition in *Note 2.14*).

[17] Helicopters with a single hydraulic circuit require low piloting loads so that pilots can still control the helicopter trajectory during the period of time necessary for landing in case of loss of the hydraulic circuit.

Indeed, these conditions would make the mechanical lever reach its end-stops on the actuator housing. Then, the input does no longer provide a position but an effort command to the actuator. It should therefore be modelled by a mechanical bond.

Mechanical kinematics of the interface stage highly depends on the actuator. In addition, this dissertation focuses on FbW technologies. Therefore, even though it has been judged necessary to clarify the type of input on hydro-mechanical actuators, no particular virtual model of the interface stage is presented in this dissertation for these actuators.

3.4.2.2. Electric Motor – DDV- and EHSV-Based Actuator

The interface stage of a DDV-based actuator is composed of several LAT motors. EHSV also includes LAT motors but usually is referred to as "coils". Therefore, both technologies will have the same interface stage model even if parameters will differ.

Each motor is mechanically interfaced with the housing and its pilot stage through the stator (subscript "*stat*") and rotor (subscript "*rot*"), respectively (also see Figure 2.4 for the topology of the DDV). Benefit is taken from standardized mechanical components, so both the stator and the rotor are modelled with a standardized mechanical body. In Figure 2.23, only the rotations around the rotor axis are shown as there are the functional motions of the motors. However, standardized mechanical bodies allow subsequent upgrading of the model for translation in the rotor axis direction if required (e.g. for a vibration study, which is relevant in a helicopter environment).

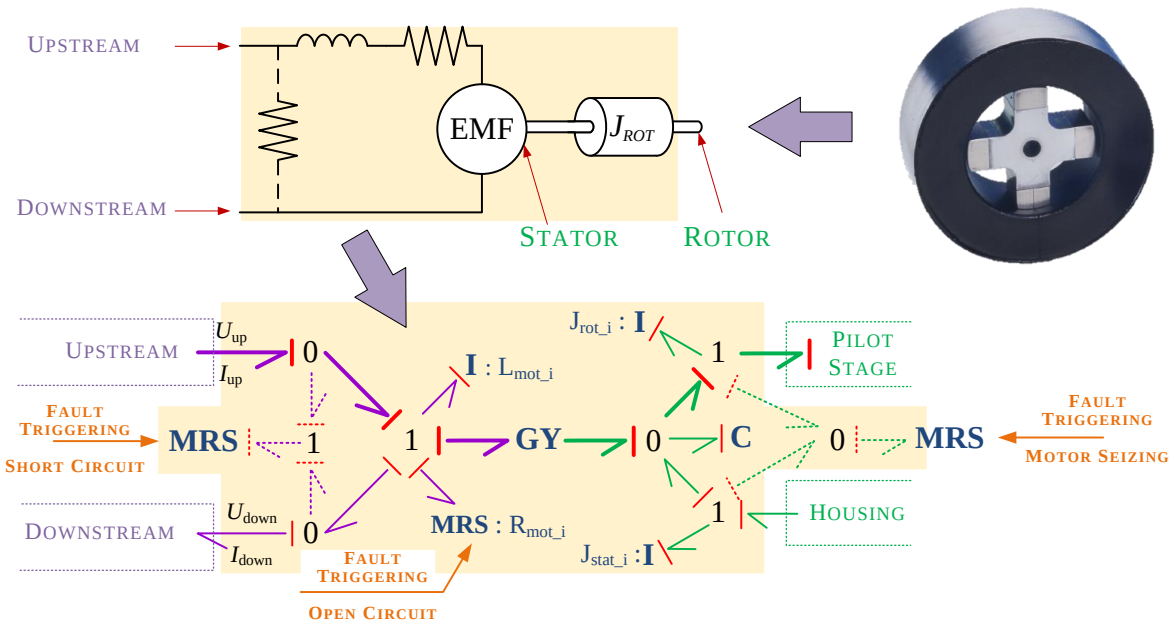

Figure 2.23 – Interface stage: electrical motor virtual model.

The interface between stator and rotor is usually the motor housing: the stator is fixed on the housing, which is linked to the rotor via hinges. Thus only one degree of freedom is left to the rotor – the rotation around its axis. It is simplified herein for readability and implementation reasons. The stator and rotor are optionally linked with a 0 junction that includes an MRS element. It represents the friction between both mechanical bodies. An increase of such friction leads to motor seizing.

Note 2.9: This interface is a highly simplified standardized mechanical interface but still shows the genericity of the proposed standardization.

In the mechanical domain, the cogging torque is equivalent to a non-linear elastic effect that depends on the relative angular position of the rotor and stator. Therefore, it is modelled as a C element in this Figure 2.23.

From an electrical point of view, the (permanent magnet) LAT motor is modelled as an equivalent DC motor. The model is based on physical topology. The upstream and downstream wirings are connected to a 1 junction, representing a serial circuit, on which the inductance, resistance and electro-magnetic force are respectively modelled with I (L_{mot}), MRS (R_{mot}) and the GY elements. In addition, electrical faults can be triggered. The short circuit corresponds to a low resistance between both wirings. Strongly increasing the resistance in the serial circuit opens the circuit.

Note 2.10: The causality on the MRS modelling motor resistance (R_{mot}) is reversed regarding the preferred causalities detailed in Figure 2.16 for hydraulics. However, the analogy should be perfect between both the hydraulic and the electric domains. This difference is reasonable as the resistance is not tending to zero but to infinity. Thus, there is no risk of dividing by zero.

More detailed models are available in the literature, e.g. **[ROM00] [XU13]**. They include for example magnetic effects. But the increased complexity is not needed for our purposes and parameters can result more difficult to be obtained for an integrator such as Airbus Helicopters.

On NH90 actuators, the interface stage is composed of four LAT motors, whereas several coils are used for the EHSV-based actuators (usually three). Such redundancy can either be represented in an object-oriented way by instantiating the same motor model several times or by using multi Bond-graphs and connecting them to a standardized mechanical body. Their connection will not create a causality conflict as the standardized mechanical body is thought to connect several standardized interfaces.

3.4.3. Pilot Stage Virtual Model

The pilot stage drives the power modulation stage from the output of the interface stage. For the same reasons as for the interface stage, no particular model of the hydro-mechanical actuator is presented

here. The hydro-mechanical actuator is usually the continuity of the lever (interface stage), but some actuators can have more complex mechanical kinematics.

3.4.3.1. Clutches on a Shaft – DDV-Based Actuator

By definition, the DDV pilot stage is the rotor shaft that drives the valves. However, in the mechanical path from the interface to the power modulation stages, passive torque limiting clutches are added. This is a way to passivate certain failures (e.g. motor seizing between rotor and stator or current hardover). Therefore, both the clutch and the shaft are included in the DDV pilot stage virtual model.

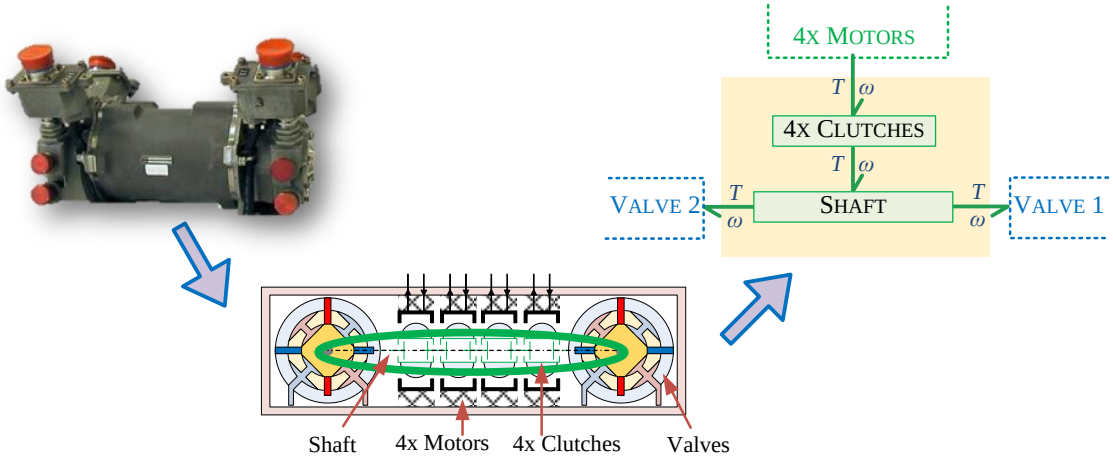

Figure 2.24 – Pilot stage: mechanical power path simplified from Figure 2.4.

On DDV actuators, the clutch is usually an open-ring linking. It functionally enables one degree of freedom in rotation (relative angular velocity) between two bodies: the motor rotor and the shaft (pilot stage). It is initially pre-loaded and its low stiffness (slightly damped) allows relative motion between both bodies when the generated torque exceeds the pre-load. In addition, sliding friction exists when relative motion occurs.

Indeed, the clutch perfectly fits within the standardized mechanical interface. Transformation ① of the standardized mechanical interface corresponds to the rotor radius (the following 0 junction could be removed but is left in order to show the same basis as Figure 2.6). Transformation ③ is a unitary ratio as the stiffness is in the same rotation axis as both mechanical bodies. Only one clutch is detailed in Figure 2.25.

On its side, the shaft is modelled as a standardized mechanical body which interacts with the four clutches and the two power modulation stages, in the case of NH90 actuators.

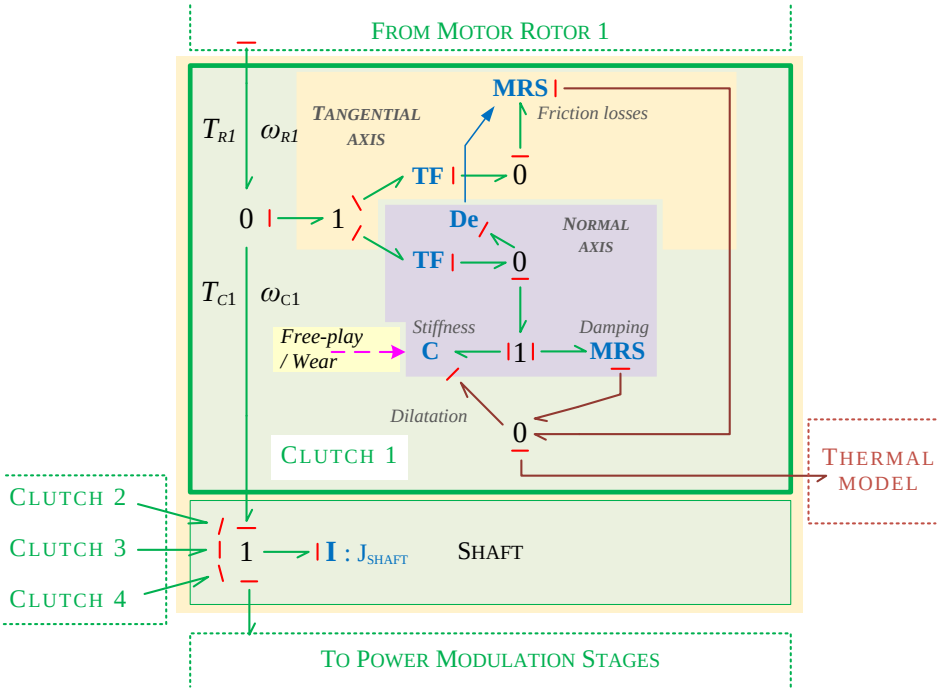

Figure 2.25 – DDV pilot stage virtual model: clutches and shaft.

Note 2.11: This clutch modelling implies that, even if it is a mechanical part, it has been chosen to model it as an interface. This makes sense as no inertial effect of the open-ring is required but compliance and friction effects are of interest.

3.4.3.2. Hydraulic Potentiometer Piloting the Spool Faces – EHSV-Based Actuator

On EHSV, the pilot stage[18] can be seen as a hydraulic potentiometer. It acts on the pressures available at the spool faces. Two[19] main technologies (Figure 2.26) exist for hydraulic potentiometers:

– the double flapper-nozzle. It consists of a movable flapper that varies the restriction at the nozzle outlets (see Figure 2.26-(a)).

– the jet-pipe. It consists of a movable jet with two collector holes that direct fluid to one or the other end faces of the spool **[THO90]**, (see Figure 2.26-(b)).

[18] On EHSV, the pilot stage is usually called first stage. The term pilot stage is introduced in this dissertation for reasons of genericity, independently of the technology.
[19] The jet deviator can be seen as a variant of the jet-pipe.

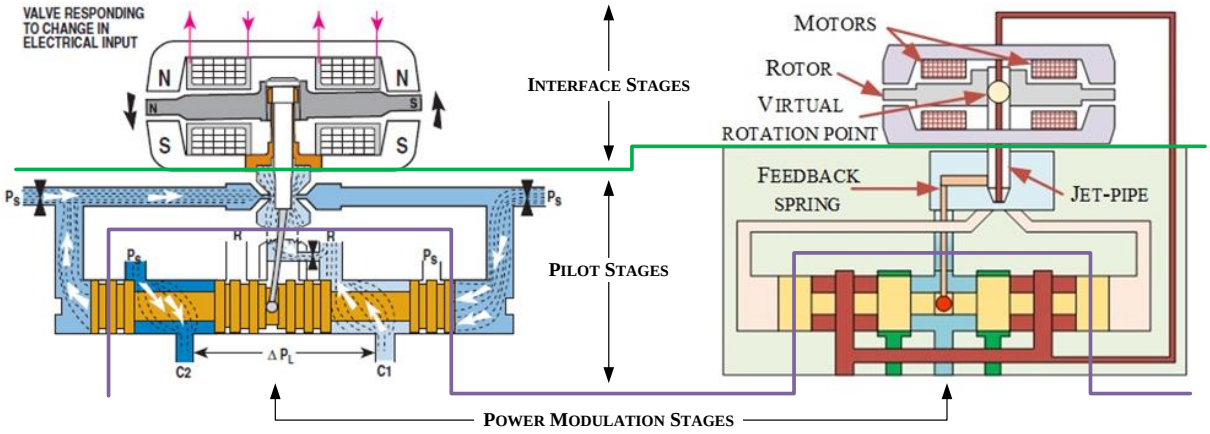

(a) – Double Flapper-Nozzle [MOO14] (b) – Jet-pipe

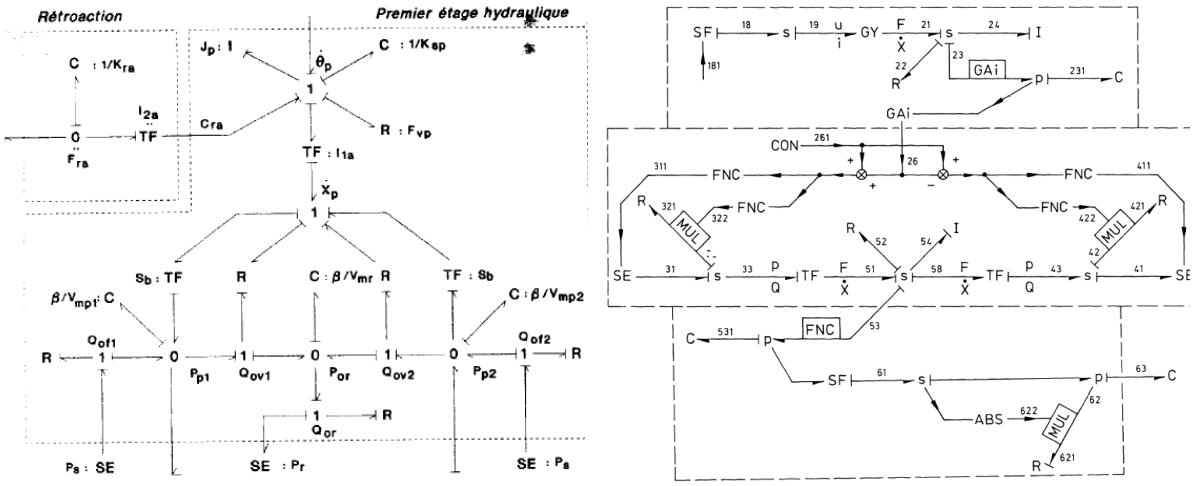

(c) – Double Flapper-Nozzle model [MAR93] (d) – Jet-pipe model [THO90]

Figure 2.26 – EHSV technologies and their pilot stage models.

In aerospace applications, jet-pipes are preferred for their lower leakage and sensitivity to fluid pollution. Unfortunately, jet pipes are complex to model (and to design). Some models are available: Thoma wrote the continuity and momentum equations and converted them into a Bond-graph model of a jet-pipe servovalve [THO90] (Figure 2.26-(d)); Somashekhar et al. proposed an analytical model [SOM06] of this type of EHSV.

Flapper-nozzle models are more often seen in the literature. Maré [MAR93] proposed the model of the first stage shown in Figure 2.26-(c). It remains almost unchanged up to today, e.g. [ROM00] or [XU13].

Note 2.12: If the cylinder model presented above is to be used, the interfacing with the double flapper-nozzle model from Maré should be done at the C element (i.e. β/V_{mp1} and β/V_{mp2}). If not, the bonds going out from P_{p1} and entering in P_{p2} should include a TF element, the ratios of which equal the spool area, in order to be consistent with a force.

3.4.4. Power Modulation Stage Virtual Model

The power modulation stage for the three considered technologies is a hydraulic valve. The valve can be linear or rotary, but in both cases the model is similar (only the type of variable and the parameters change). It has been decided to present a linear valve virtual model with two pressure inlets at the ends and a return outlet in the centre. This makes it coherent with the valve presented in Chapter 1 for the EHSV technology (Figure 1.19). A DDV-based virtual model can either include a rotary valve or an additional kinematic to the pilot stage acting as a rotary-to-linear transformation, depending on the solution implemented on the modelled actuator.

The virtual model of a hydro-mechanical valve can be viewed as the combination of two coupled submodels, each one representing one physical domain. On the one hand, the hydraulic virtual model represents the functional part of the valve that is to modulate hydraulic power. It interacts with the power distribution network virtual model. On the other hand, the mechanical virtual model provides the spool motion and forces to the pilot stage virtual model. Its interfaces are the pilot stage and housing.

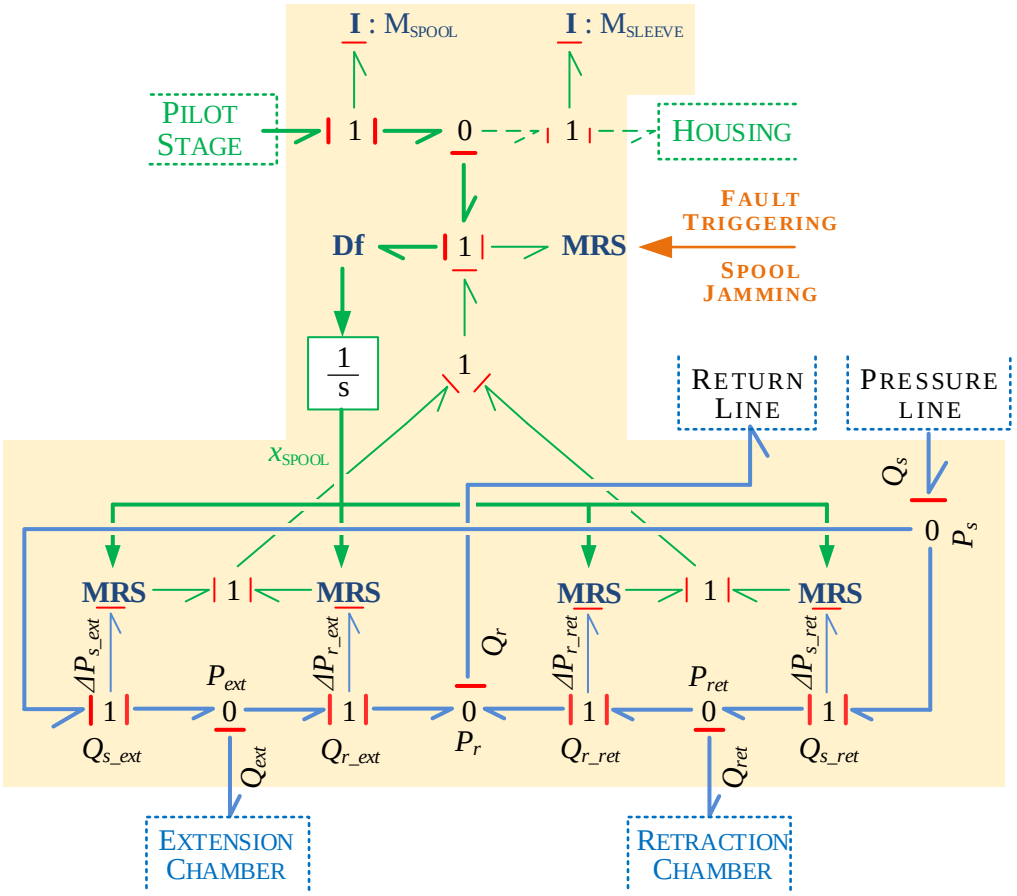

Figure 2.27 – Power modulation stage virtual model: hydro-mechanical valve.

Consistency with the cylinder model has been reached by splitting the valve with respect to the cylinder side it is aimed to provide with fluid power. Subscripts "s" and "*r*" are respectively relative to the supply and return lines.

High coupling exists between both sub-models. The valve opening modulates the hydraulic restrictions which feed/empty the cylinder chambers from the hydraulic power distribution network. The volume flow rate going through the valve creates a negative hydrodynamic flow force on the spool in the closing direction **[MER67]**. The dependency of both the pressure drop and the hydrodynamic flow force on the volume flow rate are here modelled by a RS-field modulated by the spool position. This has been introduced by **[RAB81]** at the difference that a R-field was used instead of a RS-field.

It is important to note that the valve opening corresponds to the relative position of the spool with respect to the sleeve. Most valve models consider only the spool position, which is not false as long as the sleeve is fixed, as is the case for the EHSV. On a DDV-based actuator, however, the sleeve is a back-up spool able to move within a spring-box (similarly to hydro-mechanical actuator e.g. **[MARG11]**). It is thus possible to simulate valve jamming by increasing the friction between the spool and the sleeve. A second hydraulic spool virtual model should thus be modelled for the back-up spool, which is not represented here for reasons of readability.

Such a model is not rigorously energetically consistent. Indeed, Wolfgang Borutzky **[BOR10]** provides a detailed, energetically consistent model which includes, in addition, the flow displaced by the spool motion and the flow inertia. It would be a perspective to implement such a model and compare it with our model in terms of accuracy and simulation time.

3.4.5. Closed Loop Virtual Model

On fixed-body hydro-mechanical actuators, the position loop shall be closed with bonds representing the associated kinematics from the output rod to the input lever (interface stage). This is required in order to ensure that power is transmitted and not only the position information required for position loop closure. As shown in Chapter 1 (Figure 1.17-(b)), moving body actuators do not require any additional kinematic for position loop closure.

Concerning electro-hydraulic actuators, the different loops are closed electrically. Sensors are integrated on the actuator to measure the desired variable. Typically, on aerospace actuators, the rod-housing relative position is required and on DDV-based control modules, both the angular position and the speed of the shaft are also needed. Thus position sensors are implemented and if the speed is required, it is derivated from the position.

Unfortunately, Bond-graphs do not allow measuring the generalized displacement variable, but effort and flow variables. Thus, a position sensor is a flow detector which is integrated subsequently. In practice, the position is often already available through a C element. Otherwise, if the speed is derived from the position, it has to be shown in the Bond-graph model in order to avoid measuring the speed directly in a further implementation.

Usually, position sensors are xVDT[20] which require an excitation current of several kilohertz, then the simulation step as to be as small as a few microseconds. A detailed model of an xVDT is not desirable on the actuator virtual model as it would dramatically slow the simulation. Therefore, simplified models are used including only the signal part of the sensor: a gain, an offset, a dynamic, dither and the possibility to trigger fault (constant or erratic signals).

A simplified model of the actuator closed loop has been developed with specificities of the numerical ACL including sampling, quantification, filters **[MAR00]**, time for calculation and interpolation for smoothness in the delivered signal.

4. ACTUATION SYSTEM SIMULATION

The Actuation System is an important contributor to the Flight Control System overall performance. The proposed modelling permits convenient access to the parameters influencing these performances. It also allows simulating scenarios that are not desirable to be tested in real flights. Thus, it becomes easier to evaluate an Actuation System design and establish recommendations.

In order to illustrate how it is possible to benefit from this Actuation System modelling, three scenarios are investigated. The realism is incremented between each virtual test. The first simulation involves a single actuator connected to an ideal hydraulic power generation and distribution system. The second test case is an increment of the first one: the realistic models of both the hydraulic power generation and distribution systems are added. Finally, in the third case, the three other actuators are also added, which means that the entire Actuation System is modelled.

4.1. Load Contribution to Performance

The first scenario is created[21] to emphasize the contribution on the actuator performances of the antagonist load it usually faces. In order to demonstrate this phenomenon, the hydraulic power generation and distribution systems are considered ideal (constant supply pressure without pressure drop in the pipes) and the fluid temperature is set at 70 % of T_{max} [°C] (defined in section 3.2.1).

[20] LVDT or RVDT, Linear or Rotary Variable Differential Transformers.
[21] The term “created” is used as this scenario is not representative of flight conditions. However, this scenario facilitates revealing actuator performance/load dependency.

From the centred position, three different responses to a step of desired displacement representing 25 % of the actuator full stroke are plotted:

– The actuator response without load. It shows the ideal step response of the actuator. In this case, the actuator reaches its no-load speed limitation, induced by the valve maximal opening, and then the desired position without overshoot or oscillations.
– The actuator response under a defined loading scenario in nominal operation (two hydraulic circuits are available – "2Hyd" in the figure). This curve provides the actuator nominal response affected by the load.
– The actuator response under a defined loading scenario after the loss of one hydraulic circuit ("1Hyd" in the figure). This shows a degraded performance case of the actuator.

The load scenario is a combination of a compression static load (75 % of the actuator stall load) and a sine wave dynamic load at a frequency of nearly 20 Hz (amplitude equals 25 % of the actuator stall load) – zone ③. Plotting the response to the static load first (zone ②) revealed the hydro-mechanical natural frequency of the actuator and the static error.

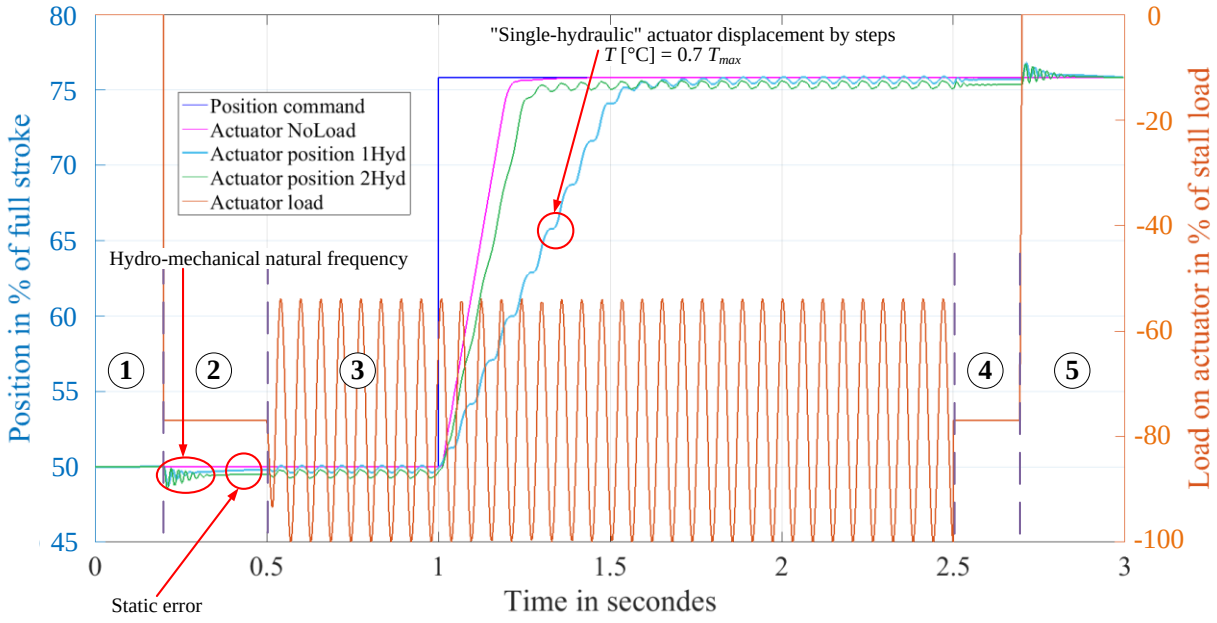

Figure 2.28 – Impact of the load on actuator response, before and after the loss of one hydraulic system.

Note 2.13: Zone ① serves for initialization. It ensures that the actuator is at equilibrium before applying on it the load scenario. Zones ④ and ⑤ emphasizes that the actuator reach the same position when removing the loads.

While the two-hydraulic supply is active, actuator response is slightly affected by the external load. When one hydraulic supply is lost, the "single-hydraulic actuator" is displaced "by steps". Indeed, at some point the actuator reaches its maximum load capability and is no longer able to provide speed.

Based on this remark, the actuator sections shall be sized considering only one remaining single hydraulic circuit and its performance shall be evaluated under the maximum static and dynamic loads.

4.2. Temperature Contribution to Performance

Figure 2.29 repeats the previous virtual test on a single hydraulic actuator but the hydraulic power generation and distribution systems are introduced considering a fluid temperature at 70 % of T_{min} [°C] (far below zero °C). This scenario is aimed at emphasizing the benefit of modelling the hydraulic network of the Actuation System, which will be included in the following simulation.

Note 2.14: In this dissertation, actuator reversibility is defined as the effort of an actuator to go in one direction (or to hold a position) while being driven in the other direction by the load which exceeds its stall load capacity. As a consequence, the pressure in the chamber that is connected to the pressure line via the valve is higher than the pressure in the supply pressure line. This induces a back flow from the chamber to the pressure line.

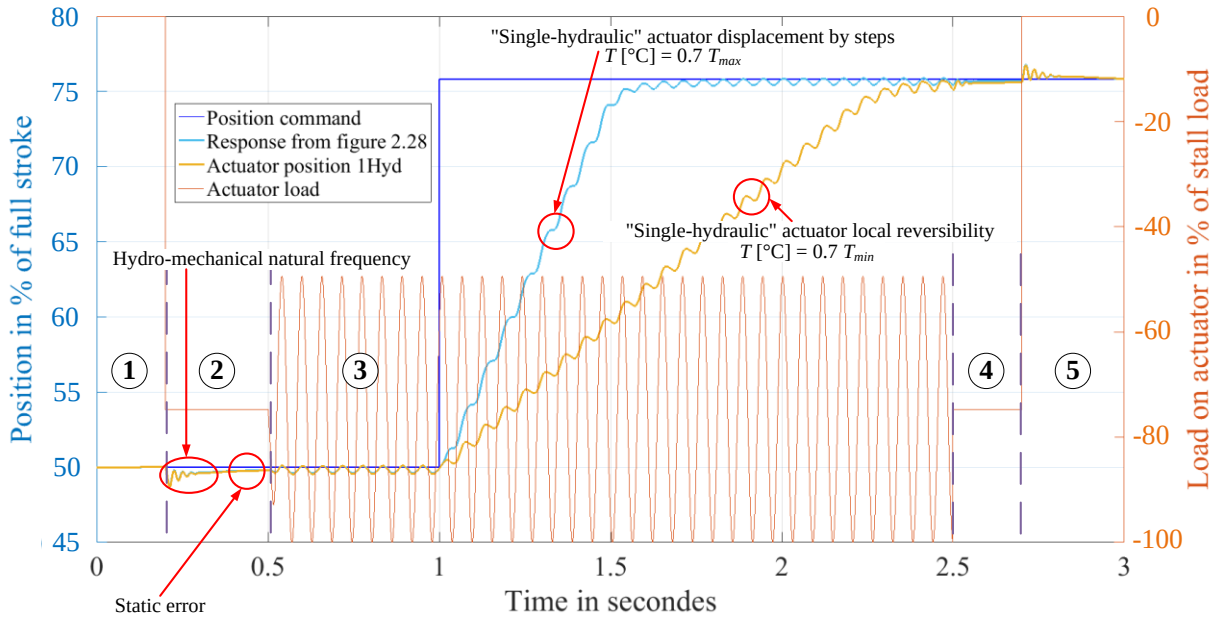

Figure 2.29 – Impact of the temperature on actuator response, similar condition as for the previous virtual test.

The single-hydraulic actuator response time is increased by a factor of nearly 2.5. The actuator is even driven backwards by the load. Indeed, in these moments, the actuator punctually and cyclically enters in reversibility (see *Note 2.14*). The back flow is observed in Figure 2.30[22] that shows both the volume flow rate and pressure drop at the valve orifice σ_{s_ext} for the time period [1.5;1.65] (approximately) of zone ③.

[22] The flow rate maximum demand corresponds to the flow induced by one actuator in motion at no-load speed.

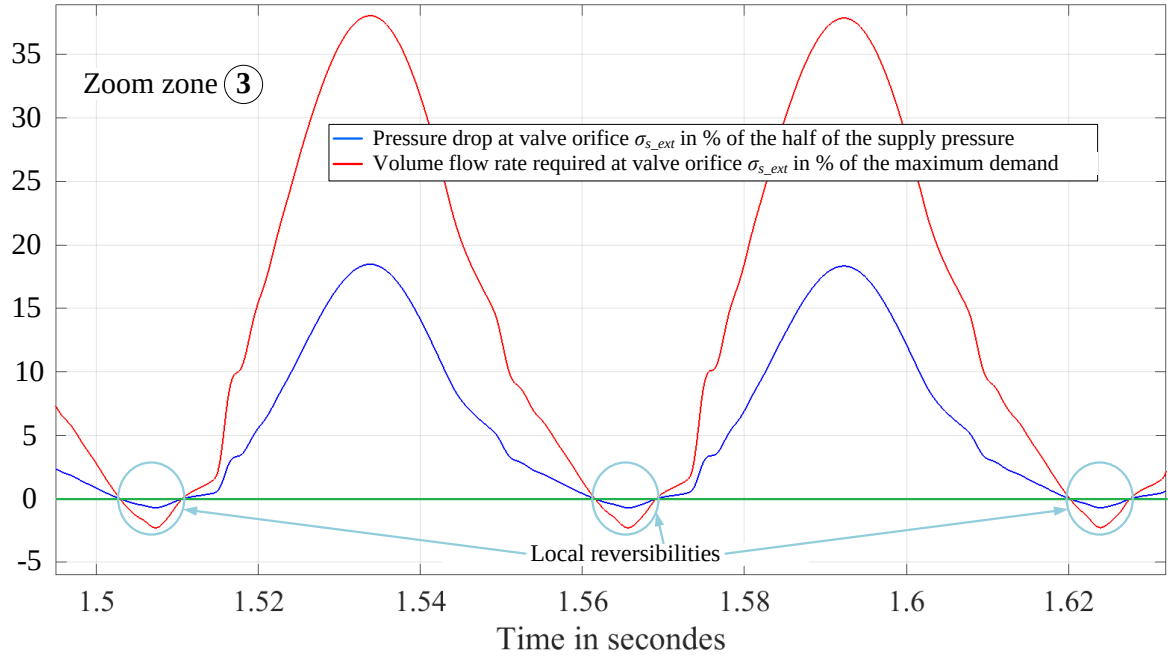

Figure 2.30 – Pressure-difference available at actuator inlet and volume flow rate required in the pressure line.

As the loading is identical to the previous test, the reversibility is due to the pressure losses in the supply and return pipes, which reduce the pressure available at the actuator inlet/outlet. This virtually decreases the actuator stall load capability.

This effect is even more perceptible when the position error (the difference between the input command and the actuator position) corresponds to the maximal opening of the valve. The fluid is no longer kept in the cylinder when the load induces higher chamber pressures than the one available at the actuator inlet/outlet.

Note 2.15: Recalling Equation 2.9, flow section σ is maximal and the pressure drop at the valve orifice ΔP is negative. Thus, the flow is negative; it goes out of the cylinder.

$$Q = c_q \sigma \sqrt{\frac{2}{\rho}|\Delta P|} sign(\Delta P) \qquad \textbf{Reminder of Equation 2.9}$$

Based on these observations and in addition to the previous recommendation, the sizing point shall be assessed considering the minimum operating fluid temperature.

4.3. Actuator Couplings

This last section emphasizes the need for simulating the entire Actuation System. The difference to the previous section is that the four actuators (three main rotor and one tail rotor actuators) are modelled.

Indeed, a coupling between the actuators exists and is illustrated in Figure 2.31. It shows that the performance of one actuator can depend on the other actuators' commands and responses.

As an example, the following test case has been simulated. On one side, a single-hydraulic actuator (the so-called "fore" actuator) faces its stall load but is required to hold a centred position – since zone ①. On the other side, the three other actuators are not exposed to any load but their input command is a ramp of 25 % of the full stroke per second – since zone ②. The induced flow demand corresponds to 30 % of the maximum pump capability. In this scenario, the fluid temperature remains at 70 % of T_{min} [°C].

After two seconds of initialisation (zone ①), it is possible to observe that the pressure-difference available at the fore actuator is near 98 % of the supply pressure. The reduction of 2 % of the supply pressure is induced by the four actuator valve leakages.

Since zone ②, the fore actuator enters in reversibility due to the pressure drop induced by the other actuator motions that require a volume flow rate. Thus, the pressure drop specified for one actuator design shall consider the potential motions of the other actuators.

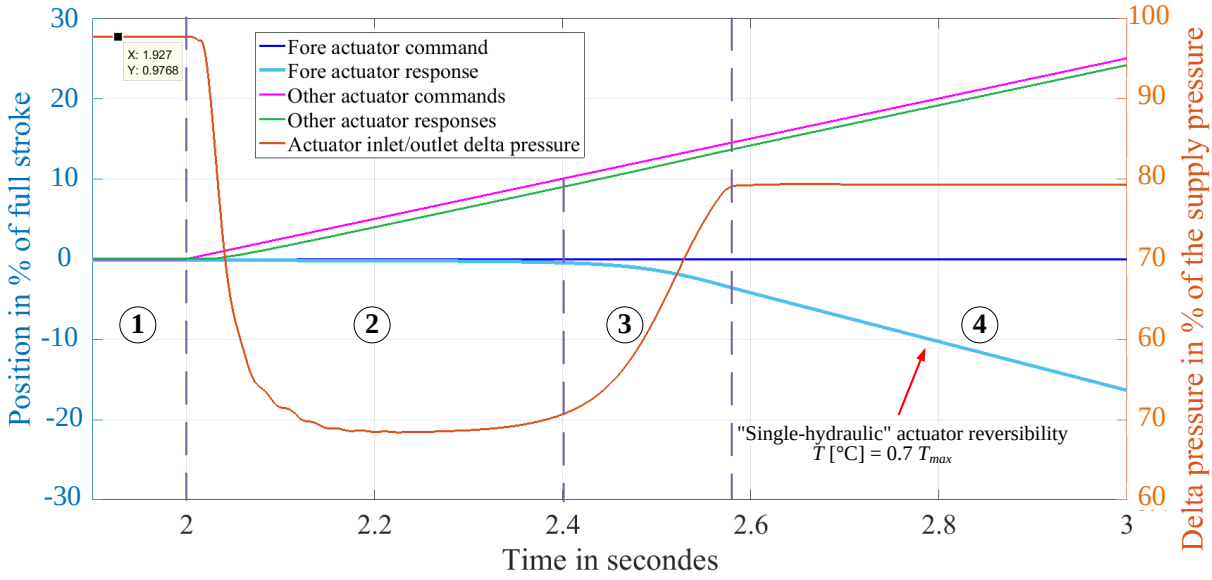

Figure 2.31 – Actuator response couplings.

It is interesting to note that actuator sinking is progressive for nearly 0.6 seconds. This can be explained as, in zone ②, the valve is almost closed[23]. The supply pressure decreases due to the other actuators motion, therefore the fore actuator enters in reversibility. But, the valve being almost closed, it creates a high restriction for the flow to get out of the cylinder. Thus the sinking is slow. However,

[23] Indeed, this small opening is induced by the load (and the closed loop gain), which causes a static error necessary to open the valve enough to provide the required pressure.

while the position error increases, the valve opening also does and thus creates less and less restriction, allowing a higher negative speed to the piston-cylinder assembly (zone ③). Once the valve reaches its maximal opening (zone ④), an equilibrium is found and the sinking continues at a constant speed.

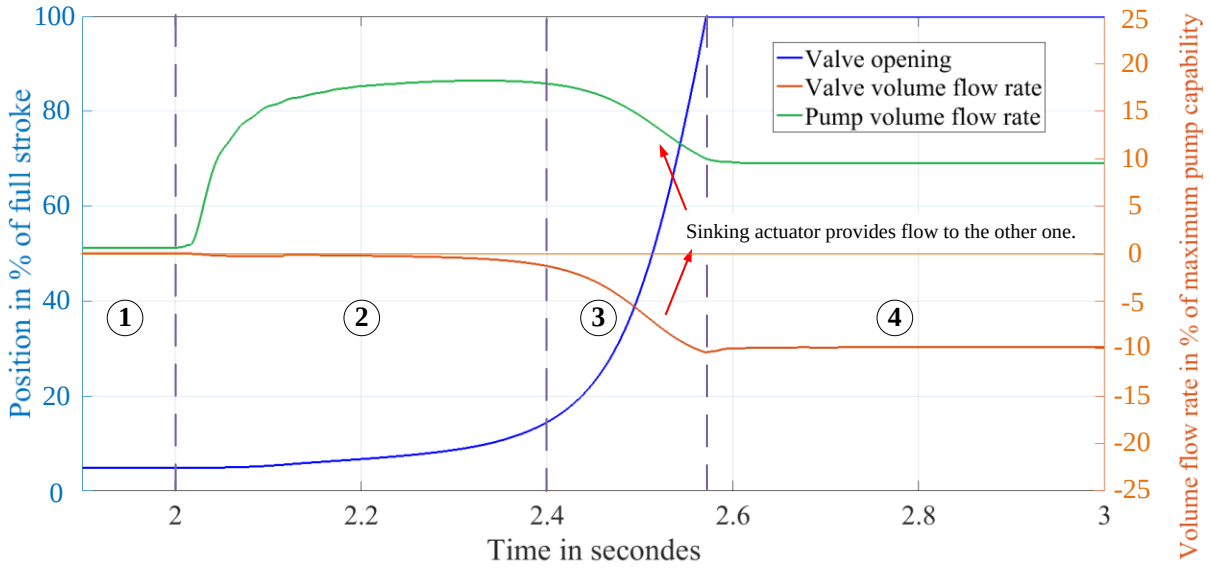

Figure 2.32 – Actuator response couplings: communicating flow rates.

Figure 2.32 shows an interesting aspect of the actuator couplings. The sinking of the fore actuator provides a volume flow rate to the hydraulic power distribution which benefits the other actuators. Therefore, a lower volume flow rate is required from the pump in zone ④.

Note 2.16: This illustrates once again the need for simulating the entire actuation system. However, no recommendations should be extracted from this observation as the actuator sinking is not desirable and shall never occur in the entire helicopter flight domain.

4.4. Actuation System Simulation

As a premise to these "coupled" simulations, it should be pointed out that each component involved in the Actuation System model has been verified unitarily, based on tests of the physical prototypes performed on test benches.

Integration tests of the Actuation System modelling have been done re-playing real command and load scenarios considering flight recordings.

Finally, this modelling has been integrated in a global flight control system model which involves the helicopter dynamics, realistic flight loads, the autopilot commands, etc. It enabled evaluating several architectures of a new Actuation System and verifying its final design at helicopter level **[COI16c]**.

5. CONCLUSION

Virtual models are widely used within the product lifecycle management from the early development phase on. They enable reducing the development time while ensuring a better fulfilment of the entire specification before the physical model is available. However, virtual models are also a potential source of error.

Therefore, in the first section, after introducing the terminology required for understanding, the modelling and simulation errors were detailed and illustrated with examples. It was concluded stating that effort must be put in architecting the models in order to reduce the number of errors.

The model architecting is addressed based on engineering and industrial needs. The Bond-graph formalism perfectly fits these needs and is therefore selected for the virtual model development. New concepts were proposed to improve model readability, balancing and readiness for further uses. Ways to model each physical domain involved in the Actuation System were detailed. Standardization of mechanical components was presented and widely used, thus highlighting their genericity. Standardized mechanical components are object-oriented and facilitate the creation of new mechanical virtual models while reducing the number of possible errors in the modelling phase.

Each subsystem of the Actuation System virtual model was detailed, component by component. An effort was made to standardize the interfaces using causal bonds, so that each subsystem from the same domain can easily be connected. This ensures correctness of further implementation in simulation software.

Finally, it was decided to simulate specific scenarios to illustrate how this modelling capitalizes knowledge and enables new studies to be carried out almost effortlessly. In this particular case, actuator sizing recommendations were provided regarding loads, temperature and Actuation System couplings. These simulations reinforce the need to implement a global Actuation System virtual model to evaluate new architectures of designs.

This complete virtual model has been used with success for a new helicopter development. Its aim is to size the actuators correctly, not only based on a sub-system specification (the actuator specification) but also based on a simulation verifying compliance with the Actuation System specification, in order to avoid oversizing or, even worse, undersizing of the actuators.

BIBLIOGRAPHY

[ASH56] ASHBY, W.R., *An Introduction to Cybernetics*, John Wiley, New York, 1956.

[ATT08] ATTAR, B., *Modélisation Réaliste en Conditions Extrêmes des Servovalves Électrohydrauliques Utilisées pour le Guidage et la Navigation Aéronautique et Spatiale*. Toulouse, France, 2008. (in French)

[BAR93] BARUS, C., *Isothermals, isopiestics and isometrics relative to viscosity*. American Journal of Science, pp87-96, 1893.

[BEA88] BEAMAN, J.J. & ROSENBERG, R.C., *Constitutive and Modulation Structure in Bond Graph Modeling*. Journal of Dynamic Systems, Measurement and Control, pp.395-402, 1988.

[BOE95] BOES, C., *Hydraulische Achsantriebe im digitalen Regelkreis*. RWTH Aachen, 1995. (in German)

[BOR10] BORUTZKY, W., *Bond Graph Methodology: Development and Analysis of Multidisciplinary Dynamic System Models*. New York: Springer-Verlag, 2010.

[BOR11] BORUTZKY, W., *Bond Graph Modelling of Engineering Systems – Theory, Applications and Software Support*. New York: Springer-Verlag, 2011.

[BRE82] BREEDVELD, P.C., *The Thermodynamic Bond Graph Concept Applied to a Flapper Nozzle Valve*. Proceedings of the 10th IMACS World Congress on Systems Simulation and Scientific Computation, volume 3, pp 395-397, 1982.

[BRE13] BREEDVELD, P.C., *Integrated Modeling of Physical Systems, Dynamic Systems part III*. Lecture notes, University of Twente, 2013.

[CEL91] CELLIER, F.E., *Continuous System Modelling*. Springer Science, 1991.

[CEL13] CELLIER, F.E., *Improvements in BondLib, the Modelica Bond Graph Library.* Proc. of the 2013 8th EUROSIM Congress on Modelling and Simulation, 2013.

[CLO80] MC CLOY, D. & MARTIN, H.R., *Control of Fluid Power – Analysis and design*. John Wiley & Sons, New York, 1968.

[COI16a] COÏC, C. & MARÉ, J.-C., *Modeling and Pre-Sizing Process for Hydrostatic Thrust Bearing with Special Consideration to Performance Robustness within a Wide Temperature Range*, International Conference on Hydraulics and Pneumatics, Praha, Czech Republic, 2016.

[COI16b] COÏC, C., FU, J. & MARÉ, J.-C., *Bond Graphs Aided development of Mechanical Power Transmission for Aerospace Electromechanical Actuators*, International Conference on Bond Graph Modelling, Montréal, Canada, 2016.

[COI16c] COÏC, C., BYZERY, R., MARGER, T. & ALLIETTA, J.-M., *Optimization of the Actuation System Sizing of a new Helicopter based on Global Modeling Approach*, Recent Advances in Aerospace Actuation Systems and Components, Toulouse, France, 2016.

[DAU00] DAUPHIN-TANGUY, G., *Les bonds graphs*, HERMES Science, Paris, 2000. (in French)

[EGG80] EGGERTH, S., *Beitrag zur Messung von Volumenströmen viskoser Flüssigkeiten in Druckleitungen.* Technische Universität Dresden, 1980. (in German)

[EIG12] EIGNER, M., GILZ, T. & ZAFIROV, R., *Proposal for functional product description as part of a PLM solution in interdisciplinary product development.* In International Design Conference, Dubrovnik, 2012.

[EUR04] EUROCOPTER, *AS332 Instruction Manual.* Marignane, 2004.

[FAI83] FAISANDIER, J., *Mécanismes hydrauliques.* Dunod, Paris, 1983. (in French)

[FU15] FU, J., MARÉ, J.-C., FU, Y. & HAN, X., *Incremental Modelling and Simulation of Power Drive Electronics and Motor for Flight Control Electro-Mechanical Actuators Application.* Proceedings of 2015 IEEE, International Conference on Mechatronics and Automation, Beijing, China, 2015.

[GAI79] GAINES, B., "General Systems Research: Quo Vadis," General Systems Yearbook, pp. 1-9 1979.

[GIL92] GILLE, J.-C., DECAULNE, P. & PELEGRIN, M., *Théorie et Calcul des Asservissements Linéaires*, Dunod, Paris, 1992. (in French)

[GUI92] GUILLON, M., *Commande et asservissement hydrauliques et électrohydrauliques.* Lavoisier, Paris, 1992. (in French)

[HOF81] HOFFMANN, W., *Dynamisches Verhalten hydraulischer Systeme, automatischer Modellaufbau und digitale Simulation.* RWTH Aachen, 1981. (in German)

[IDE66] IDEL'CHICK, I.E., *Handbook of hydraulic resistance.* Israël Program for Scientific Translations, 1966.

[JIN94] JINGHONG, Y., ZHAONENG, C. & YUANZHANG, L., *The Variation of Oil Effective Bulk Modulus With Pressure in Hydraulic Systems*. Transaction of the ASME. Journal of Dynamic Systems, Measurement and Control, pp116-144, 1994.

[KAR06] KARAM, W. & MARÉ, J.-C., *Comparison of EMA and HA performance for dynamic load simulators.* Proc. Bath Power Transmission and Motion Control Symposium – PTMC 2006, pp211-224, 2006.

[KAR12] KARNOPP, D.C., MARGOLIS, D.L., & ROSENBERG, R.C., *System dynamics: modelling, simulation, and control of mechatronic systems.* 5th ed. New York: John Wiley & Sons, 2012.

[KOR78] KORN, G.A. & WAIT, J.V., *Digital Continuous System Simulation,* Prentice-Hall, Englewood Cliffs, N.J., 1978.

[LEB84] LEBRUN, M., *Normal Modes in Hydraulic Lines.* American Control Conference, pp.458-467, San Diego, USA, 1984.

[LEE77] LEE, K.I., *Dynamisches Verhalten der Steuerkette Servoventil - Motor- Last.* RWTH Aachen, 1977. (in German)

[LIN14] VAN DER LINDEN, F.L.J., *General Fault Triggering Architecture to Trigger Model Faults in Modelica using a Standardized Blockset*, Proceedings of the 10th International Modelica Conference, Lund, 2014.

[MAR93] MARE, J.-C. *Contribution à la modélisation, la simulation, l'indentification et la commande d'actionneurs électrohydrauliques*. Thèse d'état, Lyon, 1993. (in French)

[MAR00] MARE, J.-C., *Commande numérique - bien spécifier pour maîtriser les effets parasites*, Revue Fluides, pp 41-45, N°17, 2000. (in french)

[MAR01] MARÉ, J.-C., *Simplified model of pressure regulated, variable displacement pumps for the sizing of complex hydraulic systems*, Proceedings of the 5th International Conference on fluid Power transmission and Control, Hangzhou, pp151-155, April 3-5, 2001.

[MAR12] MARÉ, J.-C., *2-D lumped paramaters modelling of EMAs for advanced virtual prototyping*. Proc. International Conference on Recent Advances in Aerospace Actuation Systems and Components (R3ASC), p. 122-127, Toulouse, 2012.

[MAR16] MARÉ, J.-C., *Requirement-based system-level simulation of mechanical transmissions with special consideration of friction, backlash and preload*, SIMPAT1572, Simulation Modelling Practice and Theory, p58-82, 2016.

[MARG11] MARGER, T., *Valve Design of Hydro-Mechanical Servoactuator under Cost and Mixability Criteria*. Arts et Métiers ParisTech, 2011.

[MARQ11] MARQUIS-FAVRE, W. & JARDIN, A., *Bond Graph pour la Conception de Systèmes Mécatroniques*. Techniques de l'Ingénieur D 3065, 2011.

[MER67] MERRITT, H.E., *Hydraulic Control System*, John Wiley & sons, Inc., 1967.

[MIN65] MINSKY, M., *Models, Minds, Machines*, Proceedings IFIP Congress, pp. 45-49, 1965.

[MOO14] MOOG, *Type 30, Nozzle-Flapper Flow Control Servovalves*. East Aurora, 2014.

[MUV10] MUVENGEI, O. & KIHIU, J., *Bond Graph Modelling of Inter-actuator Interactions in a Multi-cylinder Hydraulic System*, International Journal of Mechanical, Industrial and Aerospace Engineering, Vol.4 (1), 2010.

[NIK33] NIKURADSE, J., *Strömungsgesetze in rauhen Rohren*, VDI-Forschungsheft 361, 1933. (in German)

[OUL06] OULD BOUAMAMA, B. and DAUPHIN-TANGUY, G., *Modélisation par bond graph, Application aux systèmes énergétiques*, Techniques de l'Ingénieur BE 8 281, 2006. (in French)

[PAY61] PAYNTER, H.M., *Analysis and Design of Engineering Systems*, The M.I.T. Press, 1961.

[PRŠ13] PRŠIĆ, D., NEDIĆ, N. & DUBONJIĆ, L., *Modeling and Simulation of Hydraulic Long Trasmission Line by Bond Graph*, Journal of Mechanics Engineering and Automation 3, pp.257-262, 2013.

[PRU70] PRUDHOMME, R., *Automatique – Tome 1, Systèmes Séquentiels à Niveau ; Systèmes Asservis Linéaires Continus*, Masson & CIE, Paris, 1970. (in French)

[RAB81] RABIE, G. & LEBRUN, M., *Modélisation par les Graphes à Liens et Simulation d'une Servovalve à deux Étages*, R.A.I.O. Automatique/Systems Analysis and Control, 15, pp.97-129, 1981.

[REC00] RECHTIN, E., *The Art of Systems Architecting*, CRC Press LLC, 2000.

[REY86] REYNOLDS, 0., *On the Theory of Lubrication and its Application to Mr. Beauchamp Tower's Experiments, including an Experimental Determination of the Viscosity of Olive Oil*, 1886.

[ROM00] ROMAN, C., *Flow Control Servovalve Model*, Imagine, Roanne, 2000.

[SAE00] S.A.E., *AIR 1362 – Aerospace Hydraulic Fluids Physical Properties*. USA, 2000.

[SAE12] S.A.E., *ARP 994 – Recommended Practice for the Design of Tubing Installations for Aerospace Fluid Power Systems*. USA, 2012.

[SOM06] SOMASHEKHAR, S.H., SINGAPERUMAL, M. & KUMAR, R.K., *Modelling the Steady-State Analysis of a Jet Pipe Electrohydraulic Servo Valve*. Proceedings of the Institution of Mechanical Engineers, Part I, Journal of System and Control Engineering, vol. 220, pp.109,130, 2006.

[SJÖ10] SJÖLUND, M., BRAUN, R., FRITZSON, P. & KRUS, P., *Towards Efficient Distributed Simulation in Modelica Using Transmission Line Modeling*. 3rd International Workshop on Equation-Based Object-Oriented Languages and Tools, Norway, 2010.

[TCH79] TCHOUPRAKOV, Y., *Commande Hydraulique et Automatismes Hydrauliques*, Ed MIR, Moscow, 1979.

[THO75] THOMA, J.U., *Introduction to Bond Graphs and their applications*, Pergamon Press, 1975.

[THO90] THOMA, J.U., *Simulation by Bondgraphs - Introduction to Bond Graphs and their applications*, Springler-Verlag, 1990.

[THO99] THOMA, J.U. & HALIN, H.J., *Bondgraphs and Practical Simulation*, Simulation Practice and Theory 7, pp.401-417, Elsevier, 1999.

[VDI04] VDI GUIDELINE 2206, *Entwicklungsmethodik für mechatronische Systeme – Design methodology for mechatronic systems*, Beuth, 2004. (in German)

[VEL03] VELAZQUEZ, G. & MARÉ, J.-C., *Bottom-up design of a variable displacement vane pumps for automotive gearbox*, Proceedings of the 8th Scandinavian International Conference on Fluid Power, Tampere, Finland, 2003.

[XU13] XU, Y., *Modelling and Control of a High Performance Electro-Hydraulic Test Bench*, INSA de Lyon, 2013.

[ZEI76] ZEIGLER, B.P., *Theory of Modelling and Simulation*, John Wiley, New York, 1976.

Websites:

[web20Sim] www.20sim.com, accessed on 20/07/2016.

[webAME] www.plm.automation.siemens.com/en_us/products/lms/imagine-lab/amesim/, accessed on 20/07/2016.

[webBAR] http://www.barnesballscrew.com/how-a-ball-screw-works/ accessed on 02/09/2016

[webDYM] www.3ds.com/products-services/catia/products/dymola, accessed on 20/07/2016.

[webMAT] www.mathworks.com/products/matlab/, accessed on 20/07/2016.

CHAPITRE 3

METHODES DE DIMENSIONNEMENT DE PALIERS FLUIDES LINEAIRES SOUS CONTRAINTES AERONAUTIQUES

L'introduction de cette dissertation adressait les limitations actuelles des technologies de joints dynamiques et des moyens de guidages. Les paliers fluides linéaires ont été identifiés comme une alternative intéressantes pour le guidage en translation de l'ensemble piston-tige, en générant un effort de recentrage, au coût d'une faible fuite de fluide entre les chambres. Les paliers fluides pourraient être la clé de l'augmentation des performances des actionneurs sans dégrader excessivement sa durée de vie.

Le terme palier fluide inclus les paliers hydrostatiques, hydrodynamiques et hybrides. Comme leurs noms l'indiquent, les deux premiers types de paliers fluides listés utilisent respectivement :

Les forces hydrostatiques, générée par la pression sur une surface « fixe ».

Les effets hydrodynamiques du fluide, créés par la variation de pression induite par un déplacement relatif de deux surfaces.

Un palier fluide est qualifié d'hybride lorsqu'il combine les deux effets susnommés. Appliqués aux cas des actionneurs hydrauliques, le mouvement relatif entre l'ensemble piston-tige et le corps du vérin génère un effet hydrodynamique. Aussi, la pression dans les chambres du vérin induit un effort hydrostatique. Ainsi, seuls les paliers hybrides sont candidats à la substitution des fonctions de guidages dans vérins.

Néanmoins, dans le cas d'un paliers fluide hybride, le principe de superposition s'applique pleinement, révélant ainsi l'intérêt d'étudier séparément les paliers hydrostatiques et hydrodynamiques.

Pour l'ensemble de ce chapitre, trois critères de dimensionnement des paliers sont mis en avant : la génération d'effort normal ou de recentrage du palier fluide, son débit induit et la raideur normale ou radiale associée. Le dernier critère rend compte de la volonté de générer un effort de recentrage croissant avec l'augmentation de l'excentricité de l'ensemble piston-tige dans le corps du vérin. La complexité de satisfaire ces trois critères dans une application aéronautique réside grandement dans le domaine étendu de variation de température du fluide hydraulique ().

La première partie de ce chapitre porte sur l'étude d'un filet de fluide générique. Cette section 1 a pour but de présenter les équations prise en compte dans ce type d'étude. Une attention particulière est

portée sur la non-simplification des équations de manière à mettre en évidence tous les effets permettant de générer des variations de pression dans le filet de fluide. Le résultat est l'équation de Reynolds (Equation 3.6). Chaque terme de cette équation est discuté ainsi que leur intérêt dans notre étude.

Dans la section 2, trois différents designs de surface sont étudiés : plans parallèles, plans inclinés et plan en escalier. Les équations modélisant leurs capacités respectives à générer un effort normal, leurs débits de fuite induit ainsi que leurs raideurs sont analytiquement déterminées. Table 3.1 regroupe les équations des trois critères d'intérêt pour les trois surfaces étudiées. Deux des trois surfaces sont sélectionnées pour la suite de notre étude. En effet, la solution impliquant des plans parallèles ne génère aucune raideur radiale ce qui est rédhibitoire pour notre application.

La section 3 a fait l'objet d'une communication présentée en Keynote lors de la conférence internationale sur l'hydraulique et pneumatique à Prague en 2016 **[COI16a]**. Cette section détaille la modélisation et un processus pré-dimensionnement des paliers fluides hydrostatiques sous contraintes aéronautiques. Ces contraintes induisent une attention particulière à la robustesse des performances dans l'ensemble du domaine étendu de variation de température du fluide. Afin de satisfaire l'ensemble de nos critères, un orifice tube-court (« short tube orifice » en anglais) est inséré en tant que restriction amont nécessaire à la raideur du palier. Ce type d'orifice introduit un paramètre de dimensionnement d'intérêt, lequel peut aisément être adapté de manière à répondre au dilemme force/raideur versus débit de fuite sur la plage de variation de température du fluide.

Finalement, dans la section 4, une étude de sensibilité est menée sur les paliers hybrides coniques. Elle adresse la variation des trois principaux critères de dimensionnement face aux variables temporelles (i.e. température et excentration), ainsi que face aux paramètres de dimensionnement (i.e. la forme du palier). Les dangers liés à un mauvais design de paliers fluides, sur l'ensemble de la plage de température opérationnelle, sont mis en évidence. Notamment, cela peut conduire à un effort de recentrage négatif (soit excentrant l'ensemble piston-tige dans le corps du vérin) aux faibles températures. En effet, aux basses températures, l'effort hydrodynamique induit par le mouvement relatif des surfaces du palier peut annuler et même surpasser l'effort hydrostatique, généré par la pression dans les chambres du vérin. Des recommandations concernant le dimensionnement géométrique du palier sont finalement adressées de manière à satisfaire aux mieux les critères d'effort normal, de débit de fuite induit et de raideur du palier, pour l'ensemble de la plage de température.

CHAPTER 3:

METHODS OF LINEAR FLUID BEARING DESIGN UNDER AEROSPACE CONSTRAINTS

The Introduction of this dissertation addressed the limits of current dynamic sealing and bearing devices. Linear fluid bearings were identified as an interesting alternative for guiding the piston-rod in translation and resisting to radial forces, at the cost of minor leakage. Fluid bearings would increase actuator performance without excessively reducing its lifespan. Their main function is to guide the piston-rod assembly while allowing for a relative movement between both components without mechanical contact.

The term fluid bearing includes hydrostatic, hydrodynamic and hybrid bearings. As their names indicate, hydrostatic and hydrodynamic bearings respectively make use of:

- the hydrostatic force of the fluid, generated by an existing pressure on a "fixed" surface.
- the hydrodynamic effect[24] of the fluid, created by a pressure variation induced by a relative motion between surfaces.

A fluid bearing is called hybrid when it combines both hydrostatic and hydrodynamic effects. In our application, on the one hand, the relative motion between the piston-rod assembly and the actuator housing generates a hydrodynamic effect. On the other hand, the pressure chambers create a hydrostatic effect. Therefore, purely hydrodynamic or hydrostatic bearings cannot be used in our case, but hybrid bearings can.

In order to support the analysis of the different fluid bearings, the general case of a fluid film is studied in section 1. The aim is to introduce the equations that are used later in this chapter.

Section 2 presents the different surface designs leading to the generation of a normal force by the fluid film. As a first approach, lateral flow is neglected in order to render the functioning of each solution easily understandable. Two of the three designs presented are selected for a more thorough study under aerospace constraints in the next sections.

Section 3 details a modelling and pre-sizing process for hydrostatic thrust bearings with special attention being paid to performance robustness within a wide temperature range. Thrust bearings are studied here as combining at least three of them located at different azimuths is equivalent to a

[24] It is here preferred to use the term effect rather than force as hydrodynamic force is more generally used to describe the change in fluid momentum. **[MAR93]**

cylindrical bearing, in a first approach. The piston-housing or rod-housing play is small compared to their diameters, therefore piston or rod curvature can be neglected in a first approach.

Section 4 introduces the main relations for conical hybrid bearings. Two sensitivity analyses are carried out to assess the dependency of performance on the time variables (fluid temperature and eccentricity) and the design parameters (physical shape of the bearing).

Section 5 concludes this chapter by synthesizing the proposed process and recommendations.

1. STUDY OF A FLUID FILM – REYNOLDS EQUATION

In our future application – linear fluid bearings – the fluid film is aimed to generate a centring force preventing piston-housing or rod-housing contact. Such a force is generated by the pressure in the fluid film. It is thus natural that we are interested in the Reynolds equation, which provides the differential equation modelling the pressure distribution in the film **[REY86]**.

In this section, an element of the fluid film is analysed and, by applying the continuity equation and by computing the flow rate in the film, the Reynolds equation is demonstrated. The importance of each element of the Reynolds equation is discussed and simplification is made for our application. The simplified Reynolds equation serves as a basis for the next sections.

1.1. Fluid Film under Study

As a premise to our study, the considered fluid film is described and the main variables are introduced.

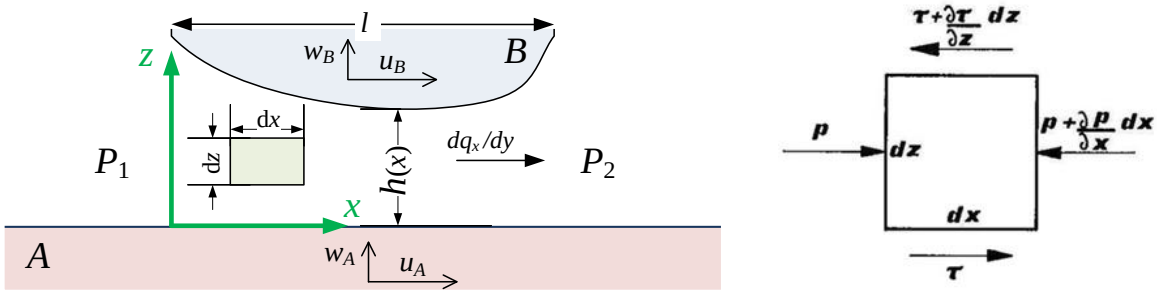

(a) – Generic fluid film with notations

(b) – Equilibrium of forces on an element of fluid **[VIE80]**

Figure 3.1 – Fluid film under study.

Fluid films involved in fluid bearings typically have a small height *h* compared to their length *l*. The length-height ratio can easily be more than several thousands. This implies that laminar flow can be considered in the film fluid[25]. Indeed, fluid film lubrication belongs to a flow class called "slow

[25] Establishment length, defined in Chapter 2 section 3.3.3, is not usually considered for fluid films.

viscous motion" **[HAM04]** where inertia effects can be neglected. This assertion is valid for the entire chapter and is verified after each pre-sizing in order to emphasize its correctness.

Figure 3.1-(a) represents the fluid film considered in our study. The film is delimited by two surfaces *A* and *B* in motion at speeds *u* and *w* (with subscript *A* and *B*) regarding respectively the *x* and *z* axes. *A* is considered to be extremely long with respect to *B* so the fluid film always exists. In addition, *A* is considered to be a plane surface so that the reference frame can be easily located; the shape defects are projected on *B*. The height of the fluid film can vary over the film length. For reasons of readability, in this figure, the length-height ratio is not representative of the order of magnitude previously described.

As a simplification for our study, the conditions are considered identical along the *y* axis. It is therefore only necessary to focus on an infinitely small slice in the *y* direction. Thus, the variable dq_x/dy is the surface flow rate[26] in the fluid film.

1.2. Continuity Equation

The continuity equation ensures the balance of mass in a volume. The difference between the output and input flows of mass from a volume of fluid must be equal to the variation of mass within the volume. Considering an element of fluid volume $dV = dx\,dy\,dz$, the continuity equation can be written as follows:

$$\left[\frac{\partial}{\partial x}(\rho u)+\frac{\partial}{\partial y}(\rho v)+\frac{\partial}{\partial z}(\rho w)\right]dx\,dy\,dz=-\frac{\partial \rho}{\partial t}dx\,dy\,dz \qquad \textbf{Equation 3.1}$$

where:

- *t* is the time [s]
- *v* is the surface speed along the *y* axis [m/s]

As detailed above, there is no variation along the *y* axis. Thus, after this simplification, it is possible to integrate the continuity equation in order to study a surface element $dS = h\,dx$.

$$\int_0^h\left[\frac{\partial \rho}{\partial t}+\frac{\partial}{\partial x}(\rho u)+\frac{\partial}{\partial z}(\rho w)\right]dz=0 \qquad \textbf{Equation 3.2}$$

This integral can be solved using Leibniz's integral rule for the second term, leading to:

$$h\frac{\partial \rho}{\partial t}+\frac{\partial}{\partial x}\left(\rho\int_0^h u\,dz\right)+\rho\left(w_B-w_A-u_B\frac{\partial h}{\partial x}\right)=0 \qquad \textbf{Equation 3.3}$$

The next step, described in section 1.3, is thus to compute the remaining integral, which corresponds to the surface flow rate dq_x/dy. Each term of updated Equation 3.3 is then commented in section 1.4.

[26] The term "surface" is used in contrast to "volume" when the three dimensions are considered.

1.3. Surface Flow Rate Calculation

The surface flow rate dq_x/dy is obtained by applying the equilibrium of forces to the surface element of fluid $dS = h\,dx$. Forces applied to this element are the pressure on both sides along the x axis and the shear stress on the z axis. Figure 3.1-(b) presents these forces on the element of fluid as seen by Viersma **[VIE80]**.

Laminar flow implies that the shear stress τ is due to the viscosity of the fluid under motion.

$$\frac{\partial P}{\partial x} = -\frac{\partial \tau}{\partial z} = \mu \frac{\partial^2 u}{\partial z^2} \qquad \textbf{Equation 3.4}$$

Double integration with respect to z variable provides a relation between the pressure distribution along the x axis and the coordinate z. The two boundary conditions required are defined by the speeds of the two solids A and B which the fluid speed equals at $z = 0$ and $z = h$. A second integration, over the entire height of the fluid film, is thus required in order to obtain the surface flow rate expression.

$$\frac{dq_x}{dy} = \frac{-1}{12\mu}\frac{\partial P}{\partial x}h^3 + \frac{u_A + u_B}{2}h \qquad \textbf{Equation 3.5}$$

Finally, the surface flow is the combination of the pressure-induced flow (Poiseuille – first term of the right part of Equation 3.5) and the velocity-induced flow (Couette – second term) **[ROW83]**.

1.4. Reynolds Equation

The Reynolds equation is obtained by including the surface flow rate (Equation 3.5) into the continuity equation in the form presented in Equation 3.3. The partial derivation applied to the Couette part of the flow reveals three more terms.

$$\underbrace{\frac{\partial}{\partial x}\left(\frac{\rho h^3}{12\mu}\frac{\partial P}{\partial x}\right)}_{\text{Poiseuille}} = \underbrace{\frac{\partial}{\partial x}\left[\frac{\rho h\left(u_A+u_B\right)}{2}\right]}_{\text{Couette}} + \underbrace{h\frac{\partial \rho}{\partial t}}_{\text{Local Expansion}} + \underbrace{\rho\left(w_B - w_A - u_B\frac{\partial h}{\partial x}\right)}_{\text{Squeeze}}$$

$$\underbrace{\frac{h\left(u_A+u_B\right)}{2}\frac{\partial \rho}{\partial x}}_{\text{Density Wedge}} \quad \underbrace{\frac{\rho h}{2}\frac{\partial}{\partial x}\left(u_A+u_B\right)}_{\text{Stretch}} \quad \underbrace{\frac{\rho\left(u_A+u_B\right)}{2}\frac{\partial h}{\partial x}}_{\text{Physical Wedge}} \quad \underbrace{\rho\left(w_B - w_A\right)}_{\text{Normal}} \quad \underbrace{-\rho u_B\frac{\partial h}{\partial x}}_{\text{Translational}} \qquad \textbf{Equation 3.6}$$

It is important to know that all these terms exist. It seems even more relevant to state whether each term is of importance or not for the calculation of the pressure distribution in the fluid film. In his book **[HAM04]**, Hamrock presents the Reynolds equation in the same manner as Equation 3.6 and details the physical meaning of each term. However, in this dissertation it makes sense to also discuss their effects and reasons why some of them can be neglected in the rest of our study.

- *Stretch*. The variation of speed along x axis of the surfaces A and B is not considered in this chapter as the surfaces consist of rigid solids. (This does not mean that the speed of each surface does not vary with time.)
- *Density wedge*. Also referred to as thermal wedge **[BLA60]**, it corresponds to the evolution of density in the fluid film. Even if this effect cannot be neglected for parallel surfaces, Jacques Faisandier demonstrates in **[FAI83]** the minor importance it has, compared to the physical wedge. Also, it is important to recall that the experimental frame associated with the fluid model developed in Chapter 2 only allows density variation if there is a change of pressure or temperature. The change of pressure along the x axis could possibly be implemented, but it would require considering several volumes in the film fluid, which is not desirable. Effort is made in the next sections to obtain a virtual lumped parameter model for the bearings as the density wedge can be neglected. Regarding the temperature variation along the x axis, this is outside the experimental frame. The fluid temperature can only vary with time in our virtual models.
- *Physical wedge*. The variation of the film height combined with surface motions generates a pressure variation. Conical and step bearings make use of this effect by respectively causing a continuous or discontinuous change of fluid film height. Therefore, it is widely used in this chapter. However, this effect has to be combined with translational squeeze in order to perceive clearly the effect of the surface speeds.
- *Translational squeeze*. The motion of surface B forces the fluid to go through a section with a different height, thus inducing pressure variation. The combination of translational squeeze and physical wedge results in an expression that depends on the differential speed between the two surfaces. This appears clearly in Equation 3.7. As a consequence, no pressure variation is induced if no relative speed exists between surfaces A and B or if $\partial h/\partial x$ is zero.
- *Normal squeeze*. This effect is the equivalent of translational speed in normal direction z. It is important to note that no height variation with x is required. This effect is used for example in dashpots, where the fluid film is the annular leakage and normal squeeze occurs in the dashpot volume. Normal squeeze shall not be neglected. However, it is important to emphasize that radial[27] motion is not relevant for our application: linear (axial) fluid bearings. Thus, this term often equals zero, i.e. whenever equilibrium is reached in the radial position. On the contrary, translational squeeze almost always operates as actuator motion is almost always required.
- *Local expansion*. This term links the fluid density variation with time at a given position with the induced pressure. Schmid **[SCH14]** affirms that this action is not important for fluid bearings.

[27] In cylindrical applications, the fluid bearing normal force becomes a radial centring force.

Once all these effects have been described, in addition to the Poiseuille term, only the physical wedge, the translational and normal squeezes are kept for further studying. This simplified Reynolds equation is presented in Equation 3.7.

$$\frac{\partial}{\partial x}\left(\frac{\rho h^3}{12\mu}\frac{\partial P}{\partial x}\right)=\frac{\rho\left(u_A-u_B\right)}{2}\frac{\partial h}{\partial x}+\rho\left(w_B-w_A\right) \qquad \textbf{Equation 3.7}$$

Finally, the density of the left part of the equation can be taken outside of the partial derivative. The rationale is the same as for neglecting the density wedge. Thus, dividing Equation 3.7 by the fluid density and rearranging the simplified Reynolds equation leads to:

$$\frac{\partial}{\partial x}\left(\frac{h^3}{12\mu}\frac{\partial P}{\partial x}-\frac{\left(u_A-u_B\right)h}{2}\right)=\left(w_B-w_A\right) \qquad \textbf{Equation 3.8}$$

This equation concludes this section. From the continuity equation, the Reynolds equation has been obtained and the importance of each of its effects has been discussed. For surface analysis, Equation 3.8 includes the simplifications described and is used further below in this chapter as the basis of fluid bearing applications.

2. CREATING A NORMAL FORCE IN FLUID BEARINGS

Fluid bearings allow a relative movement between two solids without mechanical contact. A pressurized fluid film acts as interface between the two moving solids. The main criteria for the design of fluid bearings are usually the normal force (to counterbalance an external load), the consumed flow **[ROW83]** (main source of power dissipation) and the stiffness **[POS89]** (the ability to increase the normal force with reduction of the film fluid height).

In continuity with section 1, axial analysis will be carried out based on Equation 3.8 in order to determine the possible manners to obtain a normal force in fluid bearings. Associated consumed flow and stiffness are discussed for each case.

Normal squeeze action is not considered. Position equilibrium on the *z* axis induces no relative speed in this direction. Neglecting this effect is indeed conservative as it would dissipate energy.

2.1. Constant Height Fluid Film

2.1.1. Normal Force

A simple design could be a constant height fluid film. Once the normal squeeze action is neglected and the height variation considered to be zero, Equation 3.8 becomes simply the double derivative of the pressure with respect to *x* is zero. The pressure distribution along the fluid film is easily obtained with a double integration. Boundary conditions are those of Figure 3.2-(b).

$$\frac{\partial^2 P}{\partial x^2} = 0 \quad \Rightarrow \quad P_{(x)} = \frac{P_2 - P_1}{l} x + P_1 \qquad \textbf{Equation 3.9}$$

The pressure distribution is linear, as it could be expected for a laminar flow between parallel lines. It is independent of the surface speeds. Integration along the *x* axis from 0 to *l* gives the linear force the bearing can provide in the normal direction.

$$\frac{df_x}{dy} = \frac{(P_1 + P_2)}{2} l \qquad \textbf{Equation 3.10}$$

Generating a normal force requires thus an "external" pressure, i.e. at least pressure provided to one side of the bearing. When no axial motion exists between the two surfaces, bearings that need a source of pressure to generate a normal force are called hydrostatic.

2.1.2. Consumed Flow

The consumed flow of a constant height fluid film is given by Equation 3.5 with substitution of the pressure rate.

$$\frac{dq_x}{dy} = \frac{(P_1 - P_2)}{12\mu l} h^3 + \left(\frac{u_A + u_B}{2}\right) h \qquad \textbf{Equation 3.11}$$

In the particular case of a hydrostatic bearing, the Couette effect has to be removed as surfaces are fixed. Equation 3.11 is reduced to the Poiseuille formula.

2.1.3. Stiffness

Regarding the last design criterion, the bearing stiffness seems to be zero as the film height does not explicitly influence the pressure distribution and thus the normal force. However, the boundary pressures can be made dependent on the fluid film height. This is the case for example in hydrostatic thrust bearings, which typically involve a pad with a recess and lands – surfaces that generate the bearing force. Stiffness of the bearing is achieved by inserting a fixed hydraulic resistance – usually an orifice or a capillary tube, or, as recently proposed, a short tube orifice – between the pressure source (ideally constant) and the bearing recess **[COI16a]** (Figure 3.2-(b)). A reduction of the fluid film height induces a higher restriction on the lands and thus a higher pressure in the recess.

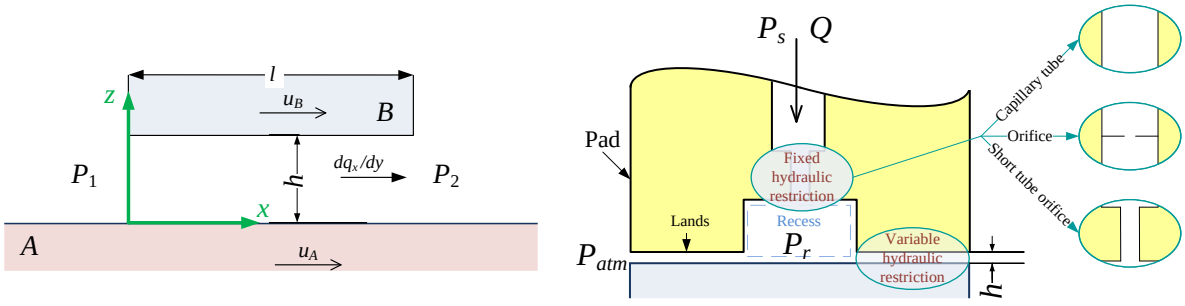

(a) – Fluid film under study (b) – Application: hydrostatic thrust bearing **[COI16a]**

Figure 3.2 – Constant height fluid film.

Hydrostatic bearings are studied in more detail in section 3. Particular attention is paid to compliance with specific aeronautical requirements.

2.2. Constant Height Gradient Fluid Film

Planar bearings with constant height gradient fluid films are usually referred to as fixed-incline slider bearings **[HAM04]**. Revolution bearings with constant height gradient fluid films are either called conical or tapered bearings **[VIE80]**. The taper height is referred as h_t .

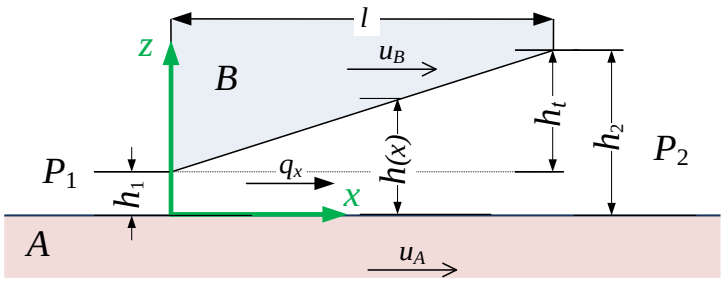

Figure 3.3 – Constant height gradient fluid film.

2.2.1. Normal Force

Integration of Equation 3.8 differs from section 2.1 in that the film height h varies with the coordinate x. It is already possible to anticipate that the double integration leads to a quadratic relation between the pressure and the fluid film height.

After proceeding to the double integration, the integration constants are found using the boundary conditions given in Figure 3.3. This finally gives the pressure distribution shown in Equation 3.12, where the height h equals $h_1 + h_t x/l$. This substitution makes the relation easier to read.

$$P_{(h)} = P_1 + (P_2 - P_1)\underbrace{\frac{(h_1/h)^2 - 1}{(h_1/h_2)^2 - 1}}_{\text{Hydrostatic effect}} + \underbrace{\frac{6\mu l}{h_t}(u_A - u_B)\frac{(h_1/h - 1)(h_2/h - 1)}{h_1 + h_2}}_{\text{Hydrodynamic effect}} \qquad \textbf{Equation 3.12}$$

Note 3.11: The hydrostatic effect corresponds to the Poiseuille term of the Reynolds equation, while the hydrodynamic effect results from the combination of both the Couette and translation squeeze terms.

In his study, Viersma **[VIE80]** obtained the same result[28] in a slightly different manner. He integrates directly with respect to h, whereas in this dissertation integration has been done with respect to x for coherence with the other sections. Hamrock noticed that the pressure gradient is zero at one point of the fluid film when boundary pressures equal zero and thus expresses the relation based on this point in **[HAM04]**. Viersma's relation is preferred here as the constants correspond to those of the boundary conditions and not to a particular point that has to be found in a further calculation.

[28] Both relations differ only in the factorization in our formula in order to have height ratios.

It is worth taking a closer look at Equation 3.12. The pressure distribution in the film fluid is the combination of two effects: hydrostatic (boundary pressures-induced) and hydrodynamic (surface speed-induced).

– *Hydrostatic effect*. It defines the pressure distribution when no relative speed exists between the two surfaces. Its contribution to the pressure distribution is a monotonic function.
– *Hydrodynamic effect*. It defines the pressure distribution based on the surface speeds only. It is a quadratic function which acts negatively if the relative speed ($u_A - u_B$) is positive.

Integration along the x axis from 0 to l provides the force f_x the bearing can provide in the normal direction. It is expressed per unit length in the following.

$$\frac{df_x}{dy} = \underbrace{\left[P_1 + (P_2 - P_1)\frac{h_1 + h_t}{2h_1 + h_t}\right]l}_{\text{Hydrostatic force}} + \underbrace{\frac{6\mu l^2}{h_t^2}(u_A - u_B)\left[\frac{2h_t}{2h_1 + h_t} + \ln\frac{h_1}{h_1 + h_t}\right]}_{\text{Hydrodynamic force}} \qquad \textbf{Equation 3.13}$$

As could be expected, if there is no hydrodynamic force, for parallel surfaces ($h_t = 0$) Equation 3.13 equals Equation 3.10. The study of the hydrodynamic axial force is less obvious. However, by writing $h_t = kh_1$ with k strictly positive, it is possible to find that the parenthesis is always negative[29]. Thus the hydrodynamic force becomes attractive when the relative speed is positive.

Note 3.2: The proportionality introduced here between h_1 and h_t must be used with caution for a conical piston. Eccentricity creates a dependency between h_1 and the azimuth, but h_t is a constant. Thus k becomes a function of the azimuth. Therefore, even if the introduction of this notation is helpful for the axial study and simplifies Equation 3.13, it is also a potential source of error for the rest of the study. It is thus not written explicitly and is not used in the rest of this section.

2.2.2. Consumed Flow

Equation 3.5 links the surface flow rate to the pressure distribution rate, which has already been calculated for the normal force computation. Substitution provides Equation 3.14.

$$\frac{dq_x}{dy} = \frac{P_1 - P_2}{(6\mu l/h_t)\left[1/h_2^2 - 1/h_1^2\right]} + \frac{(u_A + u_B)}{\left[1/h_2 + 1/h_1\right]} \qquad \textbf{Equation 3.14}$$

It is interesting to see that the speed-induced surface flow rate has no viscosity dependency. The linear relation between the surface flow rate and the relative speed is indeed due to the laminar flow.

[29] The function equals zero at $k = 0$ its derivative is always negative; thus the function decreases.

2.2.3. Stiffness

In order to study the evolution of the normal force with the change of the film height, the derivation of Equation 3.15 regarding z is calculated:

$$\frac{\partial}{\partial z}\left(\frac{df_x}{dy}\right) = -h_t\left[\left(P_2 - P_1\right)\frac{l}{\left(2h_1 + h_t\right)^2} + \frac{6\mu l^2}{h_t^2}\left(u_A - u_B\right)\left(\frac{4}{\left(2h_1 + h_t\right)^2} + \frac{1}{h_1\left(h_1 + h_t\right)}\right)\right] \quad \textbf{Equation 3.15}$$

The expression in brackets is always positive as long as the pressure difference and relative speed are both positive (i.e. $P_2 > P_1$ and $u_A > u_B$). Thus the derivate is negative while h_t is positive, inducing a decreasing force with an increasing film height. Looking at it the other way around, the decrease of the film fluid height induces an increase of the normal force, while the "greater of the two pressures, adjoining the bearing gap, prevails at the wide side of the gap" **[VIE80]**.

2.3. Discontinuous Height Fluid Film

A discontinuous height fluid film consists in having a step in the variable surface height. If both parts of surface *B*, before and after the discontinuity, are parallel to the other surface, the bearing is named after Lord Rayleigh, who first introduced this design **[RAY18]**. This is the only type of discontinuous height fluid film that is studied here. In the literature, it is also referred to as parallel-step slider bearing **[HAM04]** or stepped land piston for revolution bearing **[ETS75]**. Subscript "*st*" refers to the step discontinuity.

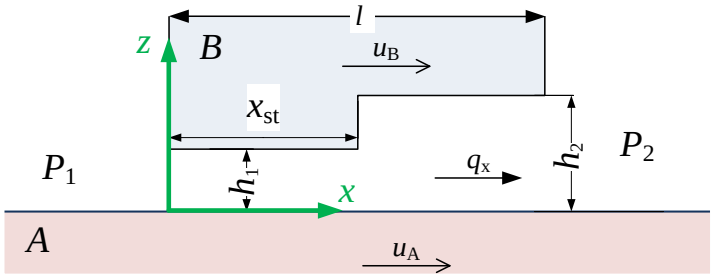

Figure 3.4 – Constant height gradient fluid film.

The study of the parallel-step slider bearing can be reduced to the study of two constant height fluid films combined with the continuity condition at the discontinuity **[FRE95]**.

2.3.1. Normal Force

The pressure distribution is found for both parts of the parallel-step bearing in the same manner as described in section 2.1.1. The initial conditions are those from Figure 3.4.

$$\begin{cases} x < x_{st} \quad \Rightarrow \quad P_{(x)} = \left(\dfrac{P_{st} - P_1}{x_{st}} \right) x + P_1 \\ x > x_{st} \quad \Rightarrow \quad P_{(x)} = \left(\dfrac{P_{st} - P_2}{l - x_{st}} \right) (l - x) + P_2 \end{cases} \qquad \textbf{Equation 3.16}$$

In order to calculate pressure P_{st} at the discontinuity, it is necessary to first determine the flow expression and then impose the equality of inlet and outlet flow rates **[FRE95]**. In this dissertation, the relation defining the discontinuity pressure is given below by anticipation:

$$P_{st} = \frac{P_1 h_1^3 / x_{st} + P_2 h_2^3 / (l - x_{st}) - 6\mu (u_B - u_A)(h_1 - h_2)}{h_1^3 / x_{st} + h_2^3 / (l - x_{st})} \qquad \textbf{Equation 3.17}$$

The contribution of the surface speeds to pressure P_{st} is positive if fluid is trapped in the step due to the surface motion.

The normal force is either obtained by integration or by analogy with section 2.1.1.

$$\frac{df_x}{dy} = \frac{(P_1 + P_{st})}{2} x_{st} + \frac{(P_{st} + P_2)}{2} (L - x_{st}) \qquad \textbf{Equation 3.18}$$

It is important to recall that the pressure at the discontinuity is dependent on the relative surface speeds. It has been chosen not to substitute the expression of P_{st} in Equation 3.18 as it has no added value and is less readable.

The parallel-step slider bearing design that maximizes the normal force is obtained when the height and length ratios equal $h_2 / h_1 = 1.866$ and $x_{st} / l = 0.718$ **[FRE97]**.

2.3.2. Consumed Flow

The consumed flow of the parallel-step slider bearing can be computed based on the parameters of both sides. The continuity equation ensures the equality of both relations.

$$\frac{dq_x}{dy} = \frac{(P_1 - P_{st})}{12\mu x_{st}} h_1^3 + \left(\frac{u_A + u_B}{2} \right) h_1 = \frac{(P_{st} - P_2)}{12\mu (l - x_{st})} h_2^3 + \left(\frac{u_A + u_B}{2} \right) h_2 \qquad \textbf{Equation 3.19}$$

It is possible to substitute P_{st} in order to have a surface flow defined by the boundary conditions.

$$\frac{dq_x}{dy} = (P_1 + P_2) \frac{\dfrac{h_2^3}{l - x_{st}}}{12\mu \left(1 + \dfrac{h_2^3}{h_1^3} \dfrac{l - x_{st}}{x_{st}} \right)} + \left(\frac{u_A + u_B}{2} \right) h_2 \frac{1 + \dfrac{h_2^2}{h_1^2} \dfrac{x_{st}}{l - x_{st}}}{1 + \dfrac{h_2^3}{h_1^3} \dfrac{x_{st}}{l - x_{st}}} \qquad \textbf{Equation 3.20}$$

The terms relative to both boundary pressures (P_1 and P_2) and surface speeds (u_A and u_B) have been separated. This facilitates assessing their contribution to the surface flow rate.

2.3.3. Stiffness

In order to study the evolution of the normal force with the decrease of the film height, the derivation of Equation 3.18 regarding z is computed:

$$\frac{\partial}{\partial z}\left(\frac{df_x}{dy}\right)=\left(\frac{1-\frac{h_2}{h_1}}{1+\frac{h_2^3}{h_1^3}\frac{x_{st}}{l-x_{st}}}\right)\left[\left(P_2-P_1\right)\frac{3l\,h_2}{2\left(l-x_{st}\right)}+\left(u_B-u_A\right)9\mu l\left(1+\frac{h_2^2}{h_1^2}\frac{x_{st}}{l-x_{st}}\right)\right] \qquad \textbf{Equation 3.21}$$

The expression in brackets is always positive as long as the pressure difference and the speed sum are both positive (i.e. $P_2>P_1$ and $u_B>u_A$). Thus, the decrease of the film fluid height induces an increase of the normal force as long as the highest pressure is on the wide side of the parallel-step bearing, as for constant height gradient bearings.

2.4. Solution Selection

Three manners to generate a normal force in fluid films have been studied in this section. These first approaches neglected lateral flows. Concrete application for aerospace actuation requires considering such flow.

However, the literature shows that parallel-step piston normal force is optimistic when discarding the lateral flow **[VOL72]**. It has therefore here been decided to focus only on the two other solutions for the rest of this chapter.

Fluid bearing integration in aerospace actuators is studied as substitution of conventional seals on pistons and bushings. In both applications, relative speed and pressure difference are involved. Therefore, the bearing could be referred to as hybrid. However, the term hydrostatic is abusively used as actuator speeds are low regarding the maximum bearing capability.

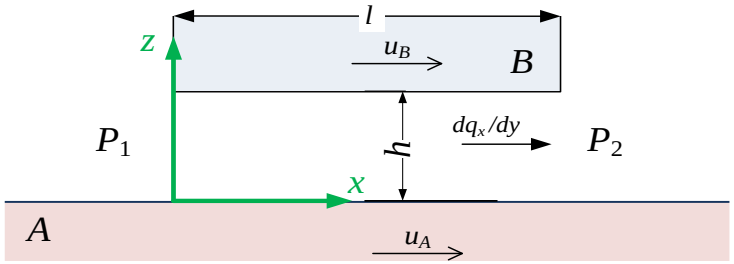	$\frac{df_x}{dy} = \frac{(P_1 + P_2)}{2} l$
	$\frac{dq_x}{dy} = \frac{(P_1 - P_2)}{12\mu l} h^3 + \left(\frac{u_A + u_B}{2}\right) h$
	No stiffness as long as the boundary pressures do not vary with the film height.
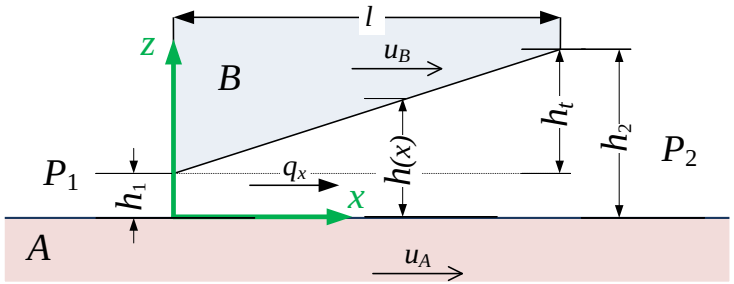	$\frac{df_x}{dy} = \left[P_1 + (P_2 - P_1)\frac{h_1 + h_t}{2h_1 + h_t} \right] l + \frac{6\mu l^2}{h_t^2}(u_A - u_B)\left[\frac{2h_t}{2h_1 + h_t} + \ln\frac{h_1}{h_1 + h_t} \right]$
	$\frac{dq_x}{dy} = \frac{P_1 - P_2}{(6\mu l / h_t)\left[1/h_2^2 - 1/h_1^2\right]} + \frac{(u_A + u_B)}{\left[1/h_2 + 1/h_1\right]}$
	$\frac{\partial}{\partial z}\left(\frac{df_x}{dy}\right) = -h_t \left[(P_2 - P_1)\frac{l}{(2h_1 + h_t)^2} + \frac{6\mu l^2}{h_t^2}(u_A - u_B)\left(\frac{4}{(2h_1 + h_t)^2} + \frac{1}{h_1(h_1 + h_t)} \right) \right]$
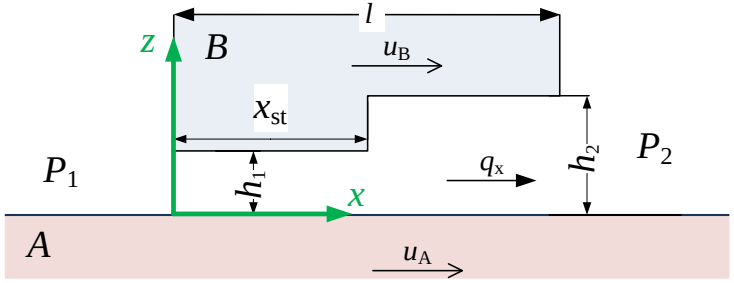	$\frac{df_x}{dy} = \frac{(P_1 + P_{st})}{2} x_{st} + \frac{(P_{st} + P_2)}{2}(L - x_{st})$
	$\frac{dq_x}{dy} = (P_1 + P_2) \frac{\frac{h_2^3}{l - x_{st}}}{12\mu\left(1 + \frac{h_2^3}{h_1^3}\frac{l - x_{st}}{x_{st}}\right)} + \left(\frac{u_A + u_B}{2}\right) h_2 \frac{1 + \frac{h_2^2}{h_1^2}\frac{x_{st}}{l - x_{st}}}{1 + \frac{h_2^3}{h_1^3}\frac{x_{st}}{l - x_{st}}}$
	$\frac{\partial}{\partial z}\left(\frac{df_x}{dy}\right) = \left(\frac{1 - h_2/h_1}{1 + (h_2/h_1)^3 (x_{st}/l - x_{st})} \right) \left[(P_2 - P_1)\frac{3l h_2}{2(l - x_{st})} + (u_B - u_A) 9\mu l \left(1 + \frac{h_2^2}{h_1^2}\frac{x_{st}}{l - x_{st}} \right) \right]$

Table 3.1 – Influence of the linear fluid bearing shape on its main design criteria.

3. DESIGN OF HYDROSTATIC THRUST BEARINGS UNDER AEROSPACE CONSTRAINTS

3.1. Background

In the common design approach of hydrostatic thrust bearings, the fluid viscosity is assumed to be constant for defining the fluid film thickness at the lands level, which offers the best combination of load capability, flow consumption and stiffness **[NIC95]**. The thrust bearing is thus optimized for a given operating temperature. This applies well to industrial applications where the fluid temperature is regulated within a narrow range.

As mentioned above, stiffness of the bearing is achieved by inserting a fixed hydraulic resistance – usually an orifice or a capillary tube – between the pressure source (ideally constant) and the bearing recess. In many embedded systems, neither the capillary tube nor the orifice meets the required performances over the extended range of temperature. On the one hand, the stiffness of the fluid bearing based on orifice design reduces too much at low temperatures. On the other hand, the consumed flow of the capillary tube design is excessive at high temperatures. An interesting alternative consists in using a short tube orifice (STO) that enables the laminar to turbulent transition to be managed by adequate sizing of its dimensions (diameter and length, typically).

*Note 3.3: This section uses knowledge about the capillary tube, orifice and variation of fluid properties with temperature. These pre-requisites are given in Chapter 2 and in **[COI16a]**.*

Note 3.4: In the present developments, the pressures indicated are gauge pressures.

3.2. Temperature Sensitivity

Most applications being industrial, cooling systems can be introduced to the hydraulic circuit to guarantee an operation near a single functioning point. Therefore, the design of a hydrostatic thrust bearing is usually optimized for a single operating point defined by temperature, bearing clearance and recess pressure (T_0, h_0 and P_{r0} – the subscript 0 refers to the design point for all parameters and variables in this dissertation). However, for power embedded systems the design is not so simple: the temperature range varies widely, typically by more than 150°C. This has been emphasized in Chapter 2 during the development of the fluid model. The sensitivity of the hydrostatic thrust bearing performance to temperature shall thus be assessed.

Some authors commented that the recess pressure of the thrust bearing, which impacts all the performances, is unchanged when the hydraulic restriction is of the capillary tube type. In contrast, the recess pressure is affected in case of use of an orifice **[ROW83]**.

This is understandable as the flows in the capillary tube and in the land are both laminar. In this case, they are equally related to the change of fluid characteristics, making, ceteris paribus, the recess pressure constant. This recess pressure only varies with the bearing clearance for a given supply pressure. For a hydrostatic thrust bearing with a capillary tube, the normalized recess pressure ($\beta_{cap} = P_r / P_s$), defined with reference to the supply pressure (P_s), is given by Equation 3.22. The parameter β_0 corresponds to the value of the normalized recess pressure at the design point.

$$\beta_{cap} = \frac{1}{1+\left(h/h_0\right)^3\left(1-\beta_0/\beta_0\right)} \qquad \textbf{Equation 3.22}$$

On its side, the orifice is designed to behave as a turbulent restriction which reacts differently to temperature variation than the bearing lands. As long as the turbulent pattern is satisfied, the orifice flow is only impacted by the fluid density, which is much less sensitive to temperature than viscosity.

In a design based on orifice as fixed restriction, the normalized recess pressure β_{orif}, can be expressed by application of the mass conservation theorem:

$$\left(h/h_0\right)^6 \beta_{orif}^2 + C_T^2 C_P \left(\beta_{orif} - 1\right) = 0 \qquad \textbf{Equation 3.23}$$

with C_T and C_P being two coefficients as defined below. The first one varies with the temperature while the second one is a constant defined by the recess pressure at design point:

$$C_T = \frac{\mu}{\mu_0}\sqrt{\frac{\rho_0}{\rho}} \qquad \textbf{Equation 3.24}$$

$$C_P = \frac{\beta_0^2}{1-\beta_0} \qquad \textbf{Equation 3.25}$$

It is relevant to notice that C_T also depends on oil pressure. However, the variation of dynamic viscosity and density due to oil pressure is negligible regarding the variation with the oil temperature.

The characteristics of a hydrostatic thrust bearing are given as dimensionless equations by Jean Frêne **[FRE95]**, obtained by division with reference values (subscript "*ref*"). A constant temperature is assumed, the normalized reference recess pressure equals one and the reference clearance is the clearance associated with the design point.

It is proposed here to use the same approach and to introduce the effect of temperature variation on performance. Therefore, the dimensionless static bearing force[30] ($\overline{W}$), the consumed flow ($\overline{Q}$) and the stiffness ($\bar{\lambda}$) become respectively:

[30] In the generic study, the fluid film normal force was named f_x. By contrast, the fluid bearing force is called *W*.

$$\overline{W} = \beta \quad \text{with} \quad W_{ref} = P_s S K_w \qquad \textbf{Equation 3.26}$$

$$\overline{Q} = \beta \frac{\mu_0}{\mu} \left(\frac{h}{h_0} \right)^3 \quad \text{with} \quad Q_{ref} = \frac{P_s h_0^3 K_w}{\mu_0} \qquad \textbf{Equation 3.27}$$

$$\overline{\lambda_{cap}} = 3\beta_{cap}(1-\beta_{cap}) \frac{h_0}{h} \qquad \textbf{Equation 3.28}$$

$$\overline{\lambda_{orif}} = 6\beta_{orif} \frac{(1-\beta_{orif})}{(2-\beta_{orif})} \frac{h_0}{h} \quad \text{with} \quad \lambda_{ref} = \frac{S K_w P_s}{h_0} \qquad \textbf{Equation 3.29}$$

where:

- S is the bearing surface (pad and recess) [m²]
- $K_w = W/(P_r S)$ is the load coefficient [-]

In Equation 3.26 and Equation 3.27, β has to be substituted by its expression obtained from Equation 3.22 or Equation 3.23 depending on the type of hydraulic fixed restriction (capillary tube or orifice). It is worth mentioning that:

- only the dimensionless flow rate is explicitly impacted by the temperature (through viscosity),
- when the restriction is made of a capillary tube, β does not depend on the temperature and, therefore, does not affect the static bearing force and stiffness. However, the flow rate increases drastically with temperature,
- when an orifice is used, the scheme is inverted. When the temperature increases, the static force and stiffness vary hugely (due to C_T) while the flow increases slowly, due to an implicit counter-effect of the dimensionless recess pressure.

3.3. A New Type of Fixed Restriction – The Short Tube Orifice

3.3.1. Characteristics of Ideal Fixed Restriction

When thrust bearings are used in an embedded hydraulic power system, their integration induces specific constraints and requirements: energy consumption must be minimized, static bearing force and stiffness must be greater than the minimum specified value for the entire range of temperature. Therefore, the bearing design based on an orifice is not acceptable because of its low stiffness at low temperatures. Unfortunately, the design based on capillary tube is not acceptable either, due to its excessive flow rate at high temperatures.

For this particular need, an "ideal" hydraulic restriction should:

- operate under laminar flow conditions at low temperatures,
- operate under turbulent flow conditions at high temperatures,
- enable selecting by design the temperature at which the transition between laminar and turbulent flow conditions occurs.

One candidate solution could have been to act on the wet perimeter of an orifice without changing its overall area. The Reynolds number is indeed sensitive to the wet perimeter **[LEW62]**. Such orifice definition would have created one degree of freedom for the laminar-turbulent transition. This option has been discarded for manufacturing reasons.

The solution selected for this purpose consists in using a short tube orifice as the hydraulic restriction of the thrust bearing.

3.3.2. STO Model Presented by Merritt

Manufacturing tolerances in addition to cost constraints usually lead to using orifices with a length L_T (short tube orifices – STO) instead of "ideal orifices". Therefore, studies were conducted on the characterization of such restriction.

In **[MER67]** the parametric model of the STO discharge coefficient was identified based on experiments and expressed as follow:

$$\begin{cases} c_q = \left[A + 64\left(\dfrac{L_T}{D_T R_e} \right) \right]^{-1/2} & for \quad \dfrac{D_T R_e}{L_T} < X \\ c_q = \left[B + C\left(\dfrac{L_T}{D_T R_e} \right)^{1/2} \right]^{-1/2} & for \quad \dfrac{D_T R_e}{L_T} > X \end{cases}$$

Equation 3.30

with A=2.28, B=1.5, C=13.74 and X=50.

This model was obtained by judicious combination of:

- the pressure loss model of a pipe with effect of the transition length to get a fully established laminar flow,
- the generic flow model of a hydraulic orifice,
- the model of a short tube orifice assuming square-edged entry and exit.

This short tube orifice model behaves as a capillary tube at very low Reynolds numbers but as an orifice with an equivalent coefficient of discharge of $c_q = [1.5]^{-1/2} \approx 0.8$ at high Reynolds numbers. It is worth mentioning that the coefficient of discharge was obtained on the basis of the well-rounded coefficient affected by the 0.5 loss coefficient due to the sharp edge entry. Introducing Equation 3.30 into the flow equation for orifices leads to the Hagen-Poiseuille equation (A can be neglected once $D_T R_e / L_T$ is sufficiently low).

The weak point of this model is that both expressions of c_q have no intersection. This generates a significant discontinuity at $D_T R_e / L_T = 50$.

3.3.3. New CFD-Based Model

The approach presented here is based on an adaptation of the former short tube orifice model considering the following requirements:

1. the model shall be continuous versus $D_T R_e / L_T$,
2. the model shall be a derivable function of $D_T R_e / L_T$,
3. the model parameters shall be identified in virtual experiments of CFD simulations,
4. the constant 64 in Equation 3.30 is maintained as it is needed for the establishment of the Hagen-Poiseuille equation at low $D_T R_e / L_T$.

Note 3.5: The two first conditions reduce numerical instability on simulation software.

The first two requirements give the two following relations between A, C and X:

$$A = B + \frac{64}{X}$$ **Equation 3.31**

$$C = \frac{128}{\sqrt{X}}$$ **Equation 3.32**

Then, almost 70 CFD simulations of different orifices were run with Fluent©. Each numerical experiment was defined by the value of the $D_T R_e / L_T$ factor, the diameter (D_T) and the length (L_T) of the STO, the pipe diameter (D_0 – upstream of the STO) and the fluid temperature. For manufacturing considerations, the entrance of the STO was assumed to be conical with a 118° cone angle instead of a square edge entry as for Merritt's model.

A design domain has been defined. Numerical experiments consider Reynolds numbers varying from 10 to 30000, the ratio L_T / D_T from 1 to 20 and the temperature covering the operating domain defined in AIR1362 for fluid MIL-PRF-83282 **[SAE00]**, typically from -40°C to +205°C.

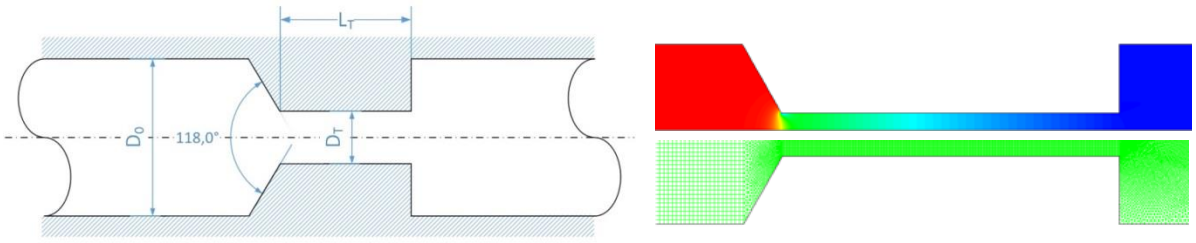

(a) – Scheme with nomenclature (b) – CFD mesh (bottom) and pressure (top)

Figure 3.5 – STO views for CFD simulation.

The CFD model was run imposing the downstream pressure and the upstream flow. The STO was meshed with 34,000 cells, K-epsilon was used as turbulent model and the wall was represented by the standard model. The flow coefficient value was then identified from the simulated upstream pressure,

according to Equation 3.23. This modus operandi allows for easy simulation of several STO geometries for a given $D_T R_e/L_T$ factor.

As first conclusions, the pressure drop is almost independent of the pipe-to-STO diameters ratio (D_0/D_T); the induced variation of c_q is in an order of 10^{-3}, which is perfectly negligible.

Then, for a given value of the $D_T R_e/L_T$ parameter, the variation of temperature also has an impact that is in the order of magnitude of the CFD simulation error and will no longer be considered for the c_q calculation.

Finally, the *A*, *B*, *C* and *X* values of the parametric model are identified using least square regression in order to adapt the model as much as possible to the simulations results. The new values specific to this STO are *A*=3.22, *B*=1.35, *C*=21.86 and *X*=35.

Figure 3.6 shows the former STO model and its discontinuity at the $D_T R_e/L_T$ transition. The CFD results and the new model are also plotted with Wuest and Von Misses asymptotes. For better readability, the new model is represented by a dotted line.

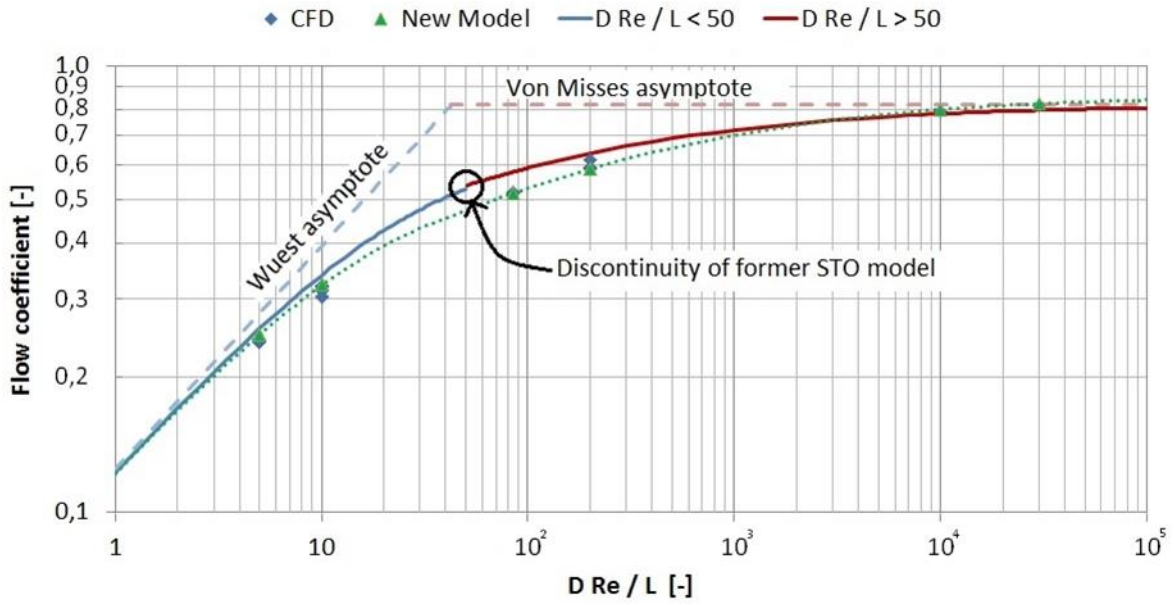

Figure 3.6 – Comparison of flow coefficients from CFD, Merritt model and the proposed new STO model.

Two main remarks can be made.

- The values of the flow coefficient differ slightly from the former model. This is due to the shape of the entrance of the STO model (cone with an angle of 118°) that is not a sharp-edge entry. Parameter *B* of Equation 3.30 now equals 1.35 instead of 1.5.
- The STO shape is also the reason why both models are not overlapping for the values of $D_T R_e/L_T$ from 10 to almost 1000.

It is interesting to note that the Wuest and Von Misses asymptotes intersect near $D_T R_e/L_T$ = 47, while Merritt gives the value 50 and for the proposed model it is 35.

It also is worth mentioning that if the intention had been to establish the new model, which is continuous and derivable, from plotted data presented in Merritt (square edge entry) **[MER67]**, the parameter values truncated after two decimals would have been A=2.24, B=1.5, C=13.75 and X=86.67.

3.3.4. Use of STO as Fixed Orifice for Hydrostatic Thrust Bearings

As defined in Equation 3.26 to Equation 3.29, the static bearing force, the flow and the bearing stiffness are highly related to the recess pressure. Therefore, the expression of the normalized recess pressure of the STO-based bearing must be identified.

The Reynolds number is the only variable of the new model of the STO flow coefficient. As it is function of the flow and used for the flow calculation, an algebraic loop must be solved. Fortunately, in the particular case of hydrostatic thrust bearings, some considerations can help:

- the ratio D_T/L_T is directly linked to the Reynolds number at the design point,
- the flow coefficient is thus only function of the ratio of the Reynolds number at the design point (R_{e0}) and at the point of study (R_e),
- the flow at the STO is considered to be equal to the flow on the lands. Therefore, the laminar equation can be used for the Reynolds calculation at the STO.

These considerations lead to the new expression that enables the algebraic loop to be removed:

$$\frac{L_T}{D_T R_e} = \frac{1}{X} C_T^2 \frac{\beta_0}{\beta} \left(\frac{h_0}{h} \right)^3 \qquad \textbf{Equation 3.33}$$

The inclusion of Equation 3.30 – considering Equation 3.33 – into the flow equation for an orifice provides the flow through the STO. Equalling it to the flow on the lands allows the determination of the normalized recess pressure. This pressure is consequently defined by one of the two following equations, depending on the value of $D_T R_e/L_T$:

$$\begin{cases} \left[\frac{AX}{64} \right] \left(\frac{h}{h_0} \right)^6 \beta^2 + \beta_0 C_T^2 \left(\frac{h}{h_0} \right)^3 \beta + \left[1 + \frac{AX}{64} \right] C_T^2 C_P (\beta - 1) = 0 \quad for \quad \frac{D_T R_e}{L_T} < X \\ \left[\frac{B\sqrt{X}}{C} \right] \left(\frac{h}{h_0} \right)^6 \beta^2 + \sqrt{\beta_0} C_T \left(\frac{h}{h_0} \right)^{4.5} \beta^{1.5} + \left[1 + \frac{B\sqrt{X}}{C} \right] C_T^2 C_P (\beta - 1) = 0 \quad for \quad \frac{D_T R_e}{L_T} > X \end{cases} \qquad \textbf{Equation 3.34}$$

Unfortunately, solving both parts of Equation 3.34 in order to get an analytical expression of the normalized recess pressure is not obvious. The recess pressure is thus calculated numerically. Consequently, the equation of the stiffness of an STO design-based hydrostatic thrust bearing is not presented. The bearing stiffness indeed equals the partial derivative of the static bearing force regarding

the clearance [FRE95]. To be conservative, the STO stiffness considered in the following is the minimum value obtained from the calculations based on Equation 3.28 and Equation 3.29, using the STO recess pressure. This can be justified as the STO should have a behaviour confined by the capillary tube and orifice responses. In practice, the stiffness based on the capillary tube is always the lowest one, considering equal normalized recess pressures.

3.4. Pre-Sizing Optimization

3.4.1. Optimization Process

It is proposed to initialize the pre-sizing process of a STO-based hydrostatic thrust bearing by using the design point (T_0, h_0 and β_0) which corresponds to $D_T R_{e0}/L_T = 35$. Such a point appears "naturally" in the model as the transition between laminar and turbulent flow conditions.

It is worth mentioning that the recess pressure expressed in Equation 3.34 only depends on:

- the design point (T_0, h_0 and β_0),
- the temperature of study (T) that impacts C_T,
- the clearance of study (h).

In order to simplify the presentation of the pre-sizing process, the optimization will be set around a particular clearance ($h/h_0 = 1$). It is indeed easiest to understand the study by plotting the requirements and results in 2D graphs. Considering h as a variable would have added a third dimension.

Criteria function G has to minimize normalized flow $\overline{Q}$ by action on vector Θ, under the vector of inequality constraints {c} over the entire temperature range.

$$J = \min_{\theta} \overline{Q}$$
$$\theta = \{T_0, h_0, \beta_0\}$$
$$\forall \overline{T} \in [-1;1], \quad \begin{cases} \overline{W} > \overline{W}_{\min} & \{c_1\} \\ \overline{\lambda} > \overline{\lambda}_{\min} & \{c_2\} \end{cases}$$

With the dimensionless temperature defined as follow:

$$\overline{T} = \frac{T - \frac{T_{max} + T_{min}}{2}}{\frac{T_{max} - T_{min}}{2}} \qquad \textbf{Equation 3.35}$$

The optimization is made possible by action on the design point. As mentioned above, the pre-design process is run around the design point clearance ($h/h_0 = 1$). Therefore, the design point is only defined by its temperature and recess pressure (T_0 and β_0).

3.4.2. Optimized Pre-Sizing

The objective is to design a hydrostatic thrust bearing satisfying the following performance requirements for the entire range of temperature:

- a dimensionless static load higher than 0.2
- a dimensionless consumed flow lower than 1
- a dimensionless stiffness higher than 0.4

The three types of hydraulic restriction – orifice, capillary tube and short tube orifice – are compared using the temperature at the design point as an optimization parameter. The results are presented in Figure 3.7, Figure 3.8 and Figure 3.9 for each restriction, depending on the temperature. The striped zone indicates the limit of the performance requirement.

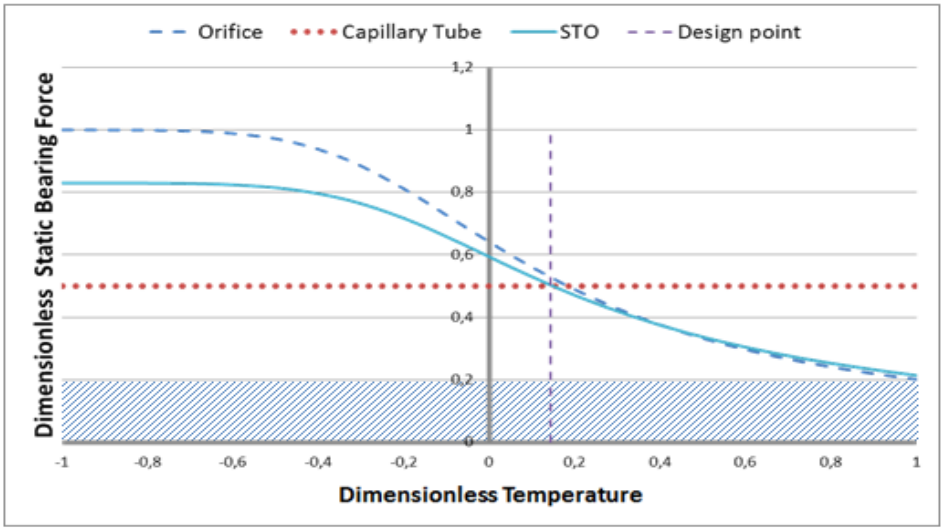

Figure 3.7 – Dimensionless static bearing force versus fluid temperature.

The dimensionless static forces of the bearings using the three different hydraulic restrictions are acceptable. The sensitivity of the STO to temperature is lower than that of the orifice but still much higher than that of the capillary tube.

If the static force requirement had not been met, the optimization would have tried to obtain a higher temperature value for the design point. This would have led to a wider range of constant static bearing forces, and thus to a higher force when the dimensionless temperature equals one. Of course, this is possible only if the other constraints are also satisfied.

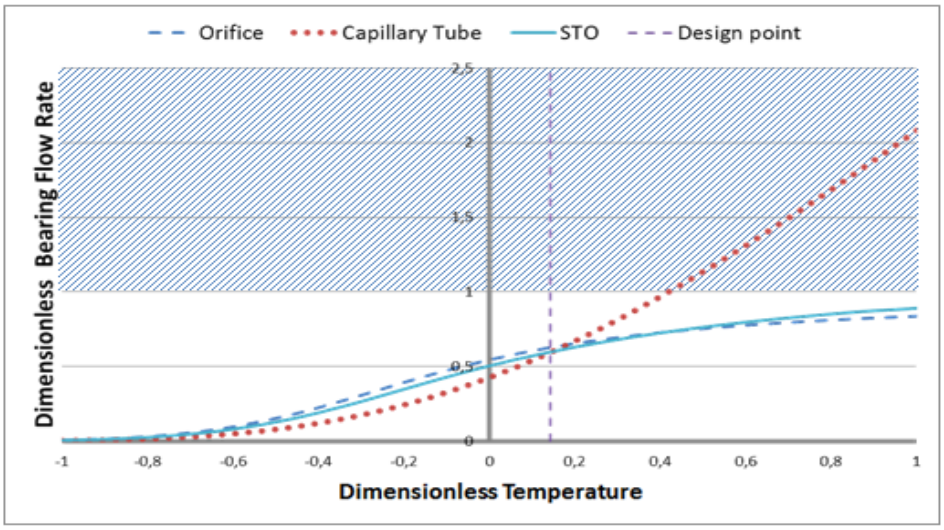

Figure 3.8 – Dimensionless bearing flow rate versus fluid temperature.

As expected, the dimensionless flow rate is slightly lower for an STO than for the orifice below the temperature of the design point and almost similar for greater values. The capillary tube cannot be selected for this embedded system application due to the high flow rate, which is more than twice the requirement value.

Finally, the stiffness of the bearing with STO is compliant with the requirement as it behaves as a capillary tube once the flow has been established as perfectly laminar.

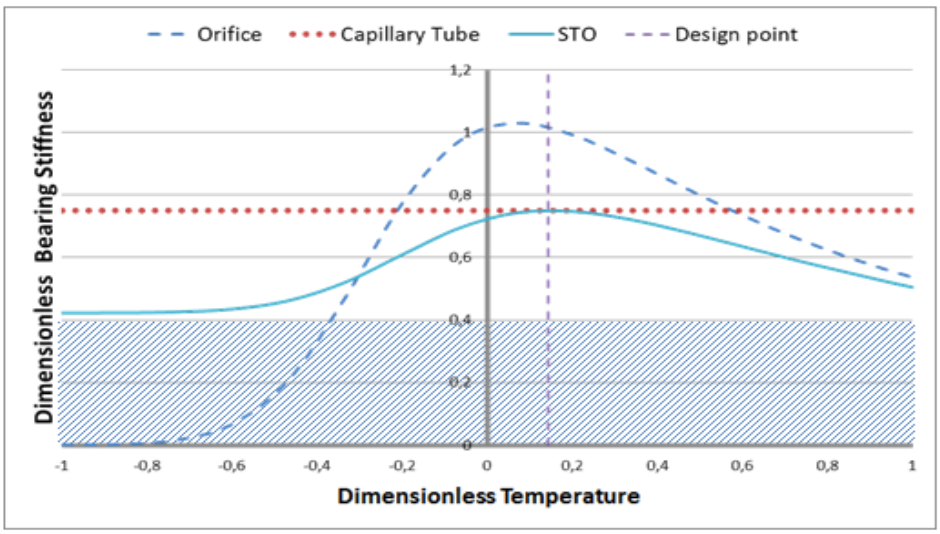

Figure 3.9 – Dimensionless bearing stiffness versus fluid temperature.

The compromise of the STO as hydraulic restriction for hydrostatic thrust bearings is a lower stiffness than the orifice around the design point temperature. However, this is perfectly acceptable as the more constraining point is at low temperatures.

As a synthesis, Table 3.2 provides the order of variation with temperature increase of the main performances for the three hydraulic restrictions discussed. The symbol "=" means constant, the sign "-" means the tendency is to decrease, whereas the sign "+" means the tendency is to increase.

	Capillary tube		Orifice		Short Tube Orifice	
	T < T0	T > T0	T < T0	T > T0	T < T0	T > T0
$\bar{W}$	=	=	-	- -	=	- -
$\bar{Q}$	+	+ + +	+ +	+	+	+
$\bar{\lambda}$	=	=	+ +	- -	=	- -

Table 3.2 – Influence of the hydraulic restriction type on hydrostatic thrust bearing parameters.

In particular, it can be remarked that the evolutions of the STO main parameters are similar to those of the capillary tube for temperatures below the design point and similar to those of the orifice for temperatures above the design point. The objective of obtaining a compromise on the behaviour for the fixed orifice is thus reached with an STO.

Note 3.6: The limit of the dimensionless approach is that the volume flow rate varies with the design point, due to the temperature effect on viscosity. This means that a loop might be necessary to calculate the flow constraints and confirm that the pre-sizing is acceptable.

3.5. Conclusion

A feasibility study was carried out to determine whether an orifice or capillary tube can be used as fixed hydraulic restriction for a hydrostatic thrust bearing designed for an embedded power system.

Respectively, low stiffness at low temperatures and a high flow rate at high temperatures were the causes of non-compliance for both technologies. For this reason, the short tube orifice was investigated as an attractive solution for making the fixed hydraulic restriction.

A new short tube orifice model, as a continuous and derivable function of $D_T R_e / L_T$, was proposed as an improvement of the existing model. Its parameters were identified by running CFD simulations. This model was used for the pre-sizing of a hydrostatic thrust bearing with the objective of meeting performance requirements within a wide range of temperatures.

Introducing a new STO model enables achieving an optimal pre-sizing of the hydrostatic thrust bearing. The key idea of the proposed design consists in exploiting the degree of freedom of the $D_T R_e / L_T$ ratio to place the temperature transition from a laminar to a turbulent flow pattern. Indeed, by configuring this temperature transition in the STO, a satisfying stiffness can be achieved at very low temperatures and a reasonable flow at very high temperatures.

4. DESIGN OF CONICAL HYBRID BEARINGS UNDER AEROSPACE CONSTRAINTS

4.1. Background

Conical hybrid bearings are well defined in the literature, mainly thanks to Viersma **[VIE80]**. From the constant height gradient axial fluid film, integration of the force and flow rate is performed on 360°, considering a possible piston eccentricity e in the housing. Indeed, the inclusion of eccentricity makes the fluid heights, h_1 and h_2, dependent on the azimuth φ (Figure 3.10).

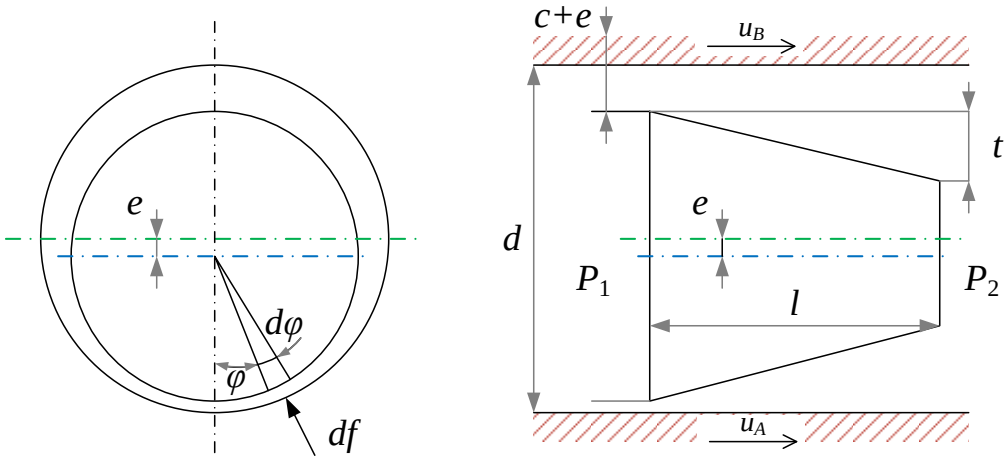

Figure 3.10 – Geometry and notations of a conical bearing from [VIE80].

The centring force W the conical hybrid bearing is able to provide is thus given, in the direction of the eccentricity, by:

$$W = \left(P_2 - P_1\right)\frac{h_t l \pi d}{4e}\left[\frac{2c + h_t}{\sqrt{\left(2c + h_t\right)^2 - 4e^2}} - 1\right] - \left(u_A - u_B\right)\frac{6\mu l^2 \pi d}{h_t e}\left[\frac{\sqrt{\left(c + h_t\right)^2 - e^2} - \sqrt{c^2 - e^2}}{h_t} - \frac{2c + h_t}{\sqrt{\left(2c + h_t\right)^2 - 4e^2}}\right]$$

Equation 3.36

The volume flow rate calculated by Viersma neglected the contribution of speed. The reason was that the leakage flow was much smaller than the displacement flow. This condition is not necessarily satisfied in our application. Consequently, the contribution of speed to the conical hybrid bearing flow has been calculated and added to the equation provided by Viersma:

$$Q=\left(P_2-P_1\right)\frac{\pi c^3 d}{12\mu l}\left[1+1.75\frac{h_t}{c}+1.5\left(1+\frac{h_t}{2c}\right)\left(\frac{e}{c}\right)^2\right]$$
$$+\left(u_A+u_B\right)\frac{\pi d}{2}\left(c+\frac{h_t}{2}\right)\left[1-\frac{\left(\frac{h_t}{2c+h_t}\right)^2}{\sqrt{1-\left(\frac{e}{c+h_t/2}\right)^2}}\right] \qquad \textbf{Equation 3.37}$$

Finally, the conical hybrid bearing stiffness can be derived from the normal force:

$$\frac{\partial W}{\partial e}=\left(P_2-P_1\right)h_t l\pi d\left[\frac{\left(2c+h_t\right)}{\left(\left(2c+h_t\right)^2-4e^2\right)^{3/2}}+\frac{1}{4e^2}\left(1-\frac{2c+h_t}{\sqrt{\left(2c+h_t\right)^2-4e^2}}\right)\right]$$
$$-\left(u_A-u_B\right)\frac{6\mu l^2\pi d}{h_t{}^2}\left[\left(\frac{1}{\sqrt{c^2-e^2}}-\frac{1}{\sqrt{\left(c+h_t\right)^2-e^2}}-\frac{4t\left(2c+h_t\right)}{\left(\left(2c+h_t\right)^2-4e^2\right)^{3/2}}\right)\right. \qquad \textbf{Equation 3.38}$$
$$\left.-\frac{h_t}{e^2}\left(\frac{\sqrt{\left(c+h_t\right)^2-e^2}-\sqrt{c^2-e^2}}{h_t}-\frac{2c+h_t}{\sqrt{\left(2c+h_t\right)^2-4e^2}}\right)\right]$$

This last equation is obviously not user-friendly, but actually only the speed, pressure, viscosity and eccentricity values are time variables.

4.2. Temperature and Eccentricity Sensitivity

The dependency on temperature of the three main design criteria (force, flow and stiffness) of the conical hybrid bearing is less complex than for the hydrostatic bearing. Indeed, the stiffness of the conical hybrid bearing comes from its tapered shape. This shape provides hydrostatic force, physical wedge and translational squeeze. Thus, unlike for hydrostatic bearings, no fixed restriction is required and the only variable affected by the temperature in the three main criteria equations is viscosity. But it is important to assess the performance variation with temperature for several eccentricities.

The three main criteria are studied for the extended range of temperature and several eccentricities. The results are presented in Figure 3.11, Figure 3.12 and Figure 3.13. In each of these figures, dashed lines show the contribution of pressure to the criteria (hydrostatic effect – subscript "*hd*"), dotted lines represent the contribution of speed (hydrodynamic effect – subscript "*hs*"), while the full lines stand for the combination of both.

Note 3.7: This study is carried out considering the data provided on the design example in ***[VIE80]****. A complete dimensionless study, such as the one carried out in the previous section, is almost impossible due to the complexity of the formula involved. Sensitivity to design parameters is thus analysed in the next section.*

Bearing data	Piston	Units
Diameter d	67	mm
Length l	50	mm
Clearance c	0.025	mm
Tapper h_t	0.05	mm

Table 3.3 – Dimensions of conical hybrid bearings used for this study from [VIE80].

Note 3.8: Pressure and speeds are taken at their maximal values so that the contribution of both effects is maximized.

The dimensionless centring forces increase with the temperature as the viscosity decreases – thus reducing the negative contribution of the hydrodynamic effect.

What is less obvious to perceive in Equation 3.36 is that, at very low temperatures, the hydrodynamic effect prevails over the hydrostatic effect. Furthermore, the eccentricity increases the coefficient which multiplies the viscosity in the hydrodynamic effect. Thus, considering the full temperature range implies designing the conical bearing at the maximal eccentricity and the lowest temperature. However, the centring force becomes negative for dimensionless temperatures below -0.9, which is not acceptable.

In this case, it is therefore recommended to reduce the dimensionless temperature range to [-0.8;1] if possible. This way, the highest eccentricity always corresponds to the maximum force. This implies indeed considering a positive stiffness regarding eccentricity.

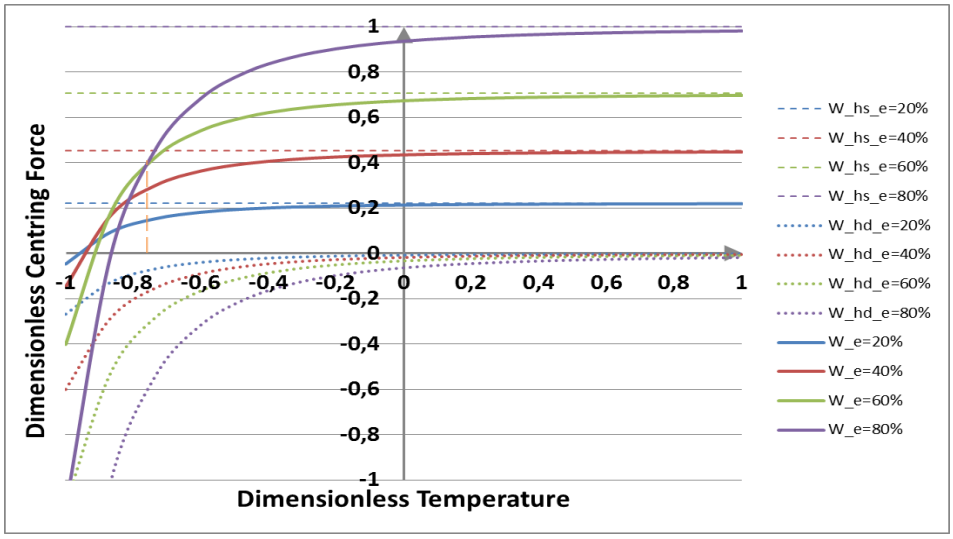

Figure 3.11 – Dimensionless centring force versus fluid temperature.

The dimensionless volume flow rate increases, as it could be expected based on Equation 3.37, with the temperature due to the laminar flow pattern. The hydrodynamic contribution to the global volume flow rate can be neglected in the extended temperature range. Indeed, below a dimensionless

temperature of -0.8, it is comparable to the hydrostatic contribution, but compared to the flow at high temperatures, both are in the order of 1%. This is consistent with Viersma's statement **[VIE80]**.

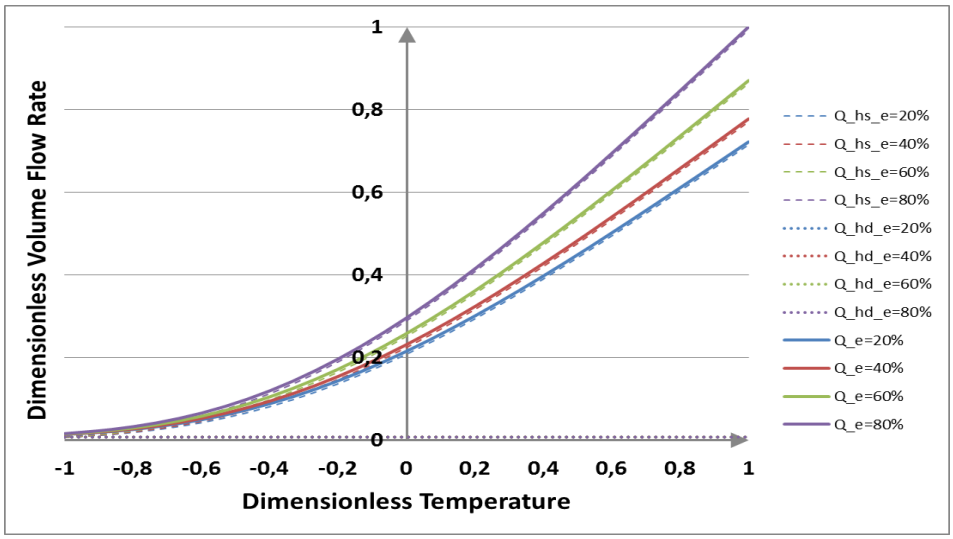

Figure 3.12 – Dimensionless volume flow rate versus fluid temperature.

The bearing should thus be designed considering the maximum eccentricity at the highest temperature, as this combination induces maximum flow.

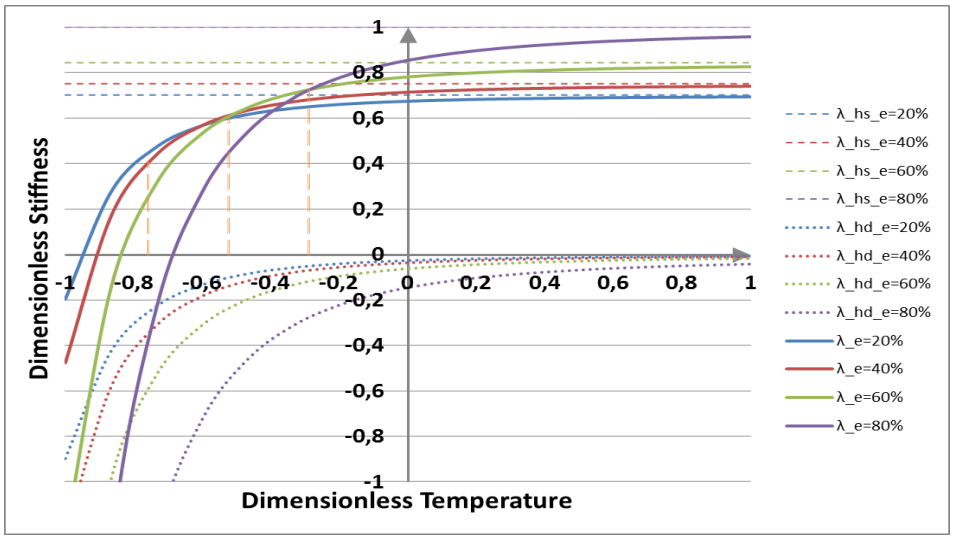

Figure 3.13 – Dimensionless stiffness versus fluid temperature.

The dimensionless bearing stiffness declines at low temperatures. With the increase of eccentricity, this decrease occurs sooner. Depending on the required minimum stiffness, it could be necessary to limit the bearing force at low temperatures in order to contain the maximum eccentricity.[31]

[31] This possibility makes sense for aeronautic applications where the flight domain can be constrained by the fluid temperature.

4.3. Design Parameter Sensitivities

For the design of conical hybrid bearings under aerospace constraints, it is reasonable to consider the pressures, speeds and diameters as inputs. The remaining parameters are the bearing length, taper height and clearance.

It is of interest to assess their impact on the three main criteria, which are also dependent on the time variables: temperature and eccentricity. Figure 3.14, Figure 3.15 and Figure 3.16 respectively show the sensitivity of the three main criteria to the bearing length, the taper height and the h_t/c ratio considering the maximum eccentricity of 0.8. This value corresponds to a fluid film height of 5 µm, which prevents fluid film rupture.

Note 3.9: In the three figures, the volume flow rate axis is on the right part of the graphs, as the flow is always positive. This provides a better scaling of the plotted curves. Both the centring force and stiffness axes are in the centre of the figures.

Note 3.10: On the three figures, one colour is used per parameter value. Full, dotted and dashed lines respectively show the centring force, bearing stiffness and volume flow rate.

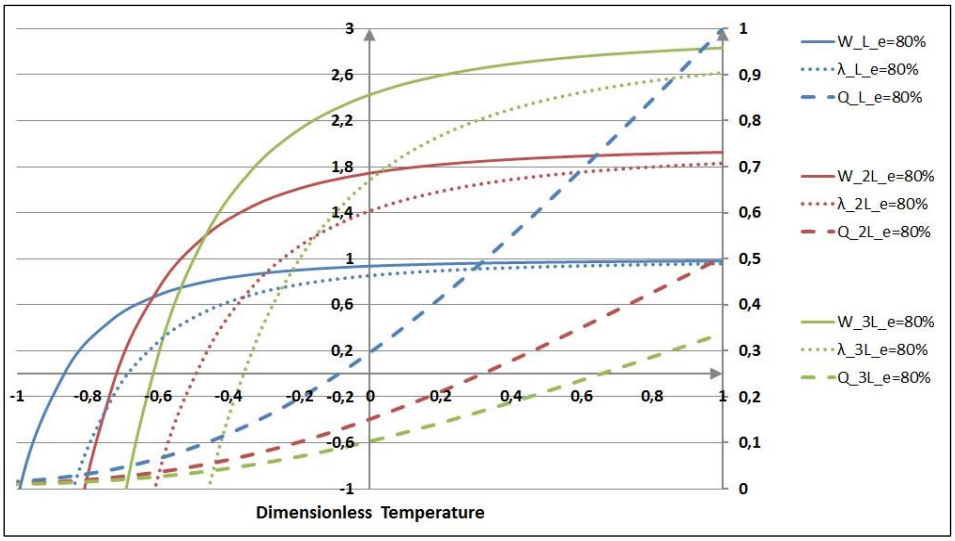

Figure 3.14 – Dimensionless main criteria versus fluid temperature for different bearing lengths.

Increasing the bearing length is tempting as it decreases the volume flow rate and increases the maximum values of both the centring force and the stiffness. However, caution should be exercised as it also makes these two criteria fall "sooner" at low temperatures.

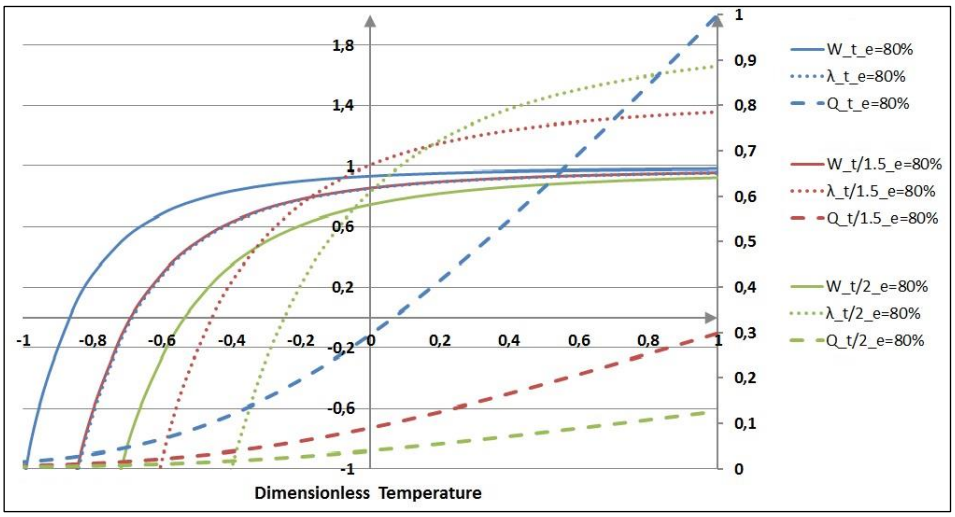

Figure 3.15 – Dimensionless main criteria versus fluid temperature for different taper heights.

The taper height is a necessary contributor to the centring force. Reducing its height clearly reduces the centring force. This effect is even more visible at low temperatures. The stiffness increases but drops dramatically sooner in the temperature axis, which not desirable. However, these disadvantages must be put into perspective with a great diminution of the volume flow rate. Dividing the taper height by 1.5 corresponds to a reduction of almost 70% of the flow rate.

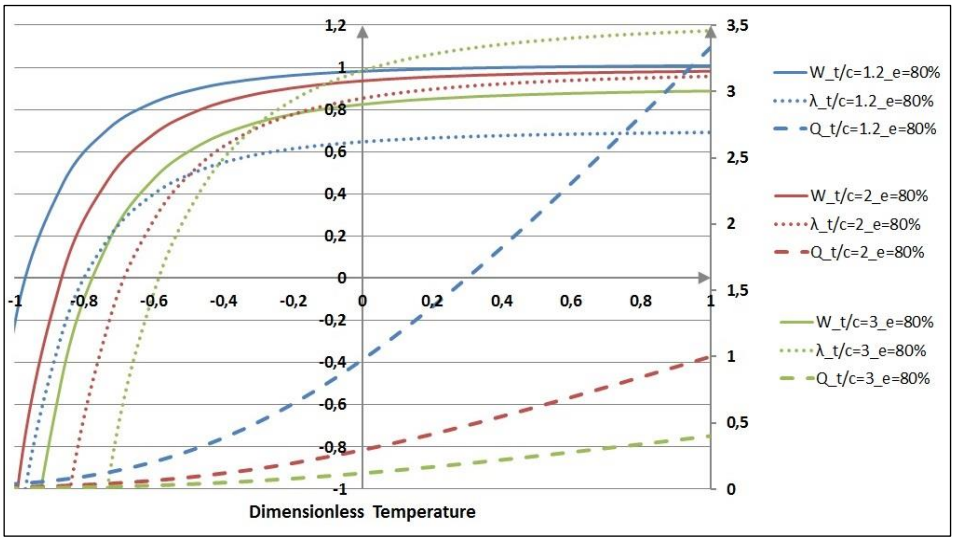

Figure 3.16 – Dimensionless main criteria versus fluid temperature for different t/c ratios.

These studies, like the previous section, are carried out considering a ratio $h_t/c = 2$. This corresponds to the ratio used by Viersma. It maximizes the bearing centring force near zero eccentricity **[FAI91]**. However, the optimal ratio for the maximum eccentricity of 0.8 is 1.2. It is therefore interesting to study the evolution of the main design criteria in order to be able to better choose the value of the h_t/c ratio while maintaining the same taper height.

By changing the ratio from 1.2 to 3, the maximum bearing centring force only decreases by 10%, while the volume flow rate is reduced by a factor 7. Caution should be exercised with respect to stiffness, which becomes negative at low temperatures, resulting in an attractive force. Thus, if margins are available on both the centring force and the stiffness at low temperatures, or if the overall extended range of temperature is not required, it would be convenient to increase this ratio in order to reduce the leakage.

4.4. Conclusion

The equations providing the three main criteria for a conical hybrid bearing were presented in this section. While the centring force equation is well-known, the volume flow rate relation was completed with the contribution of the hydrodynamic effect in this dissertation. The bearing stiffness was derived from the centring force equation.

In addition, two studies were carried out in this section. Based on a conical bearing design example proposed by Viersma, the first study assesses the dependency of the three main design criteria on temperature and eccentricity. For each criterion, the contribution of both the hydrostatic and hydrodynamic effects was emphasized. A common trend could be revealed. Considering an extended range of temperature, the characteristics of the three main criteria drop at low temperatures. Even though this is desirable for the volume flow rate, it can become unacceptable for both the centring force and the stiffness, for which negative values can be reached.

A second study assessed the sensitivity of the three main design criteria with respect to the three design parameters. Reducing the bearing length enables increasing the centring force and reducing the leakage but comes at the cost of low stiffness at low temperatures. A small diminution of the taper height or an increase of the taper height/clearance ratio are both acceptable options to reduce the leakage without a dramatic counter-effect on the other performances.

Fluid bearing friction was not addressed as it was not considered to be a key design driver. Corresponding models are available, e.g.: **[SCH97]**. Their implementation is proposed as a perspective to this study.

5. CONCLUSION

Hybrid fluid bearings were identified as a good alternative to current sealing and bearing devices. At the cost of a contained leakage, a satisfying centring force and bearing stiffness can be obtained. However, the design of such fluid bearings must be realized with caution. These performances indeed highly depend on time variables and design parameters.

Therefore, in a first section, the Reynolds equation was presented based on the equilibrium of fluid elements in a fluid film. The importance of each of its effects was discussed and associated simplification for our subsequent analysis was proposed.

Based on this simplified Reynolds equation, three different manners to generate a normal force in a fluid film were investigated in section 2. As a first approach, only the axial flow was considered. The axial study established three candidates for further investigation: hydrostatic thrust bearings, conical hybrid bearings and parallel-step piston. It was decided to focus only on the first two solutions as literature shows that parallel-step piston normal force is less promising than the others.

A pre-sizing process for hydrostatic thrust bearings with special consideration for performance robustness within an extended range of temperature was developed in section 3. This was made possible only by introducing a short tube orifice as a fixed restriction. A new STO model was proposed based on the analytic requirements and parameters identified using CFD simulations. The key idea of the proposed design consists in exploiting the degree of freedom of the $D_T R_e / L_T$ ratio to place the temperature transition from a laminar to a turbulent flow pattern. Indeed, configuring this temperature transition in the STO enables achieving a satisfying stiffness at very low temperatures and a reasonable flow at very high temperatures.

Finally, section 4 focused on a conical hybrid design under aerospace constraints. The impact of the time variables and design parameters was assessed. As final recommendation to both designs, it is important to contain as much as possible the lowest values of the temperature domain in order to optimize the design. An alternative could be to degrade the performance specified with the decrease of temperature. However, obtaining satisfying values may prove difficult.

The research performed in this chapter provides input for the high-performance actuator prototype development detailed in the next chapter (Restricted). Fluid bearings are a key technological step identified to enhance actuator performance, ensuring a satisfying lifespan.

BIBLIOGRAPHY

[BLA60] BLACKBURN, J.F., REETHOF, G. & SHEARER, J.L., *Fluid Power Control*. John Wiley & Sons, Inc., New York and London, 1960.

[COI16a] COÏC C. & MARÉ J.-C., *Modeling and Pre-Sizing Process for Hydrostatic Thrust Bearing with Special Consideration to Performance Robustness within a Wide Temperature Range*, International Conference on Hydraulics and Pneumatics, Praha, Czech Republic, 2016.

[ETS75] ETSION, I., *An Optimum Step Design for Centering of Pistons*. ASME, Journal of Fluids Engineering, 1975.

[FAI83] FAISANDIER, J., *Mécanismes Hydrauliques*. Dunod, Paris, 1983. (in French)

[FAI91] FAISANDIER, J., GRAND, S., LEBRUN, M. & THOMA, J.U., *Hydraulique et Informatique ou l'Informatique au Service de l'Hydraulique*, Promotion Presse Internationale, Paris, 1991. (in French)

[FRE95] FRENE, J., *Butées et Paliers Hydrodynamiques*. Techniques de l'Ingénieur, B5 320, 1995. (in French)

[FRE97] FRÊNE, J., NICOLAS, D., DEGUEURCE, B., BERTHE, D. & GODET, M., *Hydrodynamic Lubrication: Bearings and Thrust Bearings*. Tribology Series, 33, Elsevier, 1997.

[HAM04] HAMROCK, B.J., SCHMID, S.R. & JACOBSON, B.O. *Fundamentals of Fluid Flim Lubrication, Second Edition*. Marcel Dekker, Inc., 2004.

[LEW62] LEWIS, E.E. AND STERN, H., *Design of Hydraulic Control Systems*. McGraw-Hill, 1962.

[MAR93] MARE, J.-C., *Contribution à la Modélisation, la Simulation, l'Indentification et la Commande d'Actionneurs Électrohydrauliques*. Thèse d'état, Lyon, 1993. (in French)

[MER67] Merritt, H.E., *Hydraulic Control System*, John Wiley & sons, Inc., 1967.

[NIC95] NICOLAS, D., *Butées et Paliers Hydrostatiques*. Techniques de l'ingénieur, b5325, 1995. (in french)

[POS89] POSSAMAI, O., *Étude et Conception d'un Guidage Linéaire de Haute Précision à Palier Fluide*. Université de Compiègne, 1989. (in French)

[RAY18] RAYLEIGH, L., *Notes on the Theory of Lubrication.* Philosophical Magazine, Vol. 35 pp.1-12, 1918.

[REY86] REYNOLDS, O., *On the Theory of Lubrication and its Application to Mr. Beauchamp Tower's Experiments, including an Experimental Determination of the Viscosity of Olive Oil*. 1886.

[ROW83] ROWE, W.B., *Hydrostatic and Hybrid Bearing Design*. Butterworths, London, 1983.

[SAE00] S.A.E., *AIR 1362 – Aerospace Hydraulic Fluids Physical Properties. USA, 2000.*

[SCH14] SCHMID, S.R., HAMROCK, B.J. & JACOBSON, B.O., *Fundamentals of Machine Elements, Third Edition*. CRC Press., 2014.

[SCH97] VAN SCHOTHORST, G., *Modelling of Long-Stroke Hydraulic Servo-Systems for Flight Simulator Motion Control and System Design*. Netherland, 1997.

[VIE80] VIERSMA, T.J., *Analysis, Synthesis and Design of Hydraulic Servosystems and Pipelines*. Elsevier, 1980.

[VOL72] VOLMAN, H.J.W.M., *Berekeningen en Constructie van het Radiaal Staplager*. Ploytechn. Tijdschr., 1972.

CONCLUSION GENERALE

Le but de cette thèse était d'étudier la possible augmentation de performances des actionneurs de commandes de vol électriques pour hélicoptères. En effet, les solutions technologiques assurant l'étanchéité et le centrage de l'ensemble piston/corps du vérin ne permettent pas l'implémentation de nouvelles fonctions de pilotage, dû à leur faible durée de vie lorsqu'ils sont soumis à des déplacements hautes fréquences.

Les paliers fluides linéaires ont été identifiés comme une alternative aux systèmes d'étanchéités conventionnels afin d'améliorer les performances de l'actionneur, en admettant de légères fuites internes. Seulement cette substitution technologique ne peut être réalisé sans une totale compréhension de l'impact que cela aura sur l'actionneur lui-même, le système d'actionnement global et finalement les commandes de vols et la réponse engendrée sur le comportement de l'hélicoptère.

Il a donc été choisi d'organiser cette recherche selon trois axes principaux contribuant chacun à ce but final :

1. Présenter les différentes technologies d'actionneurs et synthétiser comment les contraintes imposées par les commandes de vol impactent leur architecture et le choix technologique associé.
2. Développer une modélisation orientée-objet du système d'actionnement dans le but d'aider le développement et de permettre un interfaçage avec le système de commandes de vol global.
3. Étudier l'implémentation de paliers fluides linéaires au sein des actionneurs en considérant les contraintes aéronautiques associées.

Dans la première partie, l'évolution incrémentale des commandes de vol, portée par les besoins naissants, a été détaillée. Les nouveaux composants, ajoutés chronologiquement aux commandes de vol conventionnelles, ont été présentés simultanément à la fonction qu'ils remplissent. Cette analyse fonctionnelle a mis en évidence le besoin de repenser le système (« re-engineering » en anglais) lors du passage aux commandes de vol électriques. Nous avons introduit une architecture ainsi qu'un vocabulaire générique afin de décrire les différentes technologies d'actionneurs et supporter leurs analyses. Nous avons recommandé la technologie d'actionneur électrohydraulique à actionnement direct du distributeur (DDV) pour les actionneurs de commandes de vol primaires et insisté sur les bénéfices liés à l'utilisation de la technologie de servovalves électrohydrauliques (EHSV) pour les fonctions non-critiques telles que certaines commandes de vol secondaires. Nous avons conclu cette partie en présentant les perspectives d'évolution des commandes de vol dans les décennies à venir.

La deuxième partie de ce mémoire consistait en la modélisation virtuelle et la simulation du système d'actionnement en utilisant le formalisme Bond-graph. Le développement des modèles virtuels a été

conduit en analogie avec la méthode d'Ingénierie Systèmes : définissant les besoins de la modélisation du point de vue ingénieur et industriel, pensant l'architecture des modèles selon ces besoins et, finalement, développant chaque sous-modèle en utilisant les principes de l'orientation-objet. Le formalisme Bond-graph, de par sa généricité multi-domaines physiques, a facilité cette approche. Une attention particulière a été portée à la compréhensibilité des modèles Bond-graphs en combinant l'état de l'art en termes de lisibilité et en améliorant la topologie des modèles. Le modèle de fluide, fonction de la température, permet l'étude du système d'actionnement sur l'ensemble de l'intervalle de température, nécessaire (car extrêmement contraignant) lors d'un développement aéronautique. Dans cette partie, nous avons proposé une standardisation des interfaces et des modèles. Les causalités préférentielles ont été attribuées aux modèles afin de s'affranchir des contraintes liées à l'implémentation des modèles dans les différents environnements de simulation. Nous avons validé cette modélisation du système d'actionnement composant par composant à l'aide de tests unitaires ainsi que dans sa globalité en réalisant des tests d'intégration. Cette modélisation a finalement été interfacée avec un model global du système de commande de vol dans le but d'aider au choix de l'architecture et du dimensionnement du système d'actionnement d'un nouvel hélicoptère.

La troisième partie était dédiée à l'étude des paliers fluides linéaires et leur utilisation pour une application système de puissance embarqué soumis à de sévères contraintes environnementales. Généralement, les paliers fluides sont utilisés dans un environnement industriel où la température du fluide est maintenue quasiment constante, contrairement à l'aéronautique où le domaine opérationnel du fluide inclus une plage de température de plus de 150°C. Considérant trois différentes technologies de paliers fluides, il a été détaillé comment celles-ci généraient un effort de centrage, une raideur radiale au prix d'une faible fuite. L'étude de la littérature existante nous a permis de sélectionner les butées hydrostatiques ainsi que les paliers hybrides fluides comme potentiels candidats à notre application. Nous avons décrit une méthode de pré-dimensionnement de la première solution technologique en utilisant un « orifice tube-court » comme restriction fixe. Nous avons en effet proposé d'influencer par design la température de transition de l'écoulement laminaire-turbulent dans l'orifice tube-court. Ceci était un élément clé pour obtenir des performances satisfaisantes en terme de force de centrage et de raideur tout en limitant le débit de fuite – ce qui n'aurait pas été possible en utilisant un orifice conventionnel ou un tube capillaire. Concernant les paliers coniques hybrides, nous avons conduit une étude de sensibilité afin d'observer l'impact des paramètres de design et des variables temporelles sur les principaux critères d'intérêt. Cela a révélé des raideur et effort de centrage du palier et inacceptables aux faibles températures, majoritairement dus à l'augmentation exponentielle de la viscosité du fluide. Finalement, nous avons recommandé de maintenir autant que faire se peut l'intervalle opérationnel de température dans le but d'optimiser le design des paliers fluides linéaires.

CONCLUSION GENERALE

La quatrième et dernière partie de ce mémoire était dédiée au développement d'un actionneur haute performances pour le contrôle actif de rotor avec l'aide de modèles virtuels. Elle se base sur les trois axes principaux investigués précédemment. La définition de l'architecture de l'actionneur, portée par les contraintes de sûreté, ainsi que le choix de technologies d'actionneur de commandes de vol électriques ont été réalisés sur la base des résultats du premier axe de ce mémoire. L'amélioration des performances tout en conservant une durée de vie acceptable a été possible grâce à l'utilisation de paliers hybrides coniques. La modélisation Bond-graph proposée a aidé le pré-dimensionnement de l'actionneur et a permis de vérifier son comportement par simulation virtuelle. Un prototype physique a été produit et est actuellement en période de tests sur des bancs d'essais dédiés.

Plusieurs améliorations possibles ont été identifiés et laissés en tant que perspectives des travaux effectués. Nous les avons organisés en deux axes principaux :

1. Les perspectives s'inscrivant dans les trois axes listés auparavant.
2. Les perspectives relatives à l'implémentation de ces axes au niveau de l'actionneur.

En analogie avec le développement d'un produit, le premier point correspondrait aux perspectives unitaires alors que le second serait les perspectives d'intégration. La priorisation des perspectives dépendrait par contre des besoins d'Airbus Helicopters et des contraintes de planning liés aux développements en cours. Cela diverge d'un cycle en V dans un schéma d'ingénierie systèmes où les tests unitaires devraient être conduits avant les tests d'intégration.

Nous avons identifié en tant que perspectives unitaires :

- Détailler le design « Top-Down » des différentes technologies d'actionneurs. Dans ce mémoire, les technologies ont été présentés sur la base de solution existante, c'est une approche dite « Bottom-Up ». Ceci ne permet pas de garder une trace de quelles architectures ont été écartées dans le développement ni les raisons de ces choix. Une approche descendante, depuis une spécification technique complète et en suivant une méthodologie d'ingénierie systèmes, pourrait mener à l'élaboration d'un outil permettant la sélection systématique d'architecture.

- Développer une modélisation thermo-hydraulique du système d'actionnement. La modélisation actuelle permet de modifier la température du système en fonction du temps de simulation mais est homogène dans la totalité du circuit. Ceci peut être atteint dans le formalisme Bond-graph en propageant quatre variables – le débit massique, la pression, la température et l'enthalpie – en lieu et place des variables d'hydraulique de puissance – le débit volumique et la pression. Il est toutefois à noter qu'augmenter le réalisme de la modélisation hydraulique à ce niveau n'a de sens que si le modèle détaillé de l'environnement du système est disponible.

- Investiguer le diagnostic de fautes des composants du système d'actionnement sur la base de l'analyse structurelle de la modélisation Bond graph. Cette étude pourrait être séparée en deux parties : la première permettrait de déterminer quelles fautes peuvent être détectées en utilisant les capteurs déjà présents à bord de l'hélicoptère, alors que la deuxième consisterait à déterminer les capteurs à ajouter afin de pouvoir détecter de nouvelles fautes. Une attention particulière devra être porté à l'isolation des fautes de manière à éviter les détections intempestives.

- Augmenter le niveau de réalisme du modèle mécanique en utilisant les Multi-Bonds dans le but de représenter tous les degrés de libertés des parties mécaniques. Ceci permettrait notamment de modéliser les interactions entre plusieurs axes. Pour donner un exemple, l'excentricité du piston par rapport au corps du vérin n'a pas été modélisé dynamiquement dans ces recherches dû aux limitation en terme de mouvement 3D du modèle.

- Développer des modèles de paliers fluides en incluant les notions de frictions et de centre de pression. Cette perspective est dépendante de la précédente. En effet, les paliers fluides génèrent des efforts normaux et de translation qui requièrent une modélisation multiaxe. L'effort de centrage est la force résultante du champ de pression ramenée au centre de pression.

Nous avons identifié, en tant que perspectives d'intégration les points suivants laissés pour des études futures :

- Conduire une analyse de sensibilité des tolérances de fabrication de paliers fluides. La production en série d'un actionneur hautes performances ne pourra démarrer uniquement si la répétabilité des performances est démontrée. Une amélioration possible du design de l'actionneur pourrait consister à usiner les paliers en tant que pièces séparées du piston ou corps du vérin et de les assembler en utilisant des joints statiques. Cette solution permettrait l'appairage des pièces qui, bien que coûteux, réduirait l'intervalle de variation du jeu au niveau des paliers et donc le débit de fuite interne.

- Analyser les résultats d'essai et vérifier le pré-dimensionnement et la modélisation de l'actionneur haute-performances. La modélisation du système d'actionnement a été vérifiée en utilisant des données de vol réelles enregistrées. Pour autant, l'introduction de nouveaux paramètres de l'actionneur haute performance peut être erronée ou, potentiellement, un effet physique négligé pour les actionneurs conventionnels joue un rôle prépondérant pour notre application.

- Investiguer le moment généré par la combinaison de plusieurs paliers fluides. En effet, les forces de chaque palier ainsi que leurs centres de pression diffèrent. Cela peut engendrer la rotation de l'ensemble piston-tige dans le corps du vérin. Cette recherche est loin d'être triviale si on s'éloigne des équations qui se trouvent dans la littérature et requiert la mise en place de moyens

d'essais dédiés. Le désaxage du piston dans le corps du vérin implique que la hauteur du cône du palier varie virtuellement en fonction de son azimut, et avec lui, toutes les effets recherchés.

- Étudier l'impact de l'introduction des paliers fluides sur la raideur et stabilité de l'actionneur ainsi que leur variation sur la totalité de la plage de température. Autant la friction du fluide que la fuite interne ont des effets stabilisateur sur l'actionneur mais réduisent sa raideur et induise une erreur statique en position. L'évolution de ces deux variables en fonction de la température est diamétralement opposée. L'étude analytique et numérique de ces propriétés serait donc un axe intéressant de recherche.

Finalement, une dernière perspective, qui sort du cadre de cette thèse mais a du sens pour un intégrateur tel Airbus Helicopters de par sa connaissance globale du design hélicoptère, est la recherche d'une potentielle amélioration de la cinématique rotor dans le but de réduire les performances requises au niveau de l'actionneur, pour un même cahier des charges de contrôle actif.

DISSERTATION CONCLUSION

The aim of this PhD dissertation was to investigate the performance augmentation of Fly-by-Wire actuators for helicopters. Indeed, current dynamic sealing and bearing devices for actuators impede the implementation of several new functions on helicopters due to their short lifespan at high frequencies. Substitution of conventional seals with linear fluid bearings was identified as a necessary technological step to enhance actuator performance, at the cost of minor leakage. However, such substitution cannot be achieved without a clear understanding of the associated impacts on the actuator itself, on the Actuation System and, finally, on helicopter flight controls.

In this dissertation, it was chosen to organize the research along the following three main axes, each of which contributes to this investigation:

1. To present the different actuator technologies and synthesize how the flight control constraints impact their architecture and the technology selection.
2. To structure an object-oriented modelling of the Actuation System aimed at supporting model-aided developments and interfacing with a global flight control system simulation model.
3. To study the implementation of linear fluid bearings on actuators under aerospace constraints.

In the first part, the need-driven incremental evolution of the helicopter flight control system was detailed. The new components, added chronologically on conventional flight controls, were organized by the function they were aimed to fulfil. This functional analysis highlighted the re-engineering induced by the Fly-by-Wire technological step. A generic architecture and wording was introduced to support the different actuator technology descriptions and analyses. The Direct Drive Valve was recommended for primary flight control actuators and the benefits of using Electro-Hydraulic Servo Valves for non-critical functions were pointed out. This first part was concluded by presenting a selection of possible further evolutions of flight controls.

The second part of this dissertation dealt with the Actuation System virtual modelling and simulation with the support of the Bond-graph formalism. Indeed, the development of virtual models was addressed in analogy with the System Engineering development method: defining the modelling needs from engineering and industrial points of view, architecting the virtual models based on these needs and, finally, developing each sub-model in an object-oriented manner. Bond-graphs facilitated this approach due to their multi-domain genericity. Special attention was paid to facilitating the understanding of the proposed Bond-graph models by combining the state of the art in readability improvement and model topology. The fluid model function of the temperature enables the behaviour of the Actuation System to be studied in an extended temperature range, as required in an aerospace environment. In this part, a standardization of components and interfaces was proposed. For this, causal

bonds are used in order to remove the constraints imposed on the simulation environment in terms of model implementation. This Actuation System modelling was validated using unitary actuator tests and integration tests of the entire system based on real data recorded during flights. It was interfaced with a global flight control system in order to help with the architecture selection and sizing of a new helicopter Actuation System.

The third part was dedicated to the study of linear fluid bearings used in an embedded power system which faces severe environmental and power consumption constraints. Indeed, this technology is usually implemented in an industrial environment, where the fluid temperature is regulated within a narrow range, as opposed to aerospace, where temperatures can vary by more than 150°C. Considering three different technologies of fluid bearings, it was detailed how they provide a centring force and radial stiffness at the cost of a contained leakage. Based on literature recommendations, hydrostatic thrust bearings and conical hybrid bearings were selected as potential candidates for aerospace actuators. A pre-sizing process of the first technology was achieved by using a short tube orifice as fixed restriction. It was proposed to manage by design the transition from a laminar to a turbulent flow pattern in the short tube orifice. This helped achieve a satisfying bearing stiffness and force with an acceptable leakage – results that had been impossible to produce using conventional orifice or capillary tubes. Regarding conical hybrid bearings, a sensitivity study was carried out on its design parameters and time variables. It revealed an unacceptable bearing stiffness and centring force at low temperatures due to the exponential increase of the fluid viscosity. Finally, it was recommended to contain as much as possible the temperature range in order to optimize the fluid bearing design.

The fourth and last part of this dissertation dealt with a model-aided development of a high-performance actuator for active rotor control. This part was based on the three main axes investigated previously. The definition of the safety-driven actuator architecture and the Fly-by-Wire technology selection for its control module were based on the first part of this dissertation. Enhanced performance with a satisfying lifespan could be achieved by using conical hybrid bearings, which ensure the function of the moving parts bearing. Actuator pre-sizing was aided by the Bond-graph models, simplified due to judicious design choices and verified by a global simulation of the Actuation System. A prototype was manufactured and is currently being tested on dedicated test benches.

This research outlines the state of the art of the helicopter Actuation System in a concise way and proposes an associated modelling representative of its static and dynamic behaviour as well as its limitations in an extended temperature range. It details new design methodologies for two technologies of fluid bearings for aerospace actuators. The combination of these results will facilitate the development of further Fly-by-Wire actuators and enable achieving higher performances.

Several improvements were identified as perspectives to the work realized. They can be divided into two main groups:

1. The perspectives relative to the three aforementioned axes, which were developed in the first three parts of this dissertation.
2. The perspectives relative to the implementation of these axes at actuator level (fourth part).

In an analogy with the development of a product, the first point would correspond to the unitary perspectives and the second point to the integration perspectives. However, the prioritization of the perspectives depends on Airbus Helicopters' needs and planning constraints linked to its on-going developments. This diverges from the System Engineering V-cycle, where unitary tests would be performed before the integration tests.

Identified as unitary perspectives, the following points have given rise to further research:

- To detail the top-down design of the different actuator technologies. In this dissertation, the actuator technologies have been addressed in a bottom-up approach. This does not permit to keep track of which actuator architectures have been discarded and of the associated rationale. A top-down design based on a complete requirement specification and following a System Engineering approach could lead to the creation of a tool which would allow for a systematic selection of architectures with respect to requirements and the state of the art of technology.
- To develop a full thermo-hydraulic model of the Actuation System. The proposed model permits to modify the temperature with respect to the simulation time, but the temperature variation along the circuit due to dissipation or thermal exchange is not computed. This can be achieved by propagating four independent variables – mass flow, pressure, temperature and enthalpy – instead of the hydraulic power variables – pressure and volume flow rate. Implementation on an acausal simulation software has been successfully achieved with the Modelica Language and is available in the Modelica Standard Library. However, using it to increase the realism of the hydraulic model makes sense only if a detailed model of its environment is available.
- To investigate the fault-diagnosis of the Actuation System components based on the structural analysis of the proposed Bond-graph models. This study could be separated into two main phases: a first phase to determine which failures can be detected using the current on-board sensors, and a second phase to identify which sensors should be added to the Actuation System in order to detect news faults. Particular attention should be paid to the fault isolation in order to avoid false detection. Bond-graphs can provide an efficient means for fault detection and isolation.
- To increase the mechanical model realism using Multi-Bonds in order to represent more degrees of freedom of a mechanical body. This would enable modelling interaction between the axes. As

an example, eccentricity of the piston with respect to the housing has not been dynamically modelled in this dissertation due to this model limitation.

- To develop Bond-graph model fluid bearings including the notions of bearing friction and centre of pressure. This perspective depends on the previous one. Indeed, fluid bearings generate normal and translational forces which require a multi-axes modelling. The normal pressure is a resultant force at the centre of pressure that has not been addressed in this dissertation.

Identified as integration perspectives, the following points have been let to further study:

- To conduct a sensitivity study of the manufacturing tolerances for the actuator fluid bearings. Serial production of the actuator can only be considered if the repeatability of the performance is proven. An improvement of the current design in order to achieve smaller tolerances could be to manufacture the bearings as individual parts separated from the piston and housing and to assemble them using static seals. The effect of pressure on the seals would naturally centre the bearings.
- To analyse the test results and verify the high-performance actuator pre-sizing and model. The Actuation System model has been verified using real flight data recordings. However, implementation of the new parameters can be mistaken or differ from the design and the manufacturing of the prototype.
- To investigate the momentum generated by the combination of several fluid bearings. Indeed, bearing forces and their centres of pressure differ. This could induce a rotation of the piston-rod assembly in the housing. This investigation is not simple and would require dedicated testing. Indeed, the de-axing of the piston in the housing implies that the tapper height virtually varies with the azimuth.
- To investigate the impact of fluid bearings on actuator stiffness and stability and their variation within the extended range of temperature. Both the fluid friction and leakage have a stabilizing effect but reduce actuator stiffness and induce a static error. However, the evolution of these two variables is diametrically opposed with respect to temperature variation. Therefore, it would be interesting to assess the impact of each factor on actuator performance within the extended range of temperature.

Finally, a last perspective for Airbus Helicopters would be to investigate the potential improvement of the rotor kinematics in order to reduce the required performance at actuator level for an equivalent active rotor control.

LIST OF ACRONYMS

ACC	Actuator Control Computer
ACL	Actuator Control Loop
AFCS	Automatic Flight Control System
APM	Auto-Pilot Module
ARP	Aerospace Recommendation Practice
ASE	Automatic Stabilization Equipment
BUPA	Back-Up Passivation Actuator
CFD	Computational flow Dynamics
CS	Certification Specifications
DDV	Direct Drive Valve
EASA	European Aviation Safety Agency
EHSV	Electro-Hydraulic ServoValve
EMA	Electro-Mechanical Actuator
FAA	Federal Aviation Administration
FAR	Federal Aviation Regulations
FbL	Fly-by-Light
FbW	Fly-by-Wire
FCC	Flight Control Computer
FCP	Flight Control Processing
FTA	Fault Tree Analysis
HACA	Hydraulic Active Control Actuator
HIL	Hardware In the Loop
HHC	Higher Harmonic Control
HMI	Human Machine Interface
HPR	High Performance Rotor
HUM	Health Usage and Monitoring
IBC	Individual Blade Control
INCOSE	International Council on Systems Engineering
JAA	Joint Aviation Authorities
JAR	Joint Aviation Requirements
LAT	Limited Angle Torque
LVDT	Linear Variable Differential Transformer
MGB	Main gear Box

LIST OF ACRONYMS

MIL	Model In the Loop
NH	NATO Helicopters
NOTAR	NO TAil Rotor
PbW	Power-by-Wire
PCB	Printed Circuit Board
PID	Proportional, Integral, Derivative
PIO	Pilot Induced Oscillations
RFLP	Requirement, Function, Logical solution and Physical element
RVDT	Rotary Variable Differential Transformers
SAE	Society of Automotive Engineers
SCAS	Stability and Control Augmentation System
SEMA	Smart Electro Mechanical Actuators
SIA	Smart Interface Actuator
SIL	Software In the Loop
STO	Short Tube Orifice
TRIM	Trim actuators
TRLx	Technology Readiness Level x
VDI	Verein Deutscher Ingenieure
V&V	Validation & Verification
xVDT	LVDT or RVDT

NOMENCLATURE

a	Fluid viscosity index	[-]
C	Capacitive effect	
c	Clearance	[m]
c_q	Flow coefficient	[-]
D	Diameter	[m]
De	Effort detector	
Df	Flow detector	
e	Effort	
e	Eccentricity	[m]
f	Flow	
F	Linear force	[N]
f	Friction factor	[-]
g	Gravitational acceleration	[m/s²]
GY	Gyrator	
h	Height	[m]
I	Inductive effect	
i	Current	[A]
J	Rotational inertia	[kg.m²]
k	Pressure-viscosity coefficient	[Pa^{-1}]
L	Length	[m]
LH	Left Hand	
M	Modulated	
m	Mass	[kg]
p	Generalized Momentum	
P	Pressure	[Pa]
P_h	Heat power	[W]
q	Generalized Displacement	
Q	Volume flow rate	[m3/s]
R	Dissipative effect	
R_e	Reynolds Number	[-]
RH	Right Hand	
Se	Effort source	
Sf	Flow source	
S	Section	[m²]
T	Torque	[N.m]
t	time	[s]
TF	Transformer	
U	Voltage	[V]
u	Linear speed in x axis	[m/s]
v	Linear speed in y axis	[m/s]
V	Volume	[m^3]
w	Linear speed in z axis	[m/s]
W	Bearing force	[N]
x	Axis of the Cartesian reference	
y	Axis of the Cartesian reference	
z	Axis of the Cartesian reference	
α_p	Fluid coefficient of thermal expansion	[$°C^{-1}$]
β	Fluid Bulk modulus	[Pa]
ΔP	Pressure-difference	[Pa]
ξ	Pressure drop coefficient	[-]
λ	Flow number	[-]
ω	Angular speed	[rad/s]
Θ	Temperature	[K]
ρ	Fluid density	[kg/m^3]
τ	Shear stress	[Pa]
μ	Fluid absolute viscosity	[Pa.s]
υ	Fluid kinematic viscosity	[m²/s]
σ	Flow cross area	[m²]